

UNIVERSIDADE DE LISBOA

FACULDADE DE CIÊNCIAS

Departamento de Física



Analysis of the Anatomical and Functional basis of Autism Spectrum Conditions using Magnetic Resonance Imaging and Electroencephalography

Ana Maria Ferreira Paradela Catarino

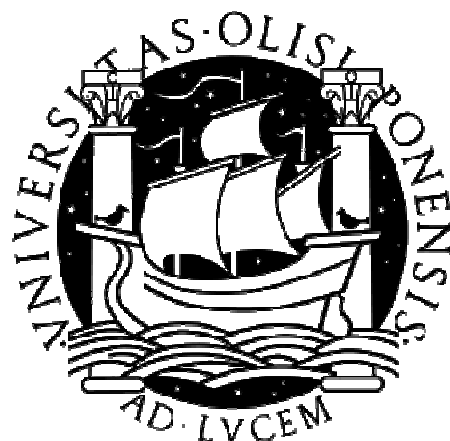
DOUTORAMENTO EM ENGENHARIA BIOMÉDICA E BIOFÍSICA

2012

UNIVERSIDADE DE LISBOA

FACULDADE DE CIÊNCIAS

Departamento de Física



Analysis of the Anatomical and Functional basis of Autism Spectrum Conditions using Magnetic Resonance Imaging and Electroencephalography

Ana Maria Ferreira Paradela Catarino

Thesis supervised by:

Professor Doutor Alexandre Andrade
Instituto de Biofísica e Engenharia Biomédica
Faculdade de Ciências, Universidade de Lisboa

DOUTORAMENTO EM ENGENHARIA BIOMÉDICA E BIOFÍSICA

2012

CONTENTS

LIST OF FIGURES	v
LIST OF TABLES	vii
LIST OF ABBREVIATIONS	ix
ABSTRACT	xi
RESUMO	xiii
PUBLICATIONS	xvii
ACKNOWLEDGEMENTS	xix
1. GENERAL INTRODUCTION	1
1.1. AUTISM SPECTRUM CONDITIONS	1
1.1.1. MECHANISM AND CAUSES	2
1.2. MAGNETIC RESONANCE IMAGING	4
1.2.1. PHYSICAL PRINCIPLES	4
1.2.2. ECHOES	9
1.2.3. SPATIAL ENCODING	11
1.2.4. FUNCTIONAL MRI	15
1.3. ELECTROENCEPHALOGRAPHY	18
1.3.1. BRAIN ANATOMY AND PHYSIOLOGY	18
1.3.2. EEG RECORDING	21
LIMITATIONS	22
TYPICAL ACTIVITY	23
1.3.3. SIGNAL ANALYSIS	24
FREQUENCY AND POWER ANALYSIS	24
EVENT RELATED POTENTIALS	25
NON-LINEAR, COMPLEXITY AND CONNECTIVITY ANALYSIS OF THE EEG SIGNAL	26

MULTISCALE ENTROPY	27
WAVELET TRANSFORM COHERENCE	28
1.3.4. APPLICATIONS OF EEG IN RESEARCH	28
2. AN MRI INVESTIGATION OF ATYPICAL CORTICAL THICKNESS IN AUTISM SPECTRUM CONDITIONS	31
2.1. INTRODUCTION	31
2.1.1. AIMS OF THE STUDY	32
2.2. METHODS	32
2.2.1. PARTICIPANTS.....	32
2.2.2. MRI ACQUISITION	35
2.2.3. CORTICAL SURFACE RECONSTRUCTION	35
2.2.4. STATISTICAL ANALYSIS	36
2.3. RESULTS.....	37
2.3.1. VARIATION OF KERNEL WIDTH	37
2.3.2. CORTICAL THICKNESS	37
2.3.3. AGE-CORTICAL THICKNESS CORRELATION	39
2.4. DISCUSSION.....	40
3. AN fMRI INVESTIGATION OF DETECTION OF SEMANTIC INCONGRUITIES IN AUTISM SPECTRUM CONDITIONS	43
3.1. INTRODUCTION	43
3.1.1. ASC AND SEMANTIC INCONGRUITIES	43
3.1.2. EEG AND fMRI IN THE STUDY OF SEMANTIC INCONGRUITIES	43
3.1.3. AIMS OF THE STUDY	44
3.2. METHODS	44
3.2.1. PARTICIPANTS.....	44
3.2.2. MRI ACQUISITION	45
3.2.3. fMRI TASK	45
3.2.4. DATA ANALYSIS.....	47
3.3. RESULTS.....	52

3.3.1.	BEHAVIOURAL PERFORMANCE	52
3.3.2.	fMRI FUNCTIONAL ACTIVATION – WITHIN-GROUP CONTRASTS.....	53
3.3.3.	fMRI FUNCTIONAL ACTIVATION – BETWEEN-GROUP CONTRASTS.....	58
3.4.	DISCUSSION.....	59
4.	ATYPICAL EEG COMPLEXITY IN AUTISM SPECTRUM CONDITIONS:	65
	A MULTISCALE ENTROPY ANALYSIS	65
4.1.	INTRODUCTION	65
4.1.1.	ASC AND FACE PROCESSING	65
4.1.2.	BRAIN COMPLEXITY IN ASC.....	66
4.1.3.	AIMS OF THE STUDY	67
4.2.	METHODS	68
4.2.1.	PARTICIPANTS.....	68
4.2.2.	EEG RECORDING	69
4.2.3.	SIGNAL ANALYSIS.....	70
4.2.4.	MULTISCALE ENTROPY.....	71
4.2.5.	POWER ANALYSIS	72
4.2.6.	STATISTICAL ANALYSIS	73
4.3.	RESULTS.....	74
4.3.1.	BEHAVIOURAL PERFORMANCE.....	74
4.3.2.	MSE ANALYSIS.....	74
4.3.3.	POWER ANALYSIS	78
4.4.	DISCUSSION.....	78
5.	INTERHEMISPHERIC FUNCTIONAL CONNECTIVITY IN AUTISM SPECTRUM CONDITIONS: AN EEG STUDY USING WAVELET COHERENCE TRANSFORM	83
5.1.	INTRODUCTION	83
5.1.1.	COHERENCE AND CONNECTIVITY	83
5.1.2.	COHERENCE AND CONNECTIVITY IN ASC	84
5.1.3.	AIMS OF THE STUDY	86

5.2. METHODS	86
5.2.1. PARTICIPANTS	86
5.2.2. EEG RECORDING	87
5.2.3. SIGNAL ANALYSIS	87
5.2.4. WAVELET TRANSFORM COHERENCE	88
5.2.5. STATISTICAL ANALYSIS	91
5.3. RESULTS	92
5.3.1. BEHAVIOURAL PERFORMANCE	92
5.3.2. WTC ANALYSIS	92
5.4. DISCUSSION	100
6. GENERAL DISCUSSION	107
6.1. UNIFYING MODELS OF ASC	107
6.1.1. ATYPICAL NEURAL CONNECTIVITY IN ASC	108
6.1.2. LIMITATIONS OF THE DATASETS USED IN THIS THESIS	109
6.2. fMRI MEASURES OF CONNECTIVITY IN ASC	110
6.2.1. LIMITATIONS ON THE INTERPRETATION OF THE fMRI STUDY DESCRIBED IN CHAPTER 3	112
6.3. EEG MEASURES OF CONNECTIVITY IN ASC	112
6.4. ANATOMICAL MEASURES OF CONNECTIVITY IN ASC	114
6.5. LIMITATIONS OF THE CONNECTIVITY THEORY IN ASC AND FUTURE PERSPECTIVES	115
6.6. CONCLUSIONS	116
REFERENCES	118

LIST OF FIGURES

Figure 1.1 – The protons’ magnetic moments align parallel or anti-parallel in the presence of an external field (a) and differences in energy states generate a positive net magnetization, in the same direction as the main field (b).	5
Figure 1.2 – When an RF pulse is applied, the net magnetization M_0 is flipped by an angle α . .	6
Figure 1.3 – The rotating frame of reference, rotating at the Larmor frequency; the RF magnetic pulse B_1 and magnetization vector M_0 will appear to be stationary.	6
Figure 1.4 – Transverse magnetization decay, due to spin-spin interactions.	7
Figure 1.5 – Decay of transverse magnetization M_{xy} due to spin-spin interactions and field inhomogeneities.....	8
Figure 1.6 – Recovery of longitudinal magnetization M_z due to spin-lattice interactions.	8
Figure 1.7 – (a) T1-weighted image of the brain, showing cerebrospinal fluid in dark, brain matter in mid-gray and adipose (fat) tissue in bright tones; (b) T2-weighted image of the brain showing cerebrospinal fluid as very bright and brain and other types of tissue in mid-gray.....	9
Figure 1.8 – Gradient echo sequence	10
Figure 1.9 - Spin echo sequence	11
Figure 1.10 – Gradients in the x, y and z axis are used for spatial encoding;	13
Figure 1.11 – Spin-echo (SE) imaging sequence	14
Figure 1.12 – Gradient echo based echo planar imaging (GE-EPI) sequence	15
Figure 1.13 – Blood Oxygen Level Dependent (BOLD) response to neural activity.....	16
Figure 1.14 – Diagram of brain anatomy showing the corpus callosum, cerebral cortex, brain stem and cerebellum, as well as the functionally segregated lobes.	19
Figure 1.15 – Diagram of a neuron’s resting potential.	19
Figure 1.16 – Neuron’s structure and stimulus propagation diagram.....	20
Figure 1.17 – Action potential being generated and propagated along the axon of a neuron (a) and a diagram illustrating a referential montage (b).	21
Figure 1.18 – Placement of electrodes on the scalp according to the International 10-20 system.	22
Figure 1.19 – Example of an EEG power graph.	25
Figure 1.20 – Averaging procedure in EEG data to extract ERP waveform.	26
Figure 2.1 – Boxplot representations of the age distribution for both Control and ASC groups.	37

Figure 2.2 – Variation of cortical thickness results with kernel width.....	38
Figure 2.3 – Group differences in cortical thickness for kernel width of FWHM = 10 mm.	39
Figure 2.4 – Group differences in cortical thickness-age correlation for kernel width of FWHM = 10 mm.	40
Figure 3.1 – Example of 1st level analysis modelation of experimental conditions.....	51
Figure 3.2 – T-maps of increased brain activity to Incongruent compared to Congruent stimuli (Concrete sentences only) in left (LH) and right (RH) hemispheres, for selected axial slices, for Control (A) and ASC (B) participants, at $p_{\text{FDR-corr}} < 0.05$ (cluster level)	54
Figure 3.3 – T-maps of increased brain activity for Congruent relative to Incongruent stimuli (Emotional sentences only) in left (LH) and right (RH) hemispheres, for selected axial slices, for Controls, at $p_{\text{FDR-corr}} < 0.05$ (cluster level).	56
Figure 4.1 – Example of stimuli sequence shown to participants, for both face and chair tasks	70
Figure 4.2 - Schematic illustration of the coarse-graining procedure	72
Figure 4.3 - Sample entropy by scale factor (SF) graphs for the chairs task, for each electrode, for each group.....	75
Figure 4.4 - Sample entropy by scale factor (SF) graphs for the faces task, for each electrode, for each group.....	75
Figure 4.5 - Sample entropy by scale factor (SF) graphs for electrode T7, for both chairs and faces task.....	76
Figure 4.6 – Electrodes that presented a significant group-by-scale factor (SF) interaction	78
Figure 5.1 – Statistical group comparison of interhemispheric coherence for the chairs task, not corrected for multiple comparisons.....	94
Figure 5.2 – Statistical group comparison of interhemispheric coherence for the faces task, not corrected for multiple comparisons.....	96
Figure 5.3 – Statistical group comparison of interhemispheric coherence, corrected for multiple comparisons using the False Discovery Rate (FDR) algorithm.....	97
Figure 5.4 - Statistical task comparison of interhemispheric coherence for the ASC group, not corrected for multiple comparisons.....	97
Figure 5.5 - Statistical task comparison of interhemispheric coherence for the Control group, not corrected for multiple comparisons	99

LIST OF TABLES

Table 2.1 - Age, verbal IQ, performance IQ and full-scale IQ for each group.....	33
Table 2.2 - Diagnosis criteria for participants in the ASC group	35
Table 3.1 - Age, verbal IQ, performance IQ and full-scale IQ for each group.....	45
Table 3.2 - Response times for each group and each sentence type	52
Table 3.3 - Accuracy scores for each group and each sentence type	53
Table 3.4 - T, Z, p FDR-corrected and uncorrected values for voxels and clusters activated more in response to Concrete Incongruent stimuli than to Concrete Congruent stimuli, for each group	55
Table 3.5 - T, Z, p FDR-corrected and uncorrected values for voxels and clusters activated more in response to Emotional Congruent stimuli than to Emotional Incongruent stimuli, for the Control group	57
Table 4.1 - Age, verbal IQ, performance IQ and full-scale IQ for each group.....	68
Table 4.2 - Accuracy (out of 10) and response times (in ms) for both tasks, for each group.....	74
Table 4.3 - Group-by-scale factor (SF) interaction significance values for each electrode site..	77
Table 6.1 - Summary of methods and results of the different studies performed in the context of this thesis	117

LIST OF ABBREVIATIONS

ADI-R	– Autism Diagnostic Interview - Revised
ADOS	– Autism Diagnostic Observation Schedule
ANOVA	– Analysis of Variance
AQ	– Autism Quotient
ASC	– Autism Spectrum Conditions
BA	– Brodmann Area
BOLD	– Blood Oxygenation Level Dependent
CC	– Concrete Congruent
CI	– Concrete Incongruent
CSF	– Cerebrospinal Fluid
DTI	– Diffusion Tensor Imaging
EC	– Emotional Congruent
EEG	- Electroencephalography
EI	– Emotional incongruent
EPI	– Echo Planar Imaging
ERC	– Event Related Coherence
ERP	– Event Related Potential
FDR	– False Discovery Rate
FFA	– Fusiform Face Area
FFT	– Fast Fourier Transform
fMRI	– functional Magnetic Resonance Imaging
FSIQ	– Full Scale Intelligence Quotient
FWHM	– Full Width at Half Maximum
GE-EPI	– Gradient Echo Echo Planar Imaging
HFA	– High Functioning Autism
ICA	– Independent Component Analysis
IQ	– Intelligence Quotient
LH	– Left Hemisphere
MEG	- Magnetoencephalography
MNI	– Montreal Neurological Institute
MPRAGE	– Magnetization Prepared Rapid Acquisition by Gradient Echo

MRI – Magnetic Resonance Imaging
MSE – Multiscale Entropy
PCA – Principal Component Analysis
PET – Positron Emission Tomography
PIQ – Performance Intelligence Quotient
RF - Radiofrequency
RH – Right Hemisphere
SD – Standard Deviation
SE – Spin Echo
SF – Scale Factor
STS – Superior Temporal Sulcus
TE – Echo time
TR – Repetition time
VIQ – Verbal Intelligence Quotient
WASI – Wechsler Abbreviated Scale of Intelligence
WTC – Wavelet Transform Coherence

ABSTRACT

Autism Spectrum Conditions (ASC) are a set of pervasive neurodevelopmental conditions defined by a triad of impairments in social interaction, communications and behavioural flexibility. Previous investigations have provided a variety of evidence of neuroanatomical and neurofunctional impairments in people with ASC, and several explanatory models for ASC have been proposed. One of the most commonly cited is the connectivity model, proposing that ASC symptoms are caused by patterns of atypical neural connectivity.

In this thesis, different algorithms were employed for the analysis of neuroanatomical and neurofunctional data acquired from people with ASC and typically developing controls. Regarding anatomy, a cortical thickness analysis was performed, using magnetic resonance imaging (MRI) data. Although differences were found between controls and ASC patients, the results were inconsistent with previous literature and did not support the connectivity model under consideration.

The findings of the functional analyses however, directly or indirectly support the connectivity model of ASC. A functional MRI (fMRI) investigation of neural activation in response to written sentences showed that people with ASC activate mainly frontal areas, whilst the Control group activates areas over all regions of the cortex. These differences indirectly suggest patterns of reduced connectivity in ASC. A multiscale entropy (MSE) analysis of electroencephalographic (EEG) data acquired during performance of a visual discrimination task demonstrated patterns of decreased EEG complexity for the ASC group relative to the Control group. This also indirectly supports the model of reduced connectivity in ASC. Finally, a wavelet transform coherence (WTC) analysis of the same EEG data set showed decreased interhemispheric EEG coherence for the ASC group relative to the Control group, providing direct evidence supporting the connectivity model of ASC.

Overall, this thesis presents a set of results congruent with the connectivity model of ASC, highlighting the importance of unification of results in ASC research.

Keywords: Autism Spectrum Conditions, connectivity model, magnetic resonance imaging, electroencephalography, multiscale entropy, wavelet transform coherence

RESUMO

As desordens do espectro do autismo (DEA) são um conjunto de condições caracterizadas por uma disfunção global do desenvolvimento neurológico, que se manifesta na infância e cujos sintomas se prolongam por toda a vida adulta. Estudos estatísticos demonstram que as DEA afectam 6 em cada 1000 indivíduos, com uma incidência maior no sexo masculino em relação ao sexo feminino (4:1). Em termos sintomatológicos, as DEA são definidas por um conjunto de disfunções na interacção social e na comunicação, desde ausência completa de desenvolvimento de linguagem a alterações subtis da semântica e pragmática. Estas desordens são também caracterizadas pela presença de padrões de comportamentos rígidos e repetitivos. Este conjunto de sintomas aponta para uma disfunção global da função cerebral em indivíduos com DEA, e inúmeras investigações têm sido realizadas na tentativa de revelar as bases neuroanatómicas e neurofuncionais das DEA. No entanto, a maior parte destas investigações consiste em estudos com pequenas amostras de população, focados em aspectos sintomatológicos específicos, o que muitas vezes resulta em investigações com resultados inconsistentes ou contraditórios entre si.

A unificação de resultados de investigações neuroanatómicas e neurofuncionais, mas também bioquímicas e genéticas, é essencial para uma melhor caracterização das DEA e consequentemente para uma melhoria nas estratégias para o tratamento e prevenção das DEA. Vários modelos de unificação para as DEA têm sido propostos nas últimas décadas, sendo que um dos modelos mais abrangentes, e presentemente um dos mais citados, é o modelo da conectividade neuronal atípica em DEA. Este modelo defende que os sintomas e comportamentos que caracterizam as DEA são o resultado de uma disfunção global da conectividade neuronal (em particular um défice de conectividade neuronal de longo alcance) em indivíduos com DEA.

O objectivo desta tese era realizar uma análise do substrato neuroanatómico e neurofuncional das DEA, utilizando dados de ressonância magnética (MRI do inglês *Magnetic Resonance Imaging*) e electroencefalografia (EEG), adquiridos em duas populações – um grupo de indivíduos com DEA e um grupo de indivíduos normais (grupo de controlo).

Relativamente ao aspecto neuroanatómico, foi efectuada uma análise de espessura cortical em imagens estruturais adquiridas por MRI. Estas imagens foram adquiridas de um grupo de 11 indivíduos com DEA e um grupo de 13 indivíduos normais. Todos os indivíduos eram do

sexo masculino, não havendo diferença de idade ou QI (quociente de inteligência) médio entre os dois grupos (Idade: DEA: 27 anos, Controlo: 34 anos, $F_{1,23} = 2.042$, $P = 0.167$; QI: DEA: 115, Controlo: 121, $F_{1,17} = 1.042$, $P = 0.323$). As imagens de MRI foram adquiridas no Wolfson Brain Imaging Centre, Universidade de Cambridge, num scanner SIEMENS MAGNETOM TrioTim de 3 Tesla, com uma resolução espacial de 1.0 mm. A análise de espessura cortical foi efectuada utilizando o software Freesurfer, enquanto que as comparações estatísticas entre grupos foram efectuadas utilizando o software SPSS v17.0. Os resultados da análise de espessura cortical mostram diversas regiões onde o grupo com DEA apresenta um aumento ou uma diminuição de espessura cortical relativamente ao grupo de Controlo. Regiões de aumento relativo de espessura cortical incluem o lobo frontal médio esquerdo, lobos parietais superiores e inferiores, bem como a circunvolução orbitofrontal medial direita. Regiões de diminuição relativa de espessura cortical incluem o lobo frontal superior esquerdo, lobos temporais superiores e sulcos pré-centrais. No entanto, estes resultados não são consistentes com os resultados de investigações anteriores de espessura cortical em DEA. Isto pode dever-se a diversos factores, como variações nos algoritmos utilizados em cada investigação para o cálculo de espessura cortical. Ainda assim, esta inconsistência de resultados, aliada a outros factores como um largo espectro de idades da população em estudo (16 a 57 anos), sugere que neste caso os resultados da análise são inconclusivos, não sendo possível estabelecer uma relação entre espessura cortical e sintomatologia em DEA.

Pelo contrário, os resultados de todas as análises neurofuncionais efectuadas no contexto desta tese apoiam directa ou indirectamente o modelo da conectividade atípica em DEA. Em primeiro lugar, foi realizada uma análise da activação neuronal em resposta a incongruências semânticas, utilizando dados de ressonância magnética funcional (fMRI) adquiridos num grupo de 12 indivíduos com DEA e 12 indivíduos normais. Como se verificou para o estudo neuranatômico, não foram detectadas diferenças de idade ou de QI entre os dois grupos (Idade: DEA: 27 anos, Controlo: 34 anos, $F_{1,23} = 2.433$, $P = 0.133$; QI: DEA: 113, Controlo: 120, $F_{1,17} = 1.086$, $P = 0.313$). As imagens de fMRI foram adquiridas no Wolfson Brain Imaging Centre, Universidade de Cambridge, com uma resolução espacial de 3.0 x 3.0 x 4.0 mm. Durante a aquisição de imagens, pediu-se aos indivíduos para lerem um conjunto de frases e decidirem se para cada frase, a palavra final era semanticamente congruente ou incongruente. As frases foram apresentadas visualmente, uma palavra de cada vez, e estavam divididas em quatro categorias – concreta congruente (e.g.: The car had a flat tyre), concreta incongruente (e.g.: The fountain pen leaked blue chocolate), emocional congruente (e.g.: The snake hissed and he felt scared) e emocional incongruente (e.g.: The scientists predicted an epidemic and

she felt hungry). A análise das imagens de fMRI foi feita utilizando o software SPM5, e os resultados demonstram que, em resposta a frases incongruentes, os indivíduos com DEA activaram maioritariamente regiões frontais (em particular o lobo temporal inferior esquerdo), enquanto que os indivíduos normais activaram uma maior variedade de regiões corticais, incluindo córtices cingulados anterior e posterior, e lobo occipitotemporal. Estas diferenças entre grupos na extensão da activação neuronal apontam indirectamente para a existência de um défice de conectividade neuronal em DEA.

Duas análises funcionais foram também efectuadas utilizando dados de EEG. Estes dados foram adquiridos num grupo de 15 indivíduos com DEA e 15 indivíduos normais, durante o processamento visual de imagens de faces e cadeiras. Como se verificou nos estudos de espessura cortical e fMRI, também neste caso não foram detectadas diferenças de idade ou QI entre os dois grupos (Idade: DEA: 31, Controlo: 29, $F_{1, 29} = 0.961$, $P = 0.335$; QI: DEA: 119, Controlo: 119, $F_{1, 28} = 0.007$, $P = 0.936$). Os dados de EEG foram adquiridos no Departamento de Psiquiatria, Universidade de Cambridge, através de um sistema Synamps de 32 canais, com frequência de aquisição de 1000 Hz e um filtro passa-banda entre 0.1 e 50 Hz.

Uma das análises efectuadas consistiu num estudo da complexidade do sinal de EEG, usando um algoritmo de cálculo de entropia em várias escalas – entropia multiescala (MSE do inglês *Multiscale Entropy*). Os resultados desta análise mostram uma redução de complexidade do sinal de EEG para o grupo de indivíduos com DEA relativamente ao grupo de controlo, em particular para regiões parietais e occipitais. A relação entre complexidade de sinais EEG e conectividade neuronal foi já comprovada em investigações prévias, e os resultados desta análise sugerem um défice de conectividade neuronal em indivíduos com DEA, em regiões posteriores do córtex, apoiando indirectamente o modelo de conectividade atípica em DEA.

Uma segunda análise efectuada nos dados de EEG pretendia estudar diferenças em coerência interhemisférica entre indivíduos com DEA e indivíduos normais. Esta análise utilizou a técnica de coerência de wavelets (WTC do inglês *Wavelet Transform Coherence*), um algoritmo cuja principal vantagem é permitir um estudo da variação da coerência em tempo e em frequência, com controlo da resolução temporal e espectral. Os resultados desta investigação demonstram uma redução de coerência inter-hemisférica no grupo com DEA, relativamente ao grupo de controlo, em todas as regiões corticais estudadas (frontal, temporal, parietal e occipital). Estudos prévios já demonstraram a existência de uma correlação entre coerência de sinais EEG e conectividade neuronal, e pode-se concluir que os resultados desta análise mostram um

défice de conectividade neuronal inter-hemisférica em DEA, apoiando directamente o modelo da conectividade atípica em DEA.

Esta tese apresenta um conjunto de análises que empregam algoritmos diversos para o estudo da anatomia e função cerebral em DEA. Os resultados destas análises apontam consistentemente para a existência de um distúrbio da conectividade neuronal em indivíduos com DEA, apoiando o modelo da conectividade atípica em DEA. É importante referir que, por conter uma variedade de análises diferentes, esta tese oferece uma perspectiva unificadora na investigação das DEA, salientando a necessidade de estudos de larga escala em DEA, que empreguem diversos níveis de análise (p.ex.: anatómica, funcional), em grandes amostras de população bem caracterizadas em termos demográficos e que incluam indivíduos num largo espectro de idades, desde a infância até à idade adulta.

Palavras-chave: Desordens do espectro do autismo, modelo de conectividade, ressonância magnética, electroencefalografia, entropia multiescala, coerência de wavelets.

PUBLICATIONS

Chapter 3 of this thesis has been published as:

Catarino A., Luke L., Waldman S., Andrade A., Fletcher P. C., Ring H. (2011) An fMRI investigation of detection of semantic incongruities in autism spectrum conditions. *European Journal of Neuroscience* 33:558-567

Chapter 4 of this thesis has been published as:

Catarino A., Churches O., Baron-Cohen S., Andrade A., Ring H. (2011) Atypical EEG complexity in autism spectrum conditions: a multiscale entropy analysis. *Clinical Neurophysiology* 122(12):2375-83

Chapter 5 of this thesis has been submitted for publication.

ACKNOWLEDGEMENTS

I would like to thank my supervisors, Dr Alexandre Andrade from the Institute of Biophysics and Biomedical Engineering, University of Lisbon, and Dr Howard Ring from the Cambridge Intellectual and Developmental Disabilities Research Group, University of Cambridge. Their helpful advice and prompt availability have contributed greatly to the successful completion of this work.

I would also like to thank all the people who have collaborated in the projects included in this thesis – Dr Lydia Vella and Ms Jennifer Landt for their help with the MRI data acquisition, Dr Paul Fletcher for his help with the MRI data analysis, Dr Owen Churches for the help with the technical aspects of EEG data acquisition and analysis, Professor Simon Baron-Cohen for his support with the EEG projects and Dr Adam Wagner and Dr Peter Watson for their statistical insight. I would also like to thank Professor Eduardo Ducla Soares for introducing me to Biomedical Engineering in the last year of my undergraduate studies, and encouraging me throughout the course of my PhD.

I would like to acknowledge my colleagues at both the Institute of Biophysics and Biomedical Engineering in Lisbon, and the Cambridge Intellectual and Developmental Disabilities Research Group, for all the helpful comments and discussions. Finally I would also like to thank all the admin staff at Cambridge and Beatriz Lampreia in Lisbon, for guiding me through the administrative side of things.

1. GENERAL INTRODUCTION

1.1. AUTISM SPECTRUM CONDITIONS

Autism Spectrum Conditions (ASC) are a set of pervasive neurodevelopmental conditions with onset in early childhood and a wide range of life-long signs and symptoms. ASC seem to affect boys more frequently than girls, with a male-to-female prevalence rate of 4.3:1. Statistical studies have shown an increase in the prevalence of ASC over the last few decades, from approximately 5 per 10.000 in the 1960's and 1970's, to 60 per 10.000 in present times (Newschaffer et al., 2007). The most likely reasons for this increase in prevalence numbers are the evolution of diagnosis methods and historical changes in the criteria for classifying behaviours consistent with ASC phenotype (Newschaffer et al., 2007). Core features of ASC include impairments in reciprocal social interactions, a restricted repetitive range of behaviours, interests and activities, and a variety of language disturbances ranging from complete absence of receptive and expressive speech to subtle disorders of semantics and pragmatics (American Psychiatric Association, 2000). Children with severe ASC often experience a lack or a significant delay in language development. In the latter case, expressive speech is usually characterized by abnormalities such as echolalia, pronoun reversal, production of utterances with no relation to conversational context, aberrant prosody, unresponsiveness to questions and a general lack of drive to communicate (Rapin and Dunn, 2003).

In addition to these characteristic social and cognitive features, atypical patterns of motor functioning and integration are also increasingly recognised as features of ASC. Amongst these are evidence of impaired motor functions (Gidley Larson and Mostofsky, 2006) as well as impaired sensorimotor integration (Haswell et al., 2009) and motor planning and control (Jansiewicz et al., 2006, Rinehart et al., 2006, Freitag et al., 2007). There is evidence that motor deficits may be correlated with the social and cognitive features of ASC (Dziuk et al., 2007), suggesting that motor symptoms may be a core feature of ASC, or a marker for the underlying neurological deficits of this condition.

Sensory functioning has also been recognised as being atypical in people with ASC. In a review by Simmons et al. (2009), the authors have gathered evidence of atypical visual perception in ASC, including perception of biological motion (Kaiser et al., 2010). Driven by the social

impairments presented by people with ASC, many studies have investigated visual face perception and processing in ASC. These studies have reported various abnormalities in face processing in the ASC population, such as atypical patterns of neuronal activation to neutral and emotional face stimuli (Schultz et al., 2000, Harms et al., 2010) and atypical gaze patterns (Kliemann et al., 2010). Past studies on sensory processing have also found evidence of atypical auditory perception (Hitoglou et al., 2010), somatosensory integration (Russo et al., 2010), and reduced adaptability to environmental changes in this population (Russo et al., 2007, Thakkar et al., 2008, Foley Nicpon et al., 2010).

Within ASC, people with Asperger's syndrome (AS) and high-functioning autism (HFA) share, with those who have more severe autism, deficits in social communication and interaction, sensory and motor functioning, whilst not experiencing the significant language impairment that also characterises severe autism.

However, language is not normal in AS and HFA and the few studies that have examined language function in these cases have reported several disturbances, including difficulties in selecting congruent humorous endings to jokes (Emerich et al., 2003), disturbed narrative skills (Losh and Capps, 2003) and difficulties in arranging sentences coherently and using context to make global inferences (Jolliffe and Baron-Cohen, 2000).

1.1.1. MECHANISM AND CAUSES

The set of signs and symptoms described above seems to suggest an overall impairment of brain function in people with ASC. In attempting to explain the wide range of features that characterise ASC, several models, both functional and anatomical, have been proposed as underlying mechanisms for this generalized disruption in neural performance.

Regarding anatomy post-mortem investigations have found evidence of abnormalities in cortical cytoarchitecture (Casanova and Trippe, 2009, Oblak et al., 2011) and neuronal migration (Korkmaz et al., 2006, Wegiel et al., 2010) in people with ASC. Increased brain volume in early stages of brain development is one of the most often reported findings of in vivo imaging studies in children with ASC (Hardan et al., 2001, Hazlett et al., 2005, Ben Bashat et al., 2007) and it is hypothesized that an overgrowth in white matter may be related with the atypical cytoarchitecture and neuronal migration patterns found in people with ASC

(Courchesne et al., 2005). Other imaging studies of brain structure in adults and children with ASC have found evidence of anatomical abnormalities in the size of specific brain structures such as the corpus callosum (Egaas et al., 1995, Piven et al., 1997) and cerebellum (Scott et al., 2009, Hodge et al., 2010).

Another common finding in brain imaging studies of ASC is altered cortical thickness. However, the direction and location of these changes is not always agreed on, with some studies reporting an increase in total brain cortical thickness in ASC groups, specifically in the temporal lobes (Hardan et al., 2006), and others a decrease in cortical thickness in specific brain regions, namely the right inferior orbital prefrontal cortex, left superior temporal sulcus and left occipito-temporal gyrus (Chung et al., 2005). Two other studies (Hardan et al., 2004, Jou et al., 2010) have also reported patterns of increased cortical gyrification in the frontal lobe of people with ASC, when compared to neurotypical controls.

A correlation between the anatomical abnormalities just described and atypical brain functioning in people with ASC is yet to be established. However, some studies suggest that these structural abnormalities may be reflected in atypical patterns of functional connectivity between neural networks in the autistic brain (Just et al., 2007, Guye et al., 2010). The connectivity model is one of the commonly cited explanatory models of atypical brain functioning in ASC. Since it was introduced by Belmonte et al. (2004b) this model has been investigated and supported by numerous publications (Courchesne and Pierce, 2005b, Just et al., 2007, Monk et al., 2009, Barttfeld et al., 2011, Wass, 2011). Atypical neural connectivity between neural networks leading to disrupted temporal integration of information has also been investigated as an explanatory model for ASC (Brock et al., 2002, Rippon et al., 2007).

The wide range of features and severity of symptoms, along with its high heritability index and high prevalence of co-morbidities with genetic syndromes, makes it likely that the underlying cause for ASC is of genetic nature. The variability of the range and severity of symptoms between individuals with ASC, along with evidence from genetic studies, tells us that ASC is a complex genetic disorder, not caused by a single mutation in a single gene, but by a wide variety of mutations in different sections of the genome (Muhle et al., 2004, Abrahams and Geschwind, 2008). In addition to this, evidence from genetic studies indicates that different atypical genotypes will give rise to different behavioural phenotypes in ASC (Abrahams and Geschwind, 2008). Also of interest is the fact that some studies have found that some genetic mutations thought to be involved in ASC are also involved with other neuropsychiatric

disorders known to occur with increased prevalence in individuals with ASC, such as schizophrenia (Burbach and van der Zwaag, 2009, Carroll and Owen, 2009) and bipolar disorder (Carroll and Owen, 2009). Environmental factors such as toxic exposure (Adams et al., 2007) or prenatal exposure to maternal infection (Atladdottir et al., 2010, Landrigan, 2010) have also been reported as possible causes for genetic mutations thought to be involved in ASC.

1.2. MAGNETIC RESONANCE IMAGING

Magnetic resonance imaging (MRI) is a medical imaging technique used to acquire high-resolution images of a certain part of the body. This technique is noninvasive and does not resort to ionizing radiation for image acquisition. Instead, it uses high strength electromagnetic fields to interfere with the magnetic moments of subatomic particles within the body. Different tissues have different magnetic properties, detected by the MRI scanner to form the final image. This section will cover the physical principles behind MRI image acquisition and reconstruction.

1.2.1. PHYSICAL PRINCIPLES

Approximately 75% of the human body is made of water. Protons are elementary particles that are part of water molecules, and are therefore abundant in the human body. Like other charged elementary particles, protons have a characteristic magnetic moment. In the MRI scanner, the main magnetic field \vec{B}_0 causes the protons' magnetic moments to align either parallel or anti-parallel to \vec{B}_0 (Figure 1.1a). These two states have slightly different energies, with the parallel state having lower energy than the anti-parallel state. For this reason, there is a slight excess of protons in the parallel state, and the sum of all the protons' magnetic moments generates the net magnetization, \vec{M}_0 , which has the same direction as the main magnetic field (Figure 1.1b).

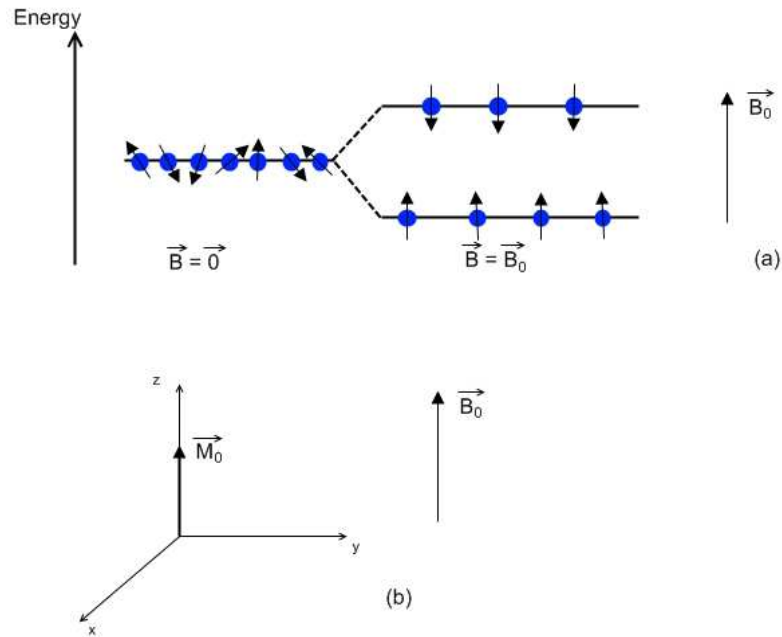


Figure 1.1 – The protons’ magnetic moments align parallel or anti-parallel in the presence of an external field (a) and differences in energy states generate a positive net magnetization, in the same direction as the main field (b).

Due to quantum mechanics laws, the alignment between the protons’ magnetic moments and the external field is not perfect. For this reason, the magnetic moments will precess around the main field’s axis (conventionally the z axis) at a frequency that is dependent on the strength of the magnetic field. This is called the Larmor frequency, and it is given by $\omega_0 = \gamma B_0$, where γ is the gyromagnetic ratio ($\gamma = 2.7 \times 10^8 \text{ rad.s}^{-1}.\text{T}^{-1}$) and B_0 the strength of the main field, in Tesla. This is the protons’ characteristic frequency, and so the protons will only be affected by electromagnetic waves with the Larmor frequency – this is called the resonance condition.

The net magnetization strength is very small compared to the strength of the main field ($\frac{M_0}{B_0} \sim 10^{-6}$), and therefore it is very hard to measure the longitudinal net magnetization. However, by applying a radiofrequency (RF) pulse in the Larmor frequency, it is possible to flip the net magnetization, by an angle α , called the flip angle. What the RF pulse does is to create a magnetic field, \vec{B}_1 , perpendicular to \vec{B}_0 , and oscillating at the Larmor frequency around the z axis. The flip angle is given by $\alpha = \gamma B_1 \tau$, where B_1 is the strength of the RF magnetic field and τ is the duration of the RF pulse (Figure 1.2).

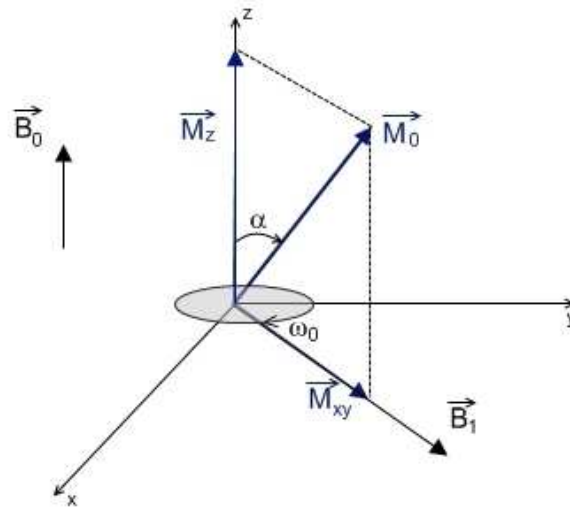


Figure 1.2 – When an RF pulse is applied, the net magnetization \vec{M}_0 is flipped by an angle α .

Since the magnetization vector \vec{M}_0 and the RF magnetic pulse \vec{B}_1 are precessing around the vertical z axis at the Larmor frequency, it is easier to consider them in a rotating frame of reference. In a frame $x'y'z'$ rotating around the $z' \equiv z$ axis at the Larmor frequency, \vec{M}_0 and \vec{B}_1 will appear to be stationary (Figure 1.3). If a 90° RF pulse is applied, the flip angle equals 90° . This means that the magnetization vector \vec{M}_0 will be in the transverse $x'y'$ plane, so the longitudinal component of the magnetization will be zero, $M_z = 0$. On the other hand, the transverse magnetization will be maximal, $M_{xy} = M_0$ (Figure 1.4a).

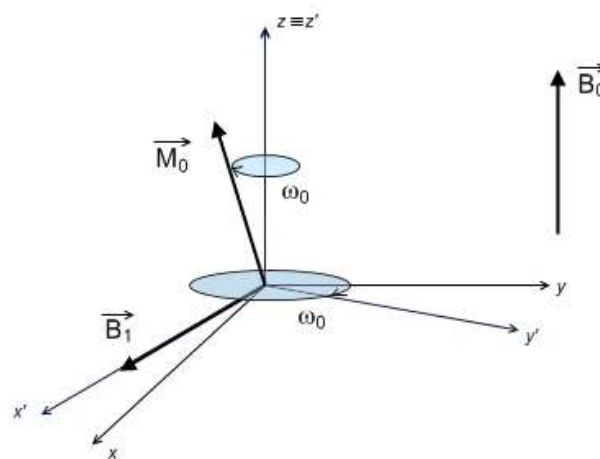


Figure 1.3 – The rotating frame of reference, rotating at the Larmor frequency; the RF magnetic pulse \vec{B}_1 and magnetization vector \vec{M}_0 will appear to be stationary.

As mentioned previously, the net magnetization is the result of the sum of the magnetic moments of all the protons. The magnetic moment of a proton precesses around the axis of the main magnetic field \vec{B}_0 at the Larmor frequency, which depends on the main magnetic field's strength. However, the protons interact with each other, and are influenced by the magnetic moments of neighbouring protons, which means that each proton experiences a magnetic field that is slightly higher or lower than that of the main magnetic field. Therefore, each proton will precess at a frequency slightly higher or lower than the Larmor frequency. After a 90° RF pulse, this interaction between protons will cause them to become out of phase with each other, and the transverse magnetization will sum up to zero. This dephasing is an exponential decay process known as spin-spin relaxation (Figure 1.4 sequence).

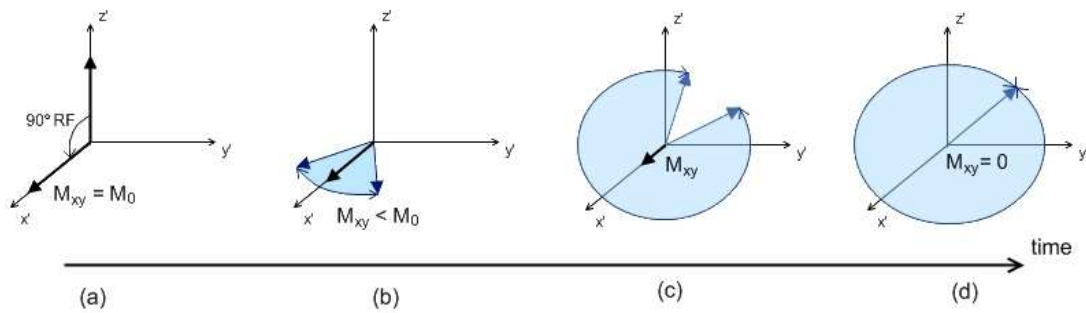


Figure 1.4 – Transverse magnetization decay, due to spin-spin interactions.

The decay of the strength of the transverse magnetization due to spin-spin relaxation is given by $M_{xy} = M_0 e^{-t/T_2}$, where t is time after the initial RF pulse, and T_2 is the spin-spin relaxation time, defined as the time the transverse magnetization signal takes to reach 37% of its original value (Figure 1.5). However, due to various factor including the presence of the patient inside the scanner, the homogeneity of the main field is affected. This leads to an increase in local inhomogeneities in the main field, which in turn accelerates the dephasing of the protons' magnetic moments and the decay of transverse magnetization. Taking into account spin-spin relaxation and the inhomogeneity of the main field, the decay of strength of the transverse magnetization is given by $M_{xy} = M_0 e^{-t/T_2^*}$, where T_2^* is a composite relaxation time that includes T_2 and the decay caused by local inhomogeneities in the main field.

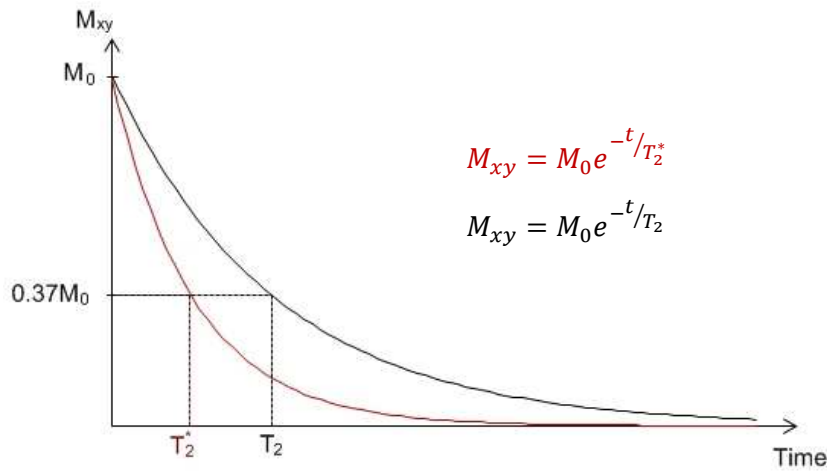


Figure 1.5 – Decay of transverse magnetization M_{xy} due to spin-spin interactions and field inhomogeneities.

Simultaneous to spin-spin decay, after the RF pulse is turned off, the protons' magnetic moments tend to go back to their equilibrium position, aligned with the main magnetic field \vec{B}_0 (Figure 1.6a). This process occurs through the loss of energy from the protons to the surrounding tissues, or lattice, and is therefore called spin-lattice relaxation. In spin-lattice relaxation, there is a recovery of the longitudinal magnetization given by

$M_z = M_0 (1 - e^{-t/T_1})$, where T_1 is the spin-lattice relaxation time, defined as the time it takes for the longitudinal magnetization to recover 63% of its original value (Figure 1.6b).

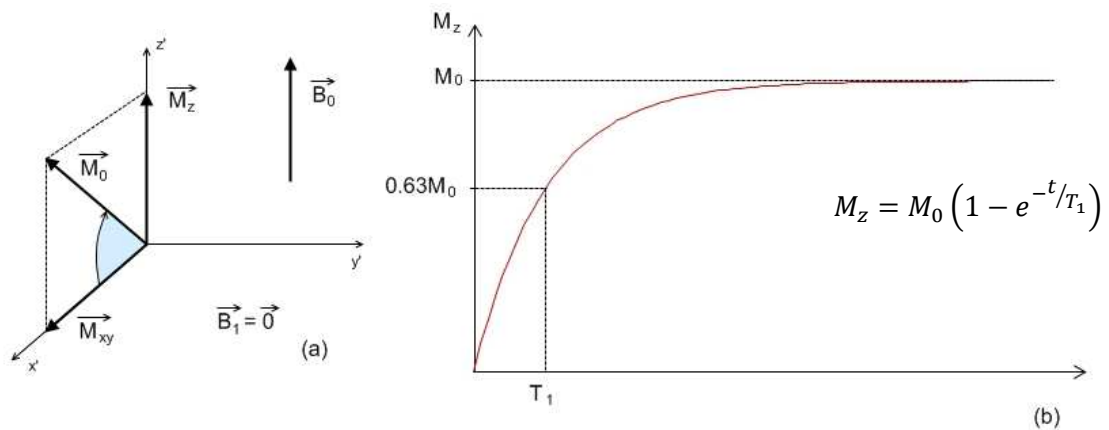


Figure 1.6 – Recovery of longitudinal magnetization M_z due to spin-lattice interactions.

Despite the 10^{-6} ratio between net magnetization and main field strength, modern MRI scanners are capable of detecting changes in transverse magnetization and measuring relaxation times T_1 , T_2 and T_2^* by having coils placed orthogonally to the main coil. Due to the fact that different tissues have different molecular compositions, each tissue has its own magnetic properties and consequently its own characteristic relaxation times, which are the basis for image contrast in MRI. T_1 -weighted images for example, have excellent contrast and are commonly used in anatomical studies. In these images fluids appear dark, water based tissues are mid-gray, and fat based tissues are very bright (Figure 1.7a). On the other hand, in T_2 -weighted images, fluids are very bright and water and fat based tissues are mid-gray. For this reason, T_2 -weighted images are commonly used for pathological studies where abnormal collections of fluid appear bright against the darker normal tissue (Figure 1.7b).

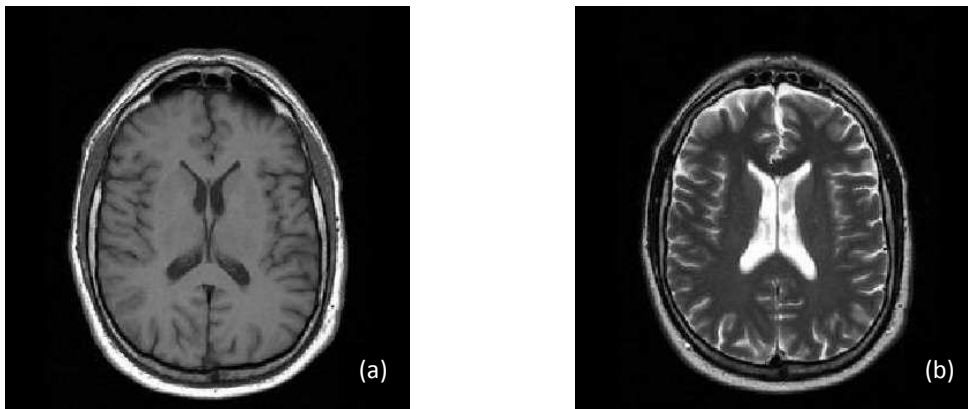


Figure 1.7 – (a) T1-weighted image of the brain, showing cerebrospinal fluid in dark, brain matter in mid-gray and adipose (fat) tissue in bright tones; (b) T2-weighted image of the brain showing cerebrospinal fluid as very bright and brain and other types of tissue in mid-gray. From www.mr-tip.com.

1.2.2. ECHOES

In MRI repetitive RF pulses are used to generate echoes of magnetization, whose intensity depends on the relaxation times T_2 and T_2^* . Different sequences of RF pulses and gradients generate different types of echoes. There are two main types of echo generating mechanisms used in modern MRI scanners: gradient echo and spin echo.

Gradient echo is generated by an initial RF pulse with a flip angle usually smaller than 90° , followed by a negative gradient in the magnetic field. Spin-spin relaxation and inhomogeneities in the main field cause the protons' magnetic moments to dephase, leading to a decay in transverse magnetization. A positive gradient in the magnetic field is then applied, compensating for the negative gradient previously described. This will cause the

protons' magnetic moments to rephase, up to the point where all the protons' magnetic moments are in phase, and transverse magnetization is maximal (Figure 1.8). This is the gradient echo, with intensity given by

$$S_{GE} = S_0 \exp\left(-\frac{TE}{T_2^*}\right) \quad (1.1)$$

Where S_0 is the signal intensity (transverse magnetization) after the initial RF pulse, T_2^* is the spin-spin and field inhomogeneity relaxation time and TE is the gradient echo time, defined as the time it takes for the echo to be formed after the initial RF pulse.

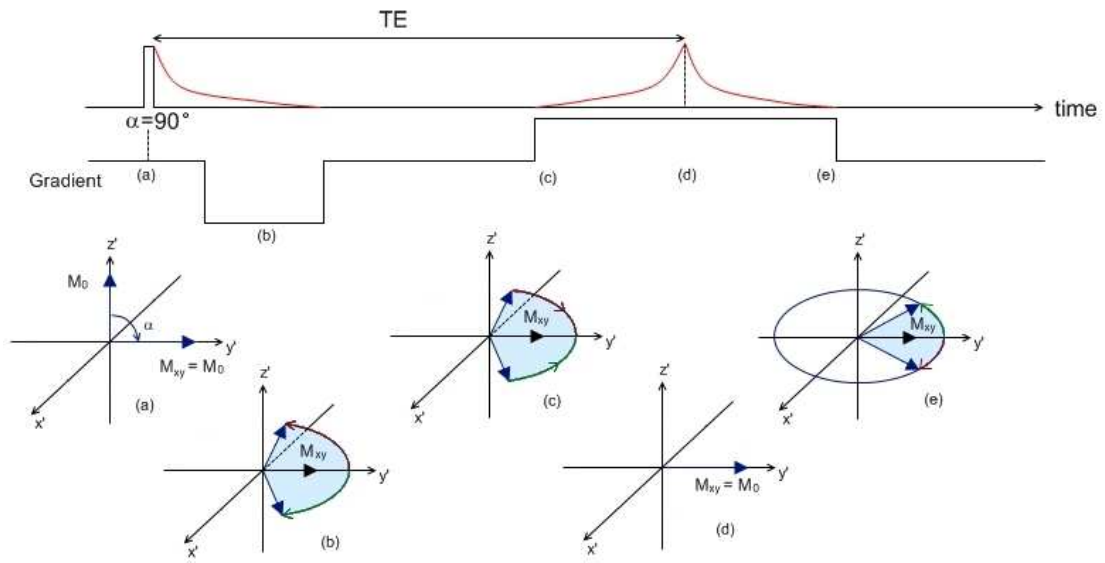


Figure 1.8 – Gradient echo sequence: the initial RF pulse is applied (a), and the negative gradient accelerates the magnetic moments dephasing and the decay of transverse magnetization (b); when the positive gradient is applied the magnetic moments begin to rephase (c), and there is a moment when all the magnetic moments are in phase again, and an echo is formed (d); the magnetic moments continue their precession around the z axis, and dephase again due to spin-spin interactions (e).

In the spin echo sequence, an initial 90° RF pulse is applied. The protons' magnetic moments start to dephase and there is decay in the transverse magnetization and signal intensity. A 180° RF pulse is then applied. This will cause the transverse magnetization to flip through 180° about the y' axis, reversing the phase angles of the protons' magnetic moments. The precession frequency of the magnetic moments will not change, and the protons will carry on experiencing the same field inhomogeneities as before. This means that after a period of time equivalent to the time gap between the 90° and the 180° RF pulses, the protons' magnetic moments will rephase and transverse magnetization will be maximal (Figure 1.9). This is called the spin echo, and its intensity is given by

$$S_{SE} = S_0 \exp\left(-\frac{TE}{T_2}\right) \quad (1.2)$$

Where S_0 is the signal intensity of the transverse magnetization after the initial RF pulse, T_2 is the spin-spin relaxation time and TE is the spin echo time, defined as the time it takes for the echo to be formed after the initial 90° RF pulse.

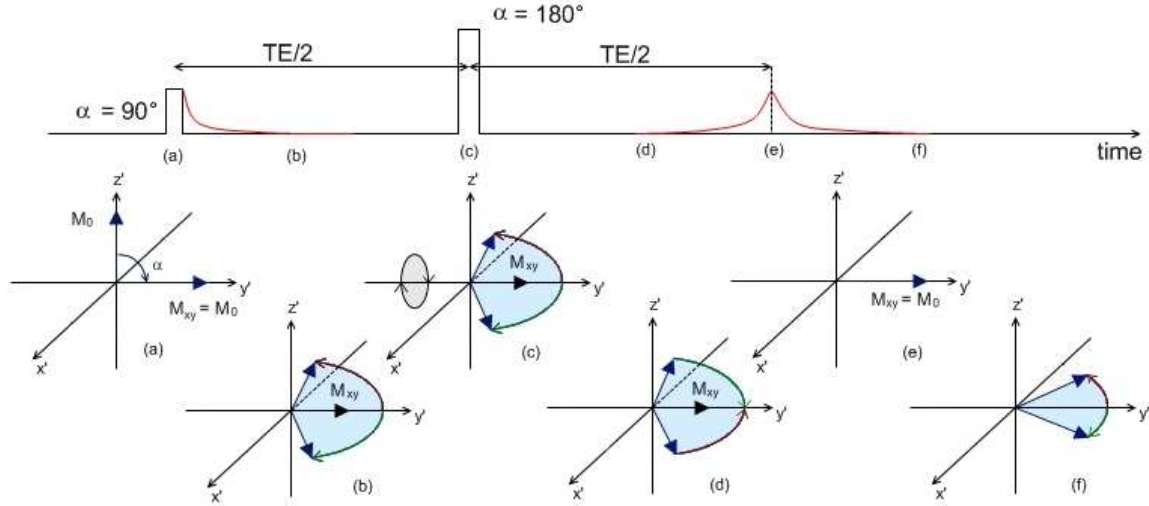


Figure 1.9 - Spin echo sequence: the initial 90° RF pulse is applied (a), the magnetic moments start to dephase and there is a decay of transverse magnetization (b); an 180° RF pulse is applied (c) which causes the magnetic moments to begin to rephase (d), and there is a moment when all the magnetic moments are in phase again, and an echo is formed (e); the magnetic moments continue their precession around the z axis, and dephase again due to spin-spin interactions (f).

1.2.3. SPATIAL ENCODING

In MRI relaxation and echo times can provide information about the average composition of a given volume. In the human body a volume can be for example the head, with the bone, brain, muscle, fat and cerebrospinal fluid (CSF) as the different types of tissue, each with characteristic relaxation times. Image reconstruction of the tissues within a volume requires a spatial encoding algorithm applied through 3-dimensional magnetic field gradients (variation of strength in the magnetic field with position):

- 1- A gradient in the z axis direction (same direction as the main magnetic field \vec{B}_0) is used for slice selection – G_{ss} ; with precessional frequency being directly proportional to field strength, this gradient will cause the protons' magnetic moment precessional frequency to vary along the main field axis; only magnetic moments precessing at the Larmor frequency will be affected by the RF pulse, and so this gradient will limit the

scope of influence of the RF pulse to a single slice orthogonal to the main field axis (Figure 1.10a)

- 2- A gradient applied for a limited amount of time, orthogonally to the main field axis, is used for phase encoding – G_{pe} ; this gradient causes a variation in the precessional frequency of the protons' magnetic moments along the G_{pe} axis, causing them to dephase; when the gradient is turned off, the magnetic moments will go back to precessing at Larmor frequency, but the difference in phase induced by the phase encoding gradient will be maintained, and magnetic moments on different coordinates along the G_{pe} axis will have different phases (Figure 1.10b)
- 3- A gradient applied orthogonally to the slice selection and phase encoding gradients is used for frequency encoding – G_{fe} ; this gradient will cause a variation in the protons magnetic moments' precessional frequencies along the G_{fe} axis; the phase and frequency encoding gradients ensure that the protons' magnetic moments have a characteristic phase and precessional frequency, according to their position in the selected slice; due to these differences in phase and frequency, the echo times will vary depending on the spatial location of the signal source, allowing accurate image reconstruction (Figure 1.10c)

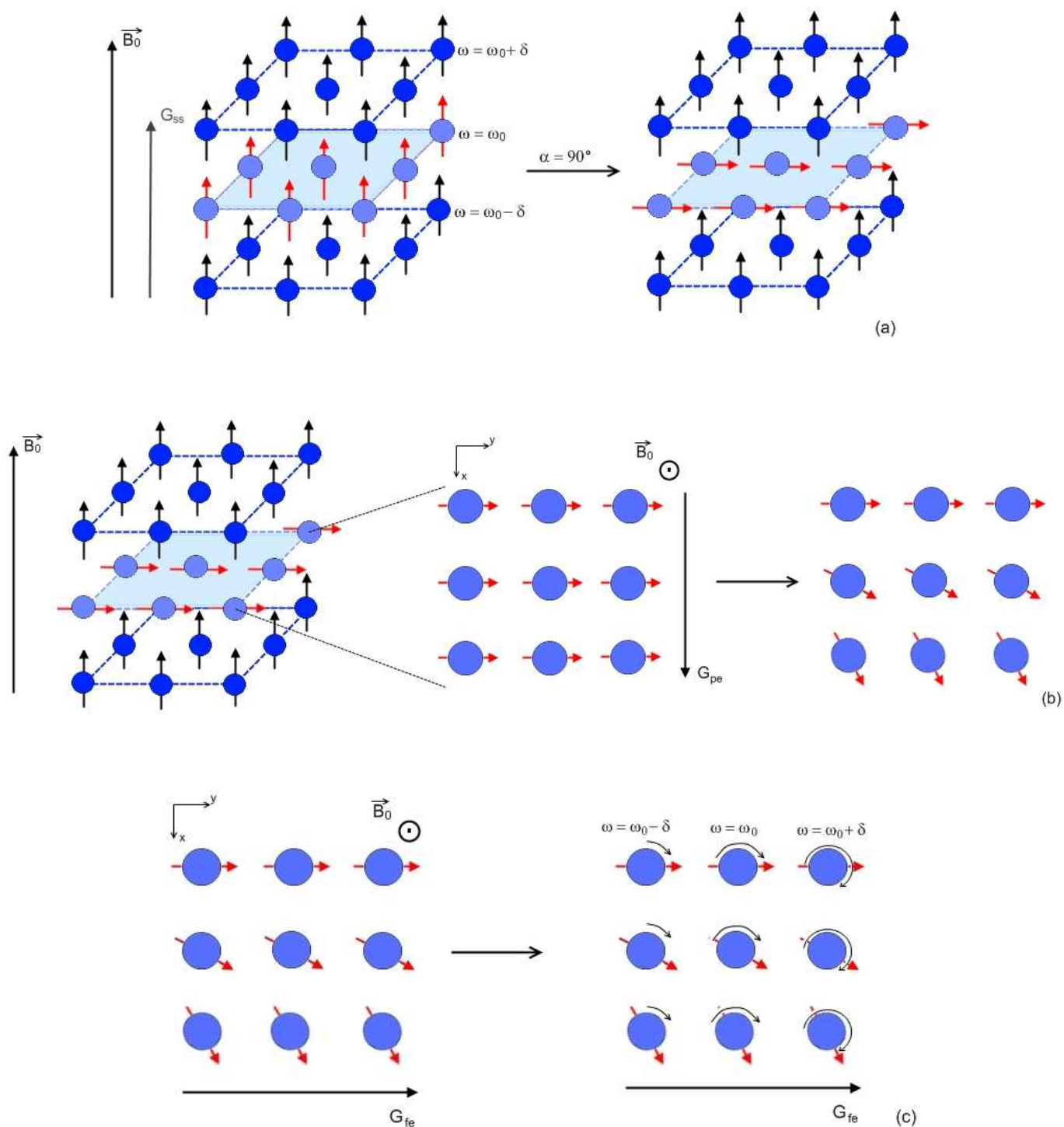


Figure 1.10 – Gradients in the x, y and z axis are used for spatial encoding; after a slice selective gradient is applied in the same direction as the main magnetic field, a position in the z axis is determined (a); a phase encoding gradient applied orthogonally to the main field axis dephases the magnetic moments according to their position along the phase encoding gradient axis (b); a frequency encoding gradient applied orthogonally to the slice selective and phase encoding gradients makes the precessional frequency vary with the position along the frequency encoding gradient axis (c); at this point each magnetic moment in the selected slice has its own characteristic phase and precessional frequency.

Different types of images can be generated by varying the timings and sequences of these spatial encoding gradients. For most gradient sequences, the frequency encoding gradient is applied last, during the signal reading stage, and for this reason it is usually called the 'readout gradient' (Figure 1.11).

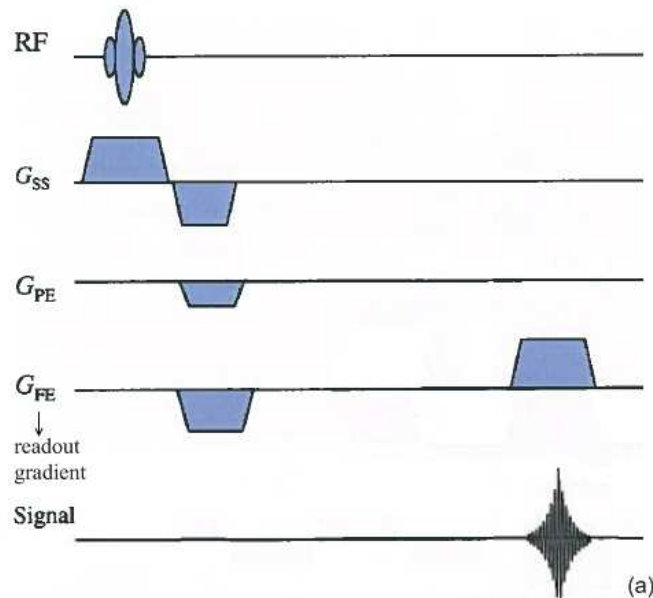


Figure 1.11 – Spin-echo (SE) imaging sequence. The frequency encoding gradient is applied during the signal reading stage, and is therefore called 'readout gradient'. Adapted from McRobbie (2007).

Each gradient sequence has their own advantages over others, concerning acquisition time, image resolution and vulnerability to artefacts. For example the gradient echo based echo planar imaging (GE-EPI) (Figure 1.12a) is a fast acquisition sequence, but has the disadvantage of providing low spatial resolution images that are prone to artefacts (Figure 1.12b). This is because in this type of sequence each spatial frequency image space (k-space) is covered in a single repetition time (the time interval between two consecutive RF pulses), limiting the amount of information that can be acquired and therefore limiting the resolution of the final image. Other sequences like the MPAGE (Magnetization Prepared Rapid Acquisition by Gradient Echo) can be used to provide high spatial resolution images, but have the disadvantage of longer acquisition times.

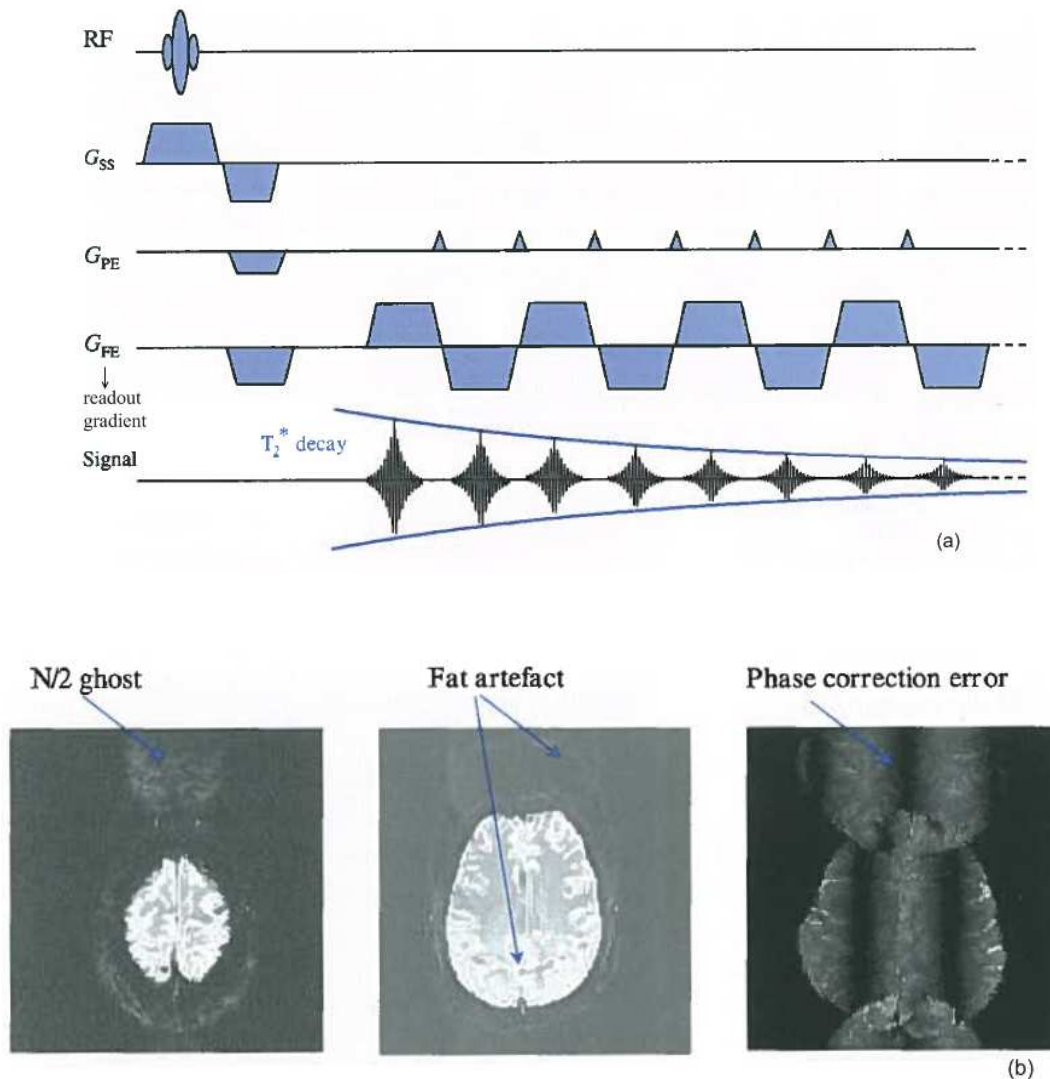


Figure 1.12 – Gradient echo based echo planar imaging (GE-EPI) sequence (a); this is a fast acquisition sequence, but it generates images of poor spatial resolution that are prone to artefacts (b). From McRobbie (2007).

1.2.4. FUNCTIONAL MRI

Functional MRI (fMRI) is used in brain imaging to detect activation of neural clusters or networks. It is based on the fact that neural activation is correlated to neurons' oxygen consumption, which causes an increase in the supply of fully oxygenated blood to the activated area, which will then have a higher concentration of oxygenated blood, compared to non-activated regions of the brain (Norris, 2006). This is called the Blood Oxygenation Level Dependent (BOLD) response (Figure 1.13).

One of the first studies to investigate the sensitivity of magnetic resonance contrasts to variations in blood oxygenation dates back to 1990 (Ogawa et al., 1990a). In this study Ogawa and colleagues (1990a), resorting to high-field *in vivo* MRI imaging of rodents' brains, showed

that MRI contrasts were sensitive to changes in blood oxygenation induced by anaesthetics, insulin-induced hypoglycemia and inhalation of gas mixtures that alter blood flow.

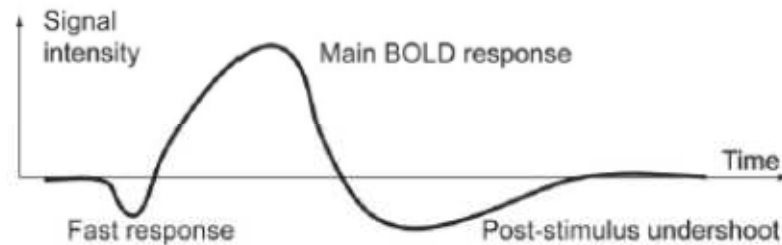


Figure 1.13 – Blood Oxygen Level Dependent (BOLD) response to neural activity.
From Norris et al. (2006).

The sensitivity of MRI to blood oxygen levels is due to the fact that haemoglobin, a protein present in the red blood cells, can be bound to oxygen molecules (oxyhaemoglobin) or not (deoxyhaemoglobin). Oxygenated blood is characterised by the presence of high levels of oxyhaemoglobin, a diamagnetic protein which is not influenced by the presence of an external magnetic field. Deoxyhaemoglobin on the other hand is a paramagnetic protein, which responds to the presence of an external field. For this reason deoxygenated blood will cause a disturbance in local field homogeneity, affecting the T_2^* relaxation time - the protons' magnetic moments, subject to stronger field inhomogeneities, will dephase faster, leading to a faster decay of transverse magnetization and a shorter T_2^* (Thulborn et al., 1982, Ogawa et al., 1990b). This difference in the relaxation time T_2^* between oxygenated and deoxygenated blood can be detected by the MRI scanner.

Echo planar imaging (EPI) sequences are usually chosen for fMRI protocols for their fast acquisition time and sensitivity to variations in magnetic susceptibility (Figure 1.12a). However, as previously described, the compromise for this is a lower spatial resolution and a higher level of artefacts (Figure 1.12b).

fMRI protocols usually include a functional paradigm that alternates between blocks or events of the activity of interest (e.g.: finger tapping, listening to specific auditory stimuli or solving simple cognitive tasks) and periods of contrasting activity or rest (baseline). In a block design paradigm, two or more conditions are alternated in blocks. Each block will have a certain duration and within each block only one condition is presented. In an event-related design paradigm, all conditions are presented in the same block. Each block will thus contain mixed

events of different types. The final fMRI images will highlight areas in the brain for which the difference in signal intensity between active and rest conditions is statistically significant.

However, to get to these final images, a series of pre-processing steps is necessary. The first step consists of realigning and coregistering all the images to each other. This will reduce the chance of motion related artifacts in the final image. The second step consists of the normalization of the images to a standard common space, usually defined by some ideal model or image templates. This step is particularly important for multi-subject studies, since it allows for inter-subject comparison and averaging. The third step consists of image smoothing, usually using a Gaussian kernel, done to improve the signal to noise ratio and to reduce artefacts caused by residual differences in functional and cortical anatomy during inter-subject averaging. Finally, the statistics are calculated, by subtracting the images acquired during the baseline periods to the ones acquired during the active periods, and looking for significant differences in signal intensity.

A general linear model is usually employed defined in matrix notation by:

$$Y = X\beta + \varepsilon \quad (1.3)$$

Where Y is a matrix representing the acquired images, X is a design matrix that encapsulates the experimental model and contains all covariates that might influence the signal, β are explanatory variables and ε the error associated with the estimation. Y and X are known *a priori*, so the statistical test consists in estimating the parameters β that minimize errors ε . Statistical inference entails testing null hypotheses ' $c\beta = 0$ ' where ' $c\beta$ ' is a contrast or a linear function of parameters that reflects the relevant question (e.g. "Is this brain region more activated by task than rest?").

fMRI is broadly used in research, in the investigation of cognitive processes such as face processing (Sato et al., 2011) and semantic integration (Visser and Lambon Ralph, 2011). It is also used in the study of neuropsychiatric conditions such as ASC (Knaus et al., 2008, Koshino et al., 2008), schizophrenia (Anticevic et al., 2011), depression (Peng et al., 2011) and bipolar disorder (Chen et al., 2011), amongst others. However, fMRI is not the only modality that can be used to investigate brain function. Positron emission tomography (PET) can also be used to assess brain function (Corbetta et al., 1993), but it requires the use of ionizing radiation. Electroencephalography (EEG) and magnetoencephalography (MEG) are also used broadly in research of cognitive function in health and disease (Deffke et al., 2007, Ring et al., 2007).

Comparative to EEG/MEG, fMRI has the advantage of having a much higher spatial resolution, but the disadvantage of a much lower temporal resolution (a few seconds in fMRI versus milliseconds in EEG/MEG). This is due to the fact that fMRI is based on the haemodynamic response to neural activity, which can be lagged behind the actual firing of the neurons up to as much as 6 seconds (McRobbie, 2007). On the other hand, although a relationship between neural activity and the BOLD effect has been demonstrated by previous research (Logothetis, 2002), the exact physiological mechanisms behind the BOLD effect are still not well known (Norris, 2006, Haller and Bartsch, 2009).

1.3. ELECTROENCEPHALOGRAPHY

Electroencephalography (EEG) is a method of measuring the electrical activity of the brain, using a set of electrodes placed on a person's scalp. To better understand the nature of EEG, a few basic notions of brain anatomy and physiology are required.

1.3.1. BRAIN ANATOMY AND PHYSIOLOGY

The brain is composed of the cerebrum, the cerebellum and the brain stem. The cerebrum is divided into two cerebral hemispheres, joined by the corpus callosum. Assisted by the cerebellum, the cerebrum is responsible for all voluntary actions of the body and motor control, as well as sensory perception and integration and higher cognitive functions. The surface of the cerebrum is covered by a thin layer (2 to 3 mm) of neuronal tissue often referred to as gray matter or cerebral cortex. Underlying it is a layer of myelinated axonal fibers often referred to as white matter.

Additionally to this anatomical mapping, the cerebral cortex is functionally segregated into four separate lobes (Figure 1.14):

- *Parietal lobe* – involved in the perception and processing of sensory information;
- *Frontal lobe* – involved in working memory, decision making and planning;
- *Occipital lobe* – involved in the perception and processing of visual information;
- *Temporal lobe* – involved in the perception and processing of auditory information, as well as in language processing

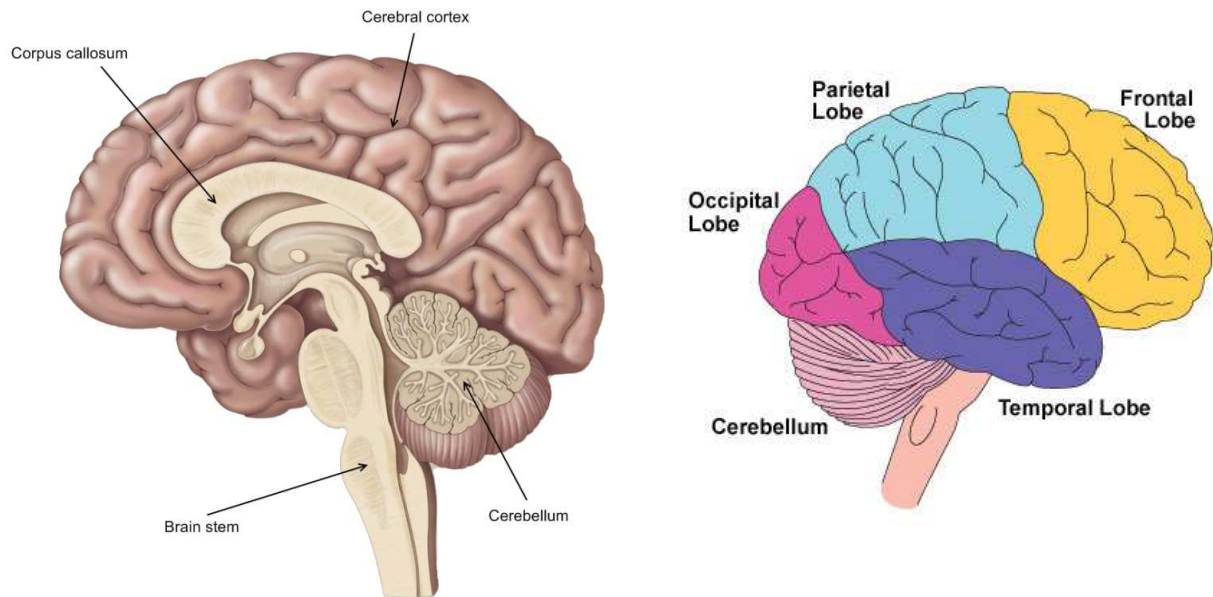


Figure 1.14 – Diagram of brain anatomy showing the corpus callosum, cerebral cortex, brain stem and cerebellum, as well as the functionally segregated lobes. From McKinley and O’Loughlin (2006) and www.braininjury.com/symptoms.shtml.

The cerebral cortex or cortical surface is a highly convoluted surface which has an average thickness of 2.5 mm in humans and a neuron density of approximately 10 000 neurons/mm² (Sholl, 1956). Neurons are electrically excitable cells that process and transmit information through the form of electrical potentials. Due to an ionic imbalance between the inside and outside of the cell, neurons have a resting potential of approximately -70 mV, and it is through the disturbance of this resting potential that an electrical signal is generated (or inhibited) (Figure 1.15).

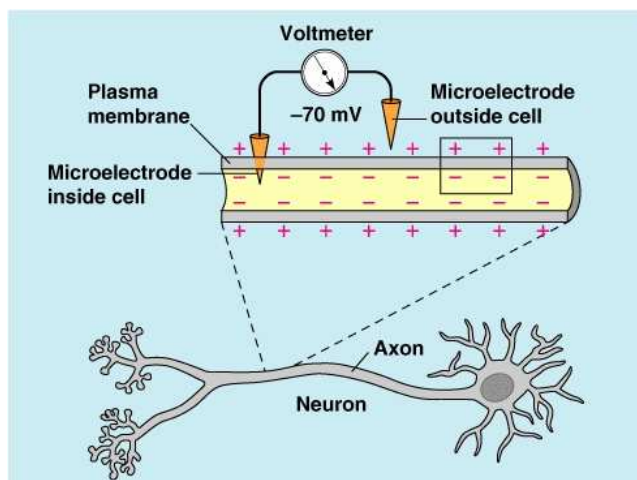


Figure 1.15 – Diagram of a neuron’s resting potential. From Marieb (2001).

In terms of structure neurons are formed by dendrites, the soma or cell body, an axon and its respective terminals. In a simplified view, one can think of a neuron’s axon terminals as being

connected to another neuron's dendrites. When a neuron fires, the electrical signal is propagated along its axon, and when it reaches the axon's terminals, neurotransmitters are released into the synapse and to the dendrites of the next neuron (Figure 1.16).

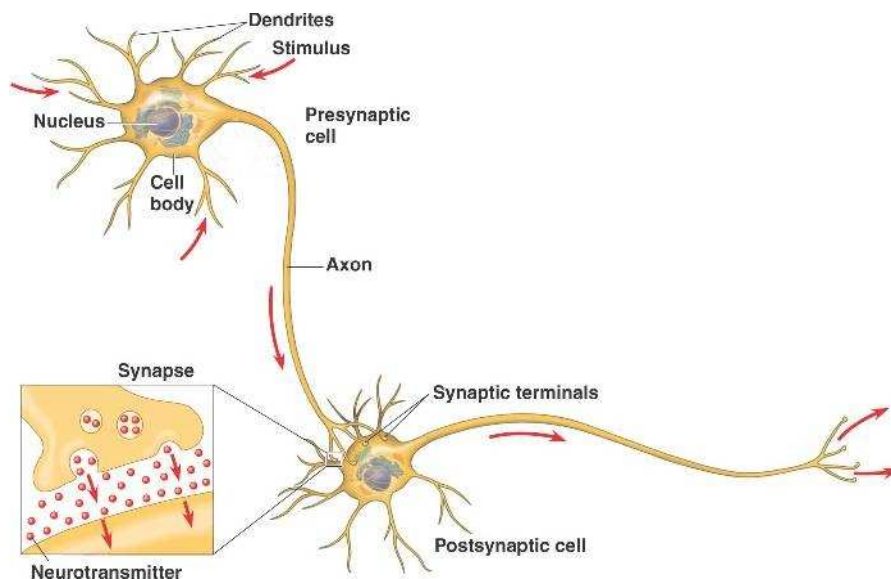


Figure 1.16 – Neuron's structure and stimulus propagation diagram. Adapted from bio1152.nicerweb.com/Locked/media/ch48/neuron.html.

These neurotransmitters can have an excitatory or an inhibitory effect. If they have an excitatory effect, they will alter the chemical properties of the receptor's membrane, causing an ionic flow through the cell membrane and increasing the receiving neuron's electric potential, leading to the generation of an action potential - an electric signal that propagates along the neuron, from the dendrites through the soma and the axon and into the next neuron. On the other hand, if the neurotransmitters have an inhibitory effect, they will cause a modification of the chemical properties of the receptor's membrane, leading to an ionic flow and a reduction of the receiving neuron's electrical potential, putting it in a state less likely to generate an action potential. However, in a more realistic model of the brain, each neuron receives inputs and sends outputs from and to hundreds of thousands of other neurons. All the excitatory and inhibitory inputs a neuron receives at a given time are averaged inside the soma and may or may not generate a new action potential. Information processing in neural networks is dependent not only on this intracellular averaging of the electric potential, but also on the firing frequency and fluctuations of firing frequency with time.

1.3.2. EEG RECORDING

When a neuron generates an action potential an electromagnetic field is generated, with the neuron acting as an electric dipole (Figure 1.17a). However, the action potentials are too transient to sum up to a measurable signal recorded from the scalp. Instead, it is believed that the EEG signal results from the aggregate of electromagnetic fields produced by excitatory and inhibitory postsynaptic potentials (Kutz, 2003). Additionally, only electric fields orthogonal to the electrode surface can be measured by the EEG electrodes. For this reason, only postsynaptic potentials generated by neurons that are perpendicular to the scalp surface can contribute to the EEG signal.

The EEG output will be a series of waveforms, or channels, each representing the electrical activity of the brain for a different location on the scalp. In a classical referential montage, each channel's waveform is obtained by subtracting the signal of a referential electrode from the signal of a scalp electrode (Figure 1.17b).

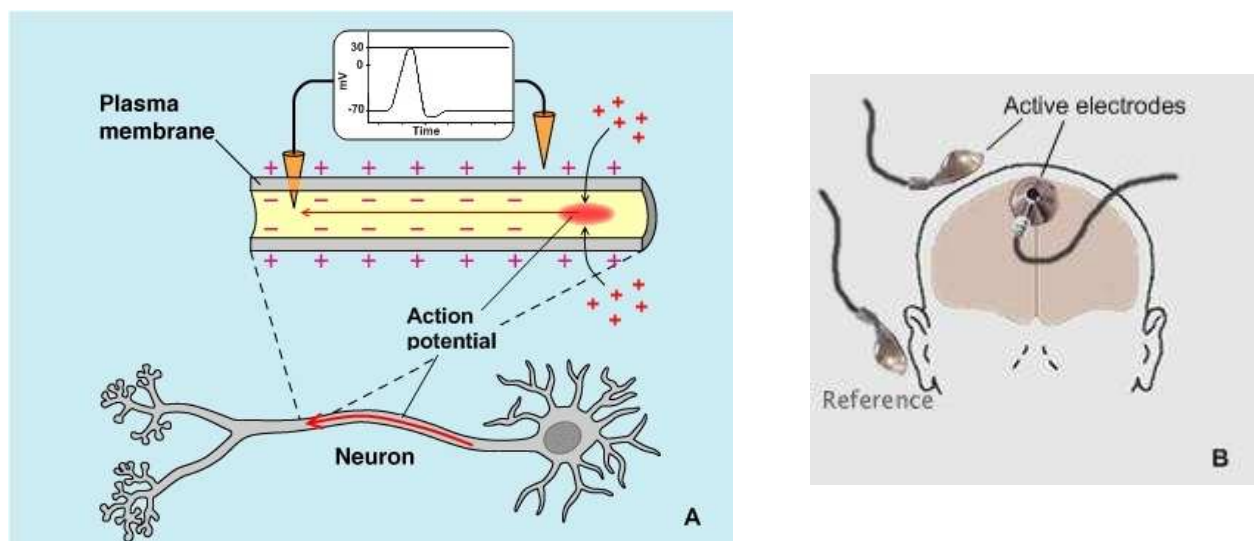


Figure 1.17 – Action potential being generated and propagated along the axon of a neuron (a) and a diagram illustrating a referential montage (b). Adapted from Marieb (2001) and www.brain-trainer.com/equipment/about_electrodes.html.

To guide the placement of the electrodes on the scalp, the International 10-20 system is usually used. This system is a globally recognized method for EEG scalp electrode location, where each electrode is named with a letter and a number. The letter (F, C, T, P or O) indicates the location on the scalp in terms of cortical region (Frontal, Central, Temporal, Parietal or Occipital, respectively) and the number defines hemisphere location – even numbers for

electrodes on the right hemisphere, odd numbers for left hemisphere locations. Electrodes on the midline are named with a 'z' instead of a number (e.g. 'Pz' for the midline electrode on the parietal region of the cortex) (Figure 1.18).

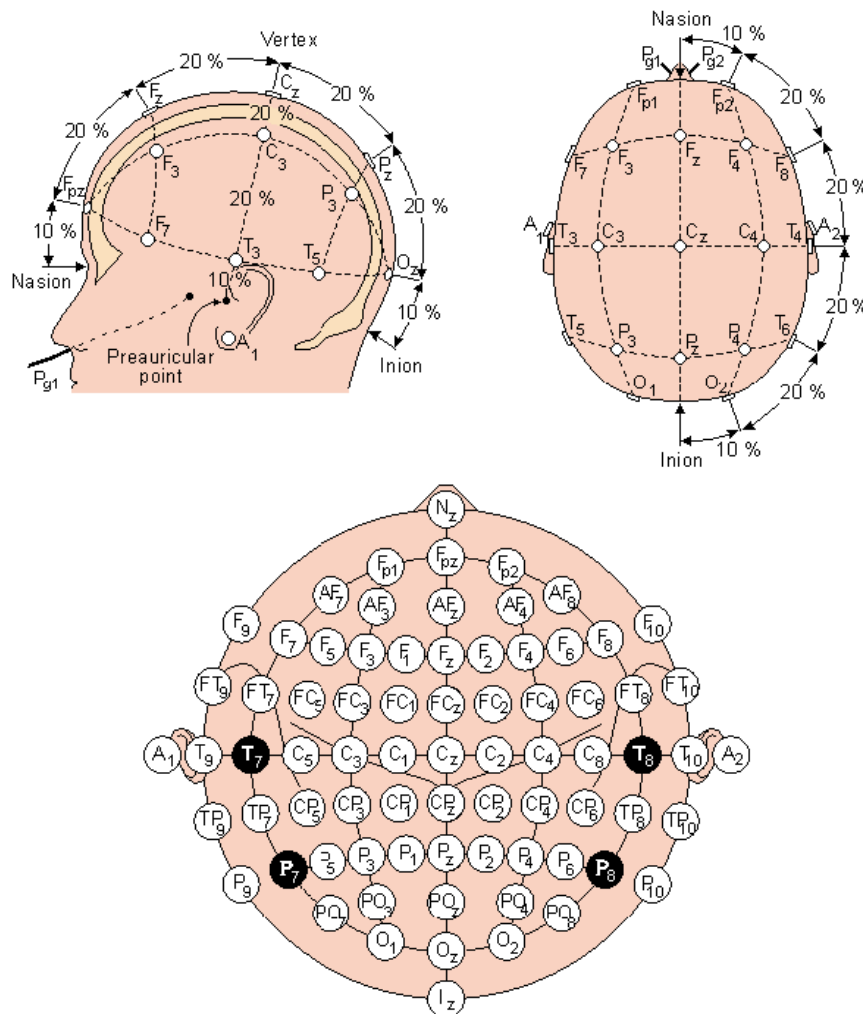


Figure 1.18 – Placement of electrodes on the scalp according to the International 10-20 system. From Sharbrough et al. (1991).

LIMITATIONS

Although EEG provides a method of measuring electrical activity in the brain with high temporal resolution, one of its major limitations is its poor spatial resolution. The electromagnetic fields generated by groups of neurons are influenced by differences in conductivity between the cortical surface, cerebrospinal fluid and skull, making source localization a difficult task – a given electrode will pick up not only the electrical signal from a set of neurons in the cortex directly underneath it, but also the signal from sets of neurons that are located further away from that electrode. Finding the underlying cortical sources of

activity through signals measured on the scalp is known as the inverse problem. Solutions for this problem usually assume a model of the source (the dipole model being the most common) and a model of the head. These models can be described in various ways, which means that there is usually more than one possible solution to the inverse problem. Anatomical and functional constraints, highly variable between individuals, are an additional difficulty to accurate head and source modeling, and consequently to solving the inverse problem (Cuffin, 1998, Michel et al., 2004).

Additional limitations of this method include the fact that EEG can only record signals originating in the cortical surface (and is therefore insensitive to deeper structures of the brain) and also its vulnerability to movement artifacts. The electrical signals generated by the neurons and captured by the scalp electrodes are very small in amplitude, and recording is often contaminated by muscle movements that generate electrical signals of higher amplitude, such as those originating from head or eye movement (such as blinks).

TYPICAL ACTIVITY

The electrical activity in an EEG measurement is usually characterized by rhythmic and transient activity. The rhythmic activity can be separated into five frequency bands:

- *Delta band (< 4 Hz)*: this frequency is characteristic of EEG recordings of babies or of sleeping adults;
- *Theta band (4 to 8 Hz)*: this frequency is often observed in EEG recordings of young children or in adults in a state of drowsiness or arousal;
- *Alpha (8 to 12 Hz)*: this frequency is observed in the EEG recordings of adults in an awake, relaxed but not drowsy state, with eyes closed;
- *Beta (13 to 30 Hz)*: this frequency is characteristic of alert or active concentration states;
- *Gamma (> 30 Hz)*: this frequency is present in EEG recordings taken during performance of complex sensory processing and working memory tasks; high frequency oscillations (> 100Hz) however, may be indicative of epilepsy (Zijlmans et al., 2011).

The presence of transient activity such as spikes and spindles is considered common in recordings of sleep states. However, if detected in recordings of awake subjects it can be an indicator of seizure activity.

1.3.3. SIGNAL ANALYSIS

The frequencies mentioned previously are well characterized in healthy individuals, for various states of consciousness (e.g. sleep, drowsiness and arousal). However, the natural rhythms recorded by EEG can be affected by pathology. For example slow waves (delta and theta), if present in awake adults, may be a sign of structural brain lesions or neuropsychiatric conditions such as schizophrenia, affective disorders and post-traumatic stress disorder (Rockstroh et al., 2007). Abnormal alpha rhythms can be observed in profoundly comatose states (Niedermeyer, 1997) and abnormal high frequency activity (beta and gamma) has been reported in EEG recordings of epileptic patients (Medvedev et al., 2011) and patients medicated with benzodiazepines (Claus et al., 2009). In many situations, visual inspection of an EEG recording by an experienced clinician is sufficient to determine a diagnosis. However, in some cases and particularly in research, analytic analysis of EEG data may be necessary.

FREQUENCY AND POWER ANALYSIS

The EEG signal is a complex waveform formed by the sum of periodic waves (e.g. sine waves) of different amplitudes and frequencies. To perform a frequency analysis of the EEG signal, it is necessary to separate the original signal into its several constituent frequencies. This is done through a Fourier transform, a mathematical operation that decomposes a function in time as a function of frequency. The Fourier transform can be defined by

$$F(k) = \int_{-\infty}^{+\infty} f(t) e^{-2\pi i k t} dt \quad (1.4)$$

Where $F(k)$ is the signal function in frequencies domain, and $f(t)$ the signal function in the time domain. The result of this transform can be represented by a power graph, where each frequency is represented in the x axis, and its relative or absolute power in the y axis (Figure 1.19). Different states of awareness (i.e.: alertness, drowsiness, sleep) and different pathologies generate variations in the power spectrum, which can help in the characterization of brain function in various conditions.

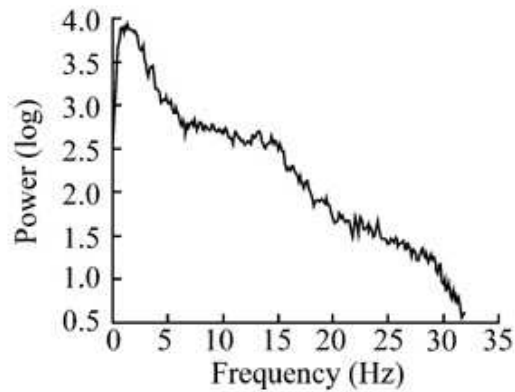


Figure 1.19 – Example of an EEG power graph.
From Feng (2003).

EVENT RELATED POTENTIALS

Power analysis of resting state EEG may provide information about the baseline activity of the brain, its characteristic frequencies and rhythm variations associated with states of sleep, drowsiness or arousal. However, to investigate brain functioning related to a specific task and cognitive process, event related potentials (ERPs) are often preferred. When performing a particular task, or when receiving a particular sensory input, there will be activation of a specific group or network of neurons. This will generate a characteristic waveform or potential in the EEG recording, within a determined onset time from the trigger stimulus – the ERP. However, amidst the background baseline activity, the ERP waveform cannot be detected. By repeating the trigger stimulus several times, and averaging the resulting waveforms within a temporally defined window around the stimuli, the background activity waveforms will sum up to zero, and the waveform of interest, the ERP, will remain, since it is time locked to the event (Figure 1.20).

When naming an ERP component, a letter is usually used to indicate polarity, followed by latency in milliseconds. The N400 component for example, will be a negative voltage deflection occurring at approximately 400 ms after stimulus onset, whilst the P100 will be a positive voltage deflection, occurring 100 ms post-stimulus.

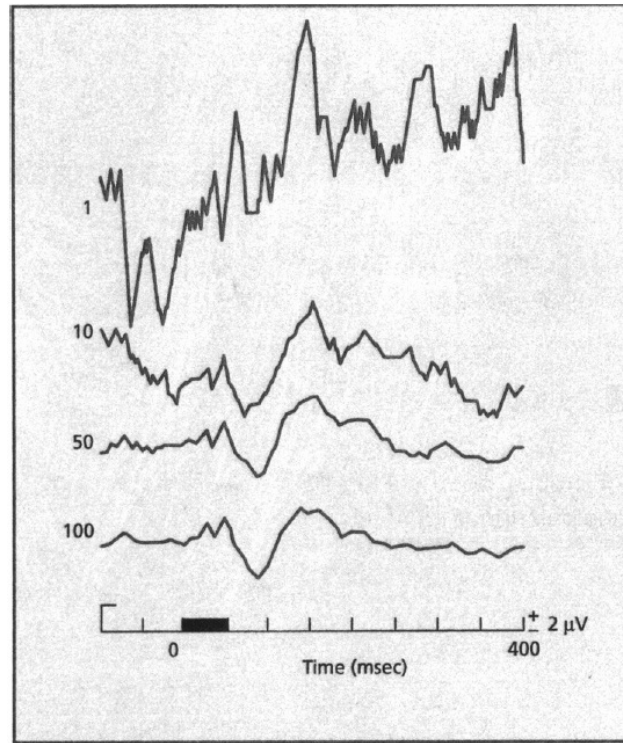


Figure 1.20 – Averaging procedure in EEG data to extract ERP waveform. This figure illustrates the resulting waveform after the averaging of 1, 10, 50 and 100 separate EEG recorded responses to a specific stimulus. Adapted from Sawyer (2011).

NON-LINEAR, COMPLEXITY AND CONNECTIVITY ANALYSIS OF THE EEG SIGNAL

Together with frequency and power analysis, ERP's provide useful information about brain function in normal and pathological brains. However, a better understanding of the neurophysiological mechanisms underlying higher brain functions can only be achieved by investigating properties underlying neural networks dynamics that fall under often used (and sometimes loosely defined) terms such as “non-linear” and “complexity” (Stam, 2005). In the last few decades, several novel mathematical concepts and analytical techniques have been introduced, capable of extracting new and meaningful information from sets of physiological data. Some examples include graph theory, synchronization likelihood measure (Stam, 2005) and multiscale entropy (MSE) (Costa et al., 2005).

In parallel, recent years have witnessed an ever-growing interest in measuring the extent to which different brain regions communicate and exchange information between each other. So called “connectivity analysis” techniques include correlation, classical coherence and wavelet transform coherence (WTC) (Lachaux et al., 2002, Pereda et al., 2005).

One of the main challenges of current neuroscience research is to combine different measures in order to obtain a richer picture of how the brain as a whole executes complex cognitive functions.

MULTISCALE ENTROPY

Physiological complexity, comprising the presence of non-random fluctuations over multiple time scales in the seemingly irregular dynamics of physiological outputs (Freeman, 1992, Glass L., 1992, Manor et al., 2010), is increasingly being recognized as contributing a novel descriptive approach to the investigation of typical and pathological developmental or degenerative states (Costa et al., 2002, 2005, Fallani et al., 2010, Ouyang et al., 2010). Whilst the interpretation of the meaning of changes in complexity varies according to the physiological parameters studied and the developmental or clinical condition being investigated, there is nevertheless increasing evidence that a variety of pathological processes are associated with atypical and often, but not always, reduced measures of physiological complexity (Escudero et al., 2006, McIntosh et al., 2008, Kang et al., 2009, Istenic et al., 2010, Manor et al., 2010, Mizuno et al., 2010, Takahashi et al., 2010, Bosl et al., 2011).

Many of the algorithms used to calculate physiological complexity are based on entropy, a physical quantity that measures the order of a system. Regular systems have lower values of entropy, whilst totally irregular systems have very high values of entropy. However, regularity is not necessarily correlated with complexity - random phenomena like white noise have very low regularity and will therefore present high values of entropy, but they do not have the structural richness of information over multiple spatial and temporal scales that characterises complex systems (Costa et al., 2002, 2005). In order to overcome this problem and differentiate between white noise and true complexity, Costa et al. (2002, 2005) introduced the method of multiscale entropy (MSE), which quantifies the complexity of a physiological signal by measuring the entropy across multiple time-scales, using a coarse-graining procedure. This method is based on the hypothesis that optimally functioning biological systems are modulated by multiple mechanisms which interact over multiple temporal scales, generating complex data composed of overlapping signals from all the interrelating mechanisms. In these circumstances, MSE analysis reveals a high value of entropy sustained for increasingly coarser time-scales. For random noise signals however, the MSE algorithm will show a decrease in entropy values as the time-scales increase. This is because a random white-noise signal carries information only on the shortest time-scale; as the time-scales

increase, since no new structures are revealed, the standard deviation of the signal decreases, causing a progressive decrease in the values of entropy (Costa et al., 2005).

It is important to note that there are several other approaches that can be used to examine complexity in physiological time series including the Hurst exponent (Lai et al., 2010), power spectral density analysis and the rate of moment convergence.

WAVELET TRANSFORM COHERENCE

Another well established tool used in the analysis of biomedical signals is coherence, used in the computation of the correlation between the spectral properties of two signals (Lachaux et al., 2002). As described above, coherence is usually used in neuroscience research for the analysis of neural connectivity. However, traditional coherence (e.g. Fourier coherence) is entirely based on frequency analysis, and therefore incapable of providing information about the temporal structure of the correlation between two signals, which is essential for the study of complex brain dynamics (Lachaux et al., 2002). Alternatively, Wavelet Transform Coherence (WTC) is a technique that allows the detection of coherence between two time series as a function of time. The WTC algorithm performs a time-frequency analysis by transforming the original signal using a wavelet function (e.g. Morlet wavelet) that can undergo time shifting and scaling in order to cover the whole time-frequency space of interest. The wavelet cross-spectrum and coherence between two signals can therefore be calculated for any time-frequency bin (Lachaux et al., 2002).

Its ability to generate time and frequency dependent coherence values and to quantify the phase-locking behaviour of two signals in a frequency-specific way makes WTC a useful tool in the study of complex and non-stationary physiological data. Of particular interest to the work of this thesis is the use of WTC in research as a tool to test hypotheses of neural over- or underconnectivity associated with pathologies of the brain.

1.3.4. APPLICATIONS OF EEG IN RESEARCH

EEG has been used widely in neuroscience research for the last few decades. The ERP method in particular has been applied in various research studies investigating cognitive processes in healthy subjects (Benau et al., 2011, Fruhholz et al., 2011) but also in pathology. In the particular case of ASC, a variety of ERP studies have reported differences in the

neurophysiological processing of information by people with ASC, when compared to a neurotypical control group. Regarding the integration of emotional stimuli for example, Dawson and colleagues (2004) have shown that unlike what happens in typically developing children, the N300 ERP does not differentiate between fearful and neutral facial expressions in children with ASC. In a similar study, Wong and colleagues (2008) have shown that ERP responses relating to face detection and processing, including mental state decoding, were weaker and/or slower in children with ASC than in typically developing children, suggesting an abnormal cortical specialization of social neural networks. On the other hand, regarding language processing, a study by Ring et al. (2007) has shown that unlike what happens in a neurotypical control group, in people with ASC the N400 ERP does not differentiate between congruent and incongruent semantic stimuli, suggesting that people with ASC do not use sentence context to predict meaning.

In addition to these findings, the wide range of features that characterize ASC are suggestive of atypical brain functioning on a global and relatively profound level. Current explanatory models of brain functioning in ASC suggest disturbances of underlying brain complexity, including atypical neural connectivity (Belmonte et al., 2004b, Courchesne and Pierce, 2005b, Just et al., 2007, Barttfeld et al., 2011, Wass, 2011) and disrupted temporal integration of information (Brock et al., 2002, Rippon et al., 2007). Supporting the hypothesis of atypical neural connectivity in ASC, is the observation that in those without ASC, improved adaptability to cognitive demands is associated with increasing physiological variability, reflected by greater scalp EEG complexity (McIntosh et al., 2008, Sitges et al., 2010). Additionally, altered neural connectivity has been associated with atypical signal complexity in schizophrenia (Friston, 1996) and Alzheimer's disease (Jeong, 2004). In the field of ASC research a recent study by Bosl et al. (2011) has shown a decrease in resting state EEG complexity in infants at high risk of ASC, when compared to normal controls, with low risk of ASC.

Regarding coherence, past studies have employed WTC analysis to the study of neural connectivity using functional magnetic resonance (fMRI), electroencephalography (EEG) and magnetoencephalography (MEG) data (Liu et al., 2006, Chang and Glover, 2010) recorded from healthy and pathological brains (Sakkalis et al., 2006, Sankari and Adeli, 2011). Sakkalis and colleagues (2006) have applied WTC to the study of functional neural connectivity in schizophrenia showing evidence supporting the 'disconnection' hypothesis in this condition. On the other hand Sankari and colleagues (2011) have used WTC to measure cortical connectivity in Alzheimer's disease patients, using the results to build a model for classification of AD. In ASC, although some investigations have provided evidence of inter and

intrahemispheric underconnectivity using traditional EEG coherence analysis (Coben et al., 2008, Isler et al., 2010), no studies have yet explored neural connectivity in this group using the WTC technique.

2. AN MRI INVESTIGATION OF ATYPICAL CORTICAL THICKNESS IN AUTISM SPECTRUM CONDITIONS

2.1. INTRODUCTION

As mentioned in Chapter 1 and as reviewed by Anagnostou and Taylor (2011), an accelerated brain volume growth in early childhood is the most common finding of anatomical studies in ASC. Another common finding of these studies is an alteration of cortical thickness in people with ASC when compared to a group of typically developing controls. It is thought that cortical thickness reflects processes of significant importance in early stages of brain development such as dendritic arborisation and pruning within grey matter (Huttenlocher, 1990) as well as changes in myelination at the grey-white matter interface (Sowell et al., 2007). It is hypothesized that abnormalities in these processes may lead to impaired cortical organization and neural connectivity in individuals with ASC (Anagnostou and Taylor, 2011).

Although it is a common finding, there is great variability across studies regarding the direction and location of group differences in cortical thickness. Whilst numerous studies report decreases of cortical thickness in ASC groups when compared to typically developing controls (Chung et al., 2005, Hyde et al., 2010, Jiao et al., 2010, Wallace et al., 2010, Scheel et al., 2011), reports of increased cortical thickness in ASC are also not uncommon (Hardan et al., 2006, Hyde et al., 2010, Jiao et al., 2010), with an absence of cortical thickness abnormalities in ASC also being reported (Hutsler et al., 2007, Hazlett et al., 2011). In addition to the disagreement in the direction of cortical thickness changes in ASC, there is also little consensus regarding the location of these group differences; in a cortical thickness study in adults with ASC, Scheel et al. (2011) reported decreased cortical thickness for the ASC group when compared to a control group in left posterior superior temporal sulcus, cuneus, right paracentral lobule, left supramarginal gyrus, inferior parietal lobule and right postcentral gyrus. Wallace et al. (2010), using similar analysis methods and software, reported cortical thinning in adolescents and young adults with ASC in left temporal and parietal lobes only. Laterality is also highly variable in cortical thickness studies in ASC, with some studies reporting group differences restricted to the left hemisphere (Jiao et al., 2010, Wallace et al., 2010) and others reporting group differences that extend to both hemispheres (Chung et al., 2005, Hyde et al., 2010, Scheel et al., 2011).

Despite this lack of consensus in the direction and location of group differences in cortical thickness, numerous studies have consistently reported significant age correlations, with a more pronounced decrease of cortical thickness with age for ASC than for Control groups, for several regions of the brain (Hutsler et al., 2007, Hardan et al., 2009, Wallace et al., 2010, Mak-Fan et al., 2011).

The heterogeneity of results across cortical thickness studies in ASC may be due to numerous factors including the variety of algorithms and techniques used to calculate cortical thickness, as well as variations in MRI image resolution across studies. Another important factor that may influence consistency of results across studies is sample heterogeneity - differences in diagnosis methods used to identify participants, participants' age group and correlation of cortical thickness results with IQ are all possible confounds (Anagnostou and Taylor, 2011). In fact, sample heterogeneity is relevant to not only cortical thickness studies, but all investigations in ASC.

2.1.1. AIMS OF THE STUDY

The first aim of this study was to perform a cortical thickness analysis on a group of individuals with ASC and a comparison group of typically developing controls. Additionally, an analysis of the variation of cortical thickness with age was performed, for both groups, to investigate possible group differences in thickness–age correlation. Despite the fact that the current study was an investigation of cortical thickness in adult age only it was hypothesized, in accordance with previous literature, that the ASC group would present a significantly more pronounced global decrease of cortical thickness with increasing age than the Control group.

2.2. METHODS

2.2.1. PARTICIPANTS

All participants in this study gave informed written consent. Twelve people with ASC (Asperger's syndrome or high-functioning autism) and 13 typically developing controls were recruited. The structural images of one ASC subject contained too many motion artefacts and this subject was excluded from the analysis. The ASC participants were recruited from the

volunteer database in the Autism Research Centre (University of Cambridge). Exclusion criteria were the presence of epilepsy or other active neurological disease, history of severe head injury or significant loss of consciousness, recreational drugs or alcohol dependence. Control participants were recruited from staff and students of the institution where the research was performed and by word of mouth to the local general population. Control participants underwent the same screening as ASC participants and in addition had no family history of ASC or other developmental disorder. All participants were male, had English as their first language and were able to speak and read fluently. All subjects were right-handed (based on self-report and assessed by the Edinburgh Handedness Inventory) and had normal or corrected to normal vision.

Participants were administered the Wechsler Abbreviated Scale of Intelligence (WASI; Wechsler, 1999) for IQ assessment, and the British Picture Vocabulary Scale (BPVS II; National Foundation for Educational Research) to confirm language level above an age equivalence of 14 years old. Participants' age and IQ details can be found in Table 2.1.

Participants in ASC and Control groups were matched for age and IQ. An analysis of variance (ANOVA) examined group differences in age, verbal IQ (VIQ), performance IQ (PIQ) and full-scale IQ (FSIQ). No significant differences were found in either case (age: $F_{1, 23} = 2.042$, $P = 0.167$; VIQ: $F_{1, 22} = 2.640$, $P = 0.119$; PIQ: $F_{1, 17} = 0.237$; $P = 0.633$; FSIQ: $F_{1, 17} = 1.042$; $P = 0.323$) (Table 2.1).

Participants Characteristics							
	Controls (n = 13)			ASC (n = 11)			Group Comparison
	Mean	SD	Range	Mean	SD	Range	
Age	34	13	18-57	27	11	16-44	$F_{1, 23} = 2.042$; $P = 0.167$
Verbal IQ ^a	121	12	100-136	113	13	86-129	$F_{1, 22} = 2.640$; $P = 0.119$
Performance IQ ^b	115	13	96-131	112	19	78-131	$F_{1, 17} = 0.237$; $P = 0.633$
Full-Scale IQ ^b	121	12	105-138	115	15	86-132	$F_{1, 17} = 1.042$; $P = 0.323$

Table 2.1 – Age, verbal IQ, performance IQ and full-scale IQ for each group; (a) – Verbal IQ score was not available for one of the control participants; (b) – These scores were only available for 10 control participants and 8 ASC participants.

All ASC participants reported that they had previously received a formal diagnosis of ASC by a qualified health or educational practitioner. Where possible (7 participants) diagnosis was confirmed using the Autism Diagnostic Interview – Revised (ADI-R; Lord et al., 1994). The ADI-R is a semi-structured interview carried out with a parent or main carer and provides the

information required to confirm diagnosis of an ASC based on ICD-10 (International Statistical Classification of Diseases and Related Health Problems – 10th revision) criteria. Where it was not possible to carry out an ADI-R, diagnosis was confirmed by contacting a relevant clinical service (5 participants). Four of these services reported taking a developmental history as part of their assessment. The remaining service did not report taking a developmental history. However, this participant was included because his scores on two other measures providing information relevant for diagnosis (see below) were consistent with his clinical report. In addition, all participants were independently assessed using Module 4 of the Autism Diagnostic Observation Schedule (ADOS; Lord et al., 2000) and the Autism Quotient (AQ; Baron-Cohen et al., 2001). The ADOS is a structured assessment providing information about the quality of Social Interaction and Communication, and the AQ is a self-administered questionnaire providing a score related to the number of autistic traits. The ADOS provides a cut-off score of 7 for ASC, and the AQ has good discriminate validity at a threshold score of 26 (out of 50) (Woodbury-Smith et al., 2005). These scores, however, do not constitute a clinical diagnosis, nor replace a systematic assessment by a clinician or ADI-R, although they may contribute to or confirm diagnosis (De Martino et al., 2008). For this reason, the three participants not meeting the threshold scores on the ADOS were included as their diagnosis had been confirmed by the ADI-R or a clinician who reported taking a developmental history to establish diagnosis. Details of ASC participants' scores and confirmation of diagnosis are shown in Table 2.2.

Participant	Source of diagnosis	Diagnosis criteria	
		AQ (ASC cut-off = 26)	ADOS Reciprocal Social Interaction and Communication Score (ASC cut-off = 7)
AS1	Clinician	32	9
AS2	ADI-R	40	9
AS3	Clinician	32	4
AS4	ADI-R	31	11
AS5	Clinician	32	10
AS6 ^a	ADI-R	28	14
AS7	Clinician	38	5
AS8	Clinician	42	7
AS9	ADI-R	31	9
AS10	ADI-R	41	14
AS11	ADI-R	23	6
AS12	ADI-R	31	16

Table 2.2 – Diagnosis criteria for participants in the ASC group; ADI-R – Autism Diagnostic Interview-Revised, AQ – Autism Questionnaire, ADOS – Autism Diagnostic Observation Schedule; (a) this participant moved excessively when the structural images were being acquired so this subject’s data was excluded from the structural analysis.

2.2.2. MRI ACQUISITION

MRI images were acquired at the Wolfson Brain Imaging Centre, University of Cambridge, on a 3 Tesla SIEMENS MAGNETOM TrioTim scanner. A T1-weighted structural image was acquired (MPRAGE sequence, voxel size = 1.0 x 1.0 x 1.0 mm, TR = 2300 ms, TE = 2.98 ms, flip angle = 9°, 176 slices, no gap).

2.2.3. CORTICAL SURFACE RECONSTRUCTION

The software FreeSurfer (<http://surfer.nmr.mgh.harvard.edu/>) was used for cortical reconstruction in this study. The standard surface-based analysis pipeline included in the software was applied to the MRI images of each subject (Dale et al., 1999, Fischl et al., 1999). The analysis started by registering each subject’s MRI volume with a Talairach atlas using an affine registration algorithm, followed by skull stripping using a deformable template model (Segonne et al., 2004). Each voxel was then classified as white matter or not white matter, depending on voxel intensity and neighbour constraints. The cerebellum and brain stem structures were identified based on their expected location according to Talairach atlas, and then removed from the image. White and pial surfaces were generated following intensity

gradients between white and grey matter, and grey matter and cerebrospinal fluid (CSF) respectively. Cortical thickness was then calculated at each vertex as the distance between the white and pial surfaces (Fischl and Dale, 2000).

Due to the fact that the cortical surface reconstruction done by FreeSurfer is a semi-automated process, manual checks and corrections were performed for each subject after the volume registration, skull stripping, identification of white matter voxels and surface reconstruction steps. For most subjects, manual corrections were necessary to fix errors in the segmentation of white matter and pial surfaces. In this case, voxels which were erroneously included or excluded from these categories had to be manually deleted or added to the segmented surfaces. This manual process added approximately one hour to the image processing time for each subject.

2.2.4. STATISTICAL ANALYSIS

Demographic and behavioural data were analysed using statistical analysis software SPSS Statistics 17.0 (IBM company). Group differences in cortical thickness and age correlations were calculated using the Qdec toolbox included in the FreeSurfer software. Qdec uses a general linear model approach to perform statistical analysis (please refer to Chapter 1 for more detail on general linear models). To investigate group differences in cortical thickness, group (ASC and Controls) was introduced as a discrete factor in the design matrix. Additionally, to evaluate differences in the correlation of cortical thickness with age across groups, age was introduced as a continuous factor in the analysis. The distribution of age for each group can be found in Figure 2.1. The results of the analysis were displayed on a surface map of an average template brain, and smoothed with Gaussian kernels of 5, 10, 15 and 20 mm full width at half maximum (FWHM). Group differences and thickness-age correlations were considered significant if they had $p_{\text{uncorrected}} < 0.01$. However, results corrected for multiple comparisons using the False Discovery Rate (FDR) algorithm implemented in the Qdec toolbox, with $p_{\text{FDR-corr}} < 0.05$, are also presented.

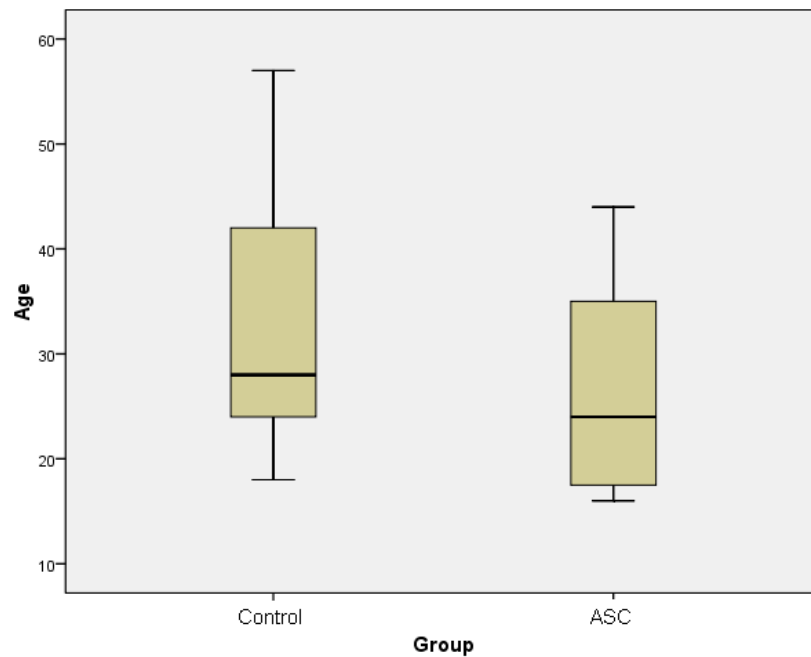


Figure 2.1 – Boxplot representations of the age distribution for both Control and ASC groups.

2.3. RESULTS

2.3.1. VARIATION OF KERNEL WIDTH

The results for the cortical thickness analysis were generated using a variety of Gaussian kernel widths, from 5 to 20 mm FWHM. Analysis using FWHM = 5 mm resulted in significant group differences distributed across numerous small clusters dispersed along various regions of the cortex. On the other hand, a larger kernel width of FWHM = 20 mm resulted in significant group differences distributed across a considerably smaller number of larger size clusters in more specific regions of the brain. The variation of results with kernel size can be seen in Figure 2.2, representing group differences in cortical thickness for the left and right hemisphere.

2.3.2. CORTICAL THICKNESS

Considering FWHM = 10 mm, areas of increased cortical thickness for the ASC group relative to the Control group were found in left middle frontal, left and right superior and inferior parietal regions and right medial orbitofrontal gyrus (areas in red in Figure 2.3). Areas of decreased cortical thickness for the ASC group relative to Controls included the left superior frontal and superior temporal regions, as well as left and right precentral sulcus (areas in blue in Figure 2.3). No group differences survived correction for multiple comparisons at $p_{\text{FDR-corr}} < 0.05$.

FWHM

Left Hemisphere

Right Hemisphere

5 mm

10 mm

15 mm

20 mm

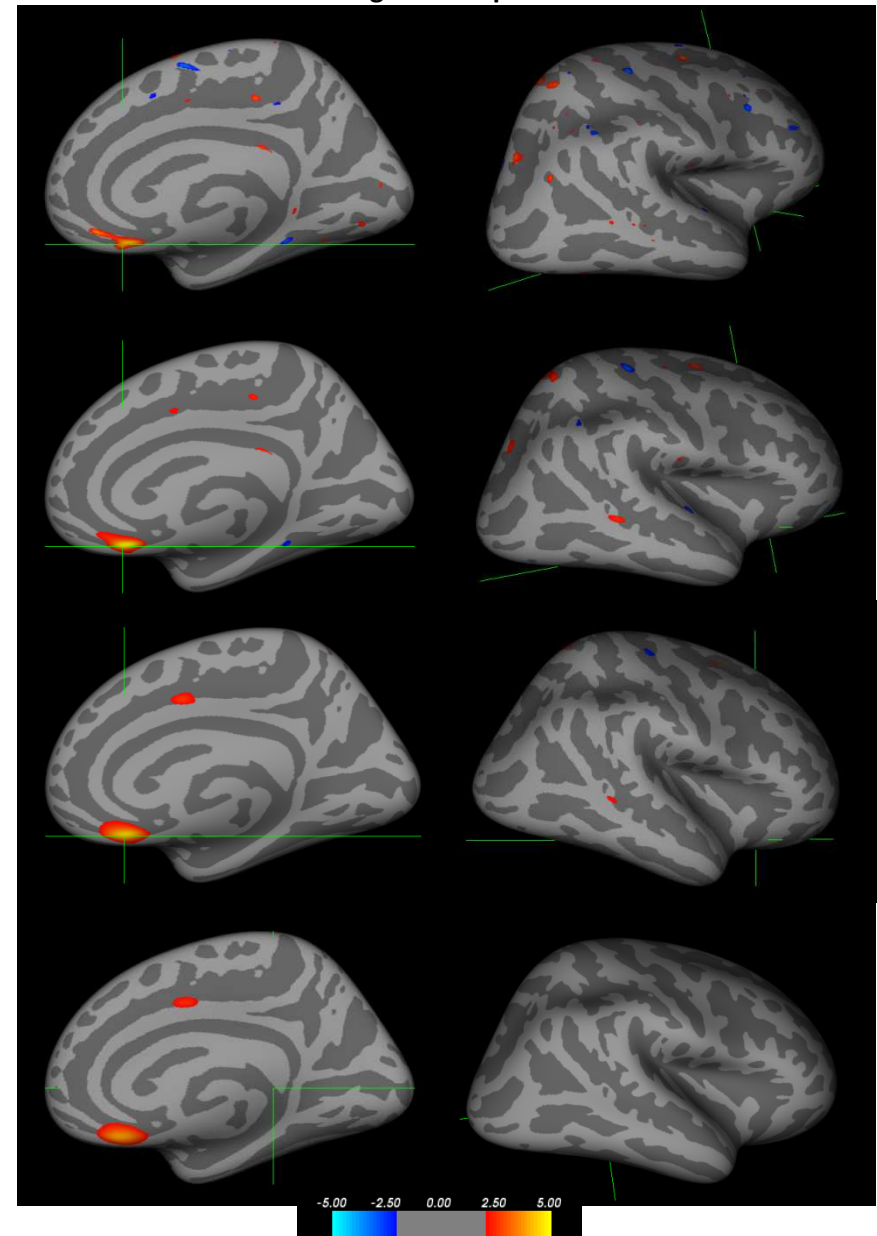
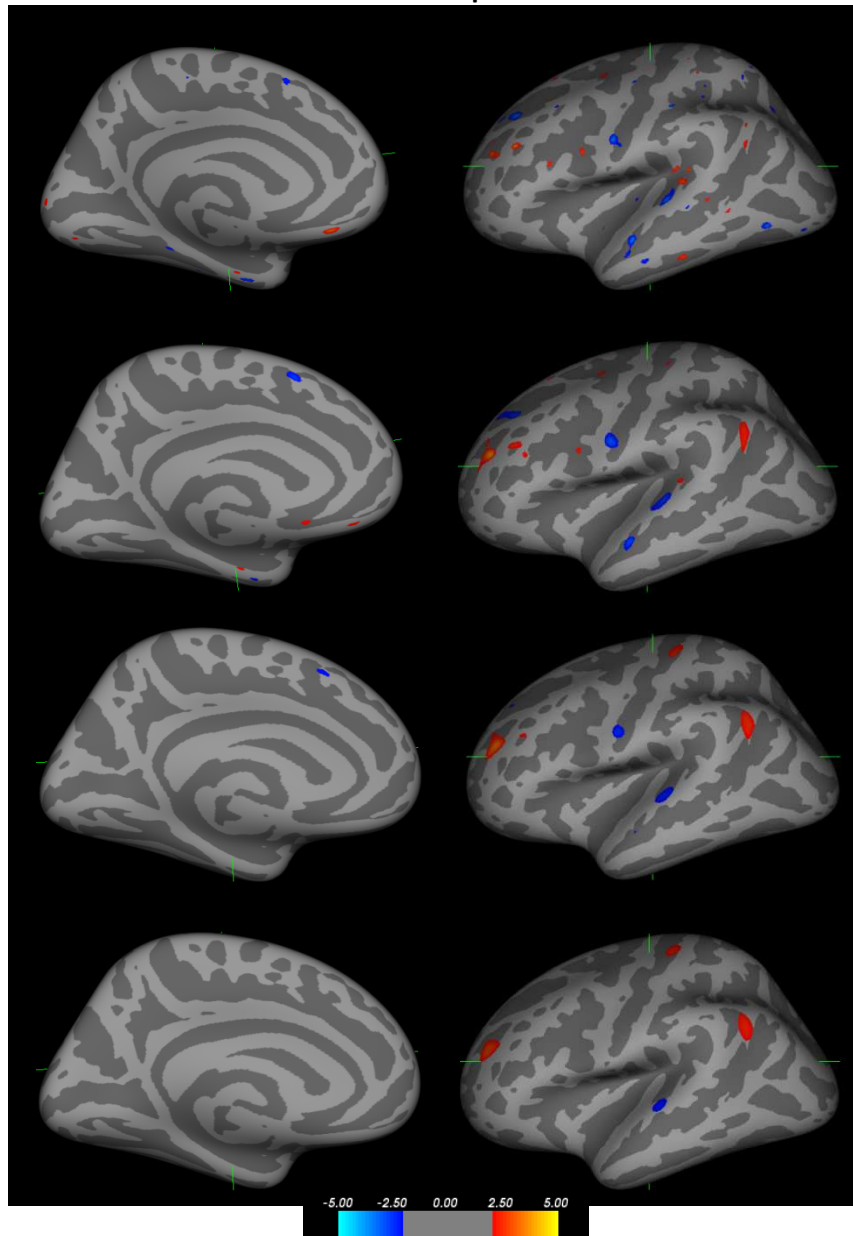
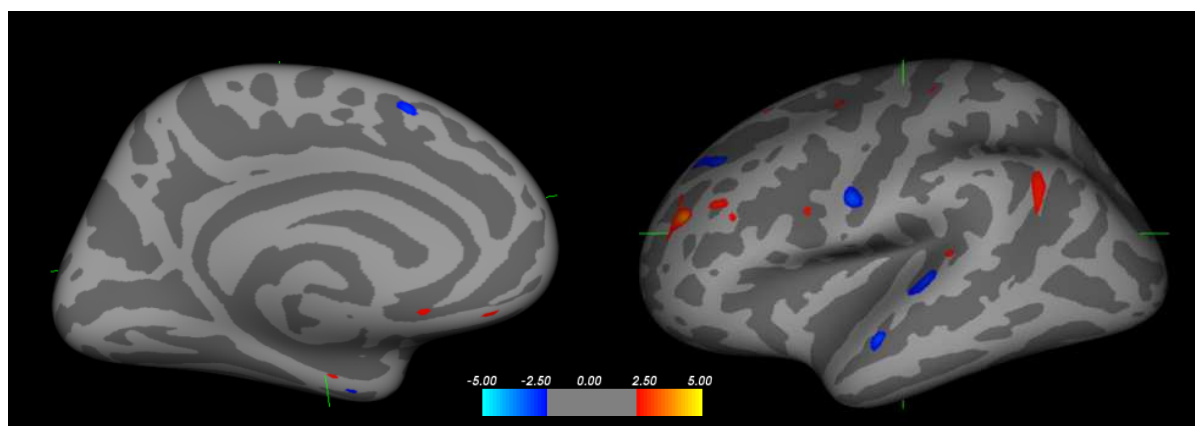


Figure 2.2 – Variation of cortical thickness results with kernel width. Areas in red represent regions of increased cortical thickness for the ASC group relative to Control, and in blue regions of decreased cortical thickness for ASC relative to Controls. Significance of group differences is presented in a logarithmic scale such that $p = 10^{-|\text{scale}|}$

Left Hemisphere



Right Hemisphere

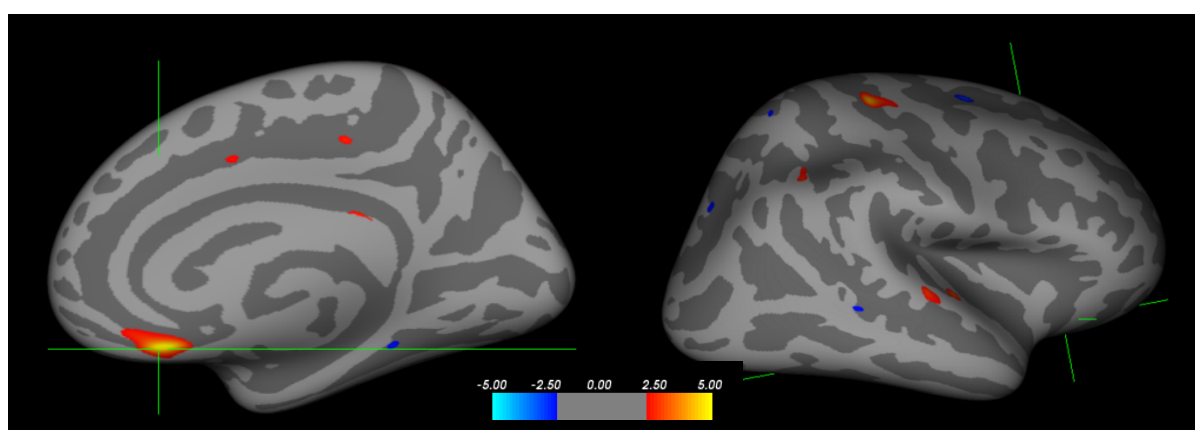
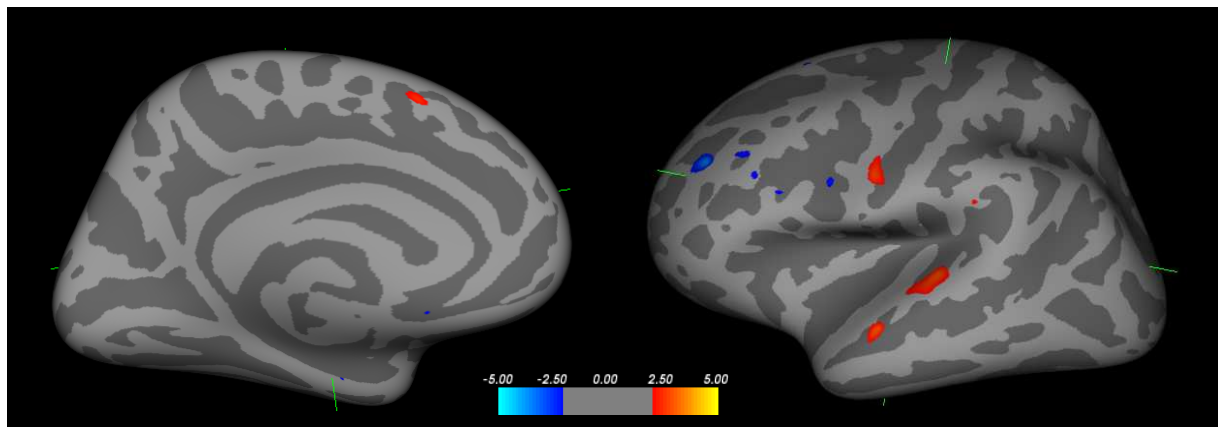


Figure 2.3 – Group differences in cortical thickness for kernel width of FWHM = 10 mm. Areas in red represent regions of increased cortical thickness for the ASC relative to the Control group, and in blue are regions of decreased cortical thickness for the ASC relative to the Control group. Significance is presented in a logarithmic scale such that $p = 10^{-|\text{scale}|}$

2.3.3. AGE-CORTICAL THICKNESS CORRELATION

For FWHM = 10 mm, analysis of the correlation between cortical thickness and age revealed a variety of group differences including clusters in the left middle frontal gyrus and right medial orbitofrontal gyrus, for which the Control group presented increasing cortical thickness with age, whilst the ASC group showed a decrease of cortical thickness with age (areas in blue in Figure 2.4). Results have also revealed areas where there was a decrease of cortical thickness with age for the Control group, but an increase of thickness with age for the ASC group. These areas are shown in red in Figure 2.4 and include both left and right superior temporal and precentral regions. No group differences in age-thickness correlation survived correction for multiple comparisons at $p_{\text{FDR-corr}} < 0.05$.

Left Hemisphere



Right Hemisphere

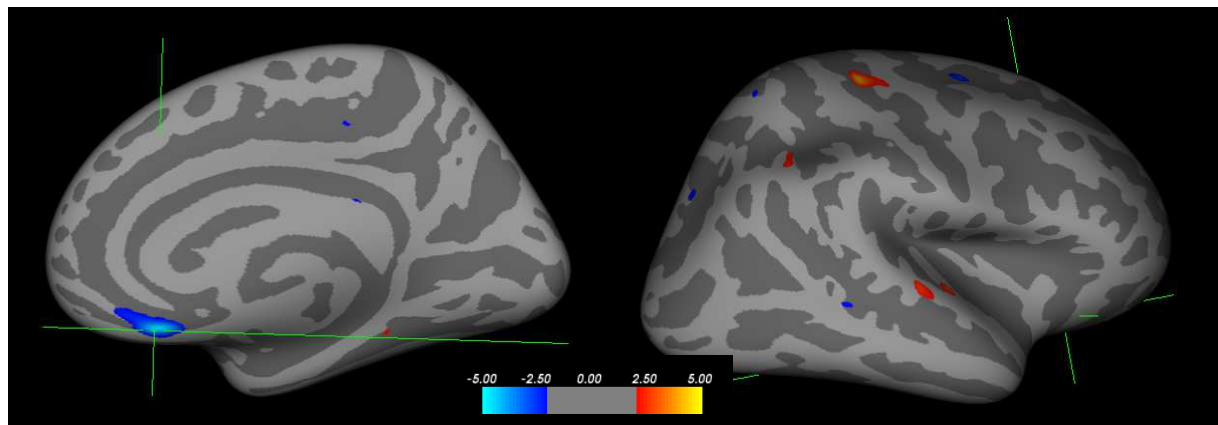


Figure 2.4 – Group differences in cortical thickness-age correlation for kernel width of FWHM = 10 mm. Areas in blue represent regions where cortical thickness increased with age for the Control group, but decreased with age for the ASC group; in red are regions where cortical thickness decreased with age for the Control group but increased with age for the ASC group. Significance is presented in a logarithmic scale such that $p = 10^{-|\text{scale}|}$

2.4. DISCUSSION

The cortical thickness analysis performed in this study revealed various regions of the brain where there were significant differences in cortical thickness between the ASC and the Control group. Although these differences did not survive correction for multiple comparisons, the analysis found areas of increased cortical thickness for the ASC relative to the Control group in the left middle frontal gyrus, left and right superior and inferior parietal regions and right medial orbitofrontal gyrus. Whilst this is consistent with the results of previous studies such as those by Hyde et al. (2010) and Hardan et al. (2006) who found evidence of increased cortical thickness in young adults and children with ASC in parietal regions, it is also in opposition to the study by Hardan et al. (2006),

which reports the absence of such thickness increases in frontal regions of the cortex. Furthermore, whilst not in opposition to them, the results of the current study are also lacking in consistency with previous investigations reporting cortical thickness increases in ASC groups relative to Control groups in the left superior temporal sulcus, left middle temporal gyrus, left and right postcentral sulci (Chung et al., 2005) and cingulate gyrii (Hyde et al., 2010, Jiao et al., 2010).

Regarding cortical thickness decreases in the ASC relative to the Control group, results follow a similar pattern. The analysis in the current study revealed thickness decreases for the ASC group in the left superior frontal and superior temporal regions, as well as left and right precentral sulcus. This is consistent with the results of previous investigations reporting thickness decreases in ASC in the left superior temporal sulcus (Chung et al., 2005, Wallace et al., 2010) and right precentral gyrus (Hyde et al., 2010, Scheel et al., 2011). Despite this, the results of the present study fail to validate the findings of numerous other investigations reporting thickness decreases in ASC in various other regions of the frontal (Chung et al., 2005, Jiao et al., 2010) and parietal cortices (Wallace et al., 2010, Scheel et al., 2011) as well as inferior temporal and fusiform gyrii (Wallace et al., 2010).

It is interesting to note that although the current study is only partially consistent with the results of previous similar investigations, it is also true that previous investigations are not consistent amongst themselves and there is generally a great heterogeneity regarding the results of cortical thickness studies in ASC. As previously mentioned in the introduction of this chapter, one of the factors that may account for such heterogeneity of results is a variation in the algorithms used to calculate cortical thickness across studies (Anagnostou and Taylor, 2011). For example the variation of kernel width explored in the context of the current study shows that smaller kernel widths give rise to group differences in small but numerous clusters across the brain, whilst larger kernel widths result in group differences represented by a smaller number of larger size clusters. As can be seen in Figure 2.2, there is a reasonable variation of results from kernel width = 5 mm to 20 mm. In the current study, because MRI images were acquired with a resolution of 1 mm it was considered adequate to present the results of the analysis with a kernel width of 10 mm, which gives a good compromise between spatial resolution and noise when identifying clusters of significant group differences. Other cortical thickness studies in ASC use kernel widths varying from 15 mm (Wallace et al., 2010, Scheel et al., 2011) to 20 mm (Hyde et al., 2010) or 30 mm (Chung et al., 2005), indicating that kernel width can be an important factor accounting for the variability of results across studies.

Another important factor to take into account when considering the heterogeneity of results across cortical thickness studies in ASC is the age of the populations recruited in each case – whilst some studies have investigated cortical thickness in children (Hardan et al., 2006, Jiao et al., 2010), others

have run similar analysis in teenagers (Chung et al., 2005, Hyde et al., 2010, Wallace et al., 2010) or adults (Scheel et al., 2011). It is known that normal aging is associated with changes in cortical thickness (Lemaitre et al., 2010, Tamnes et al., 2010, Kochunov et al., 2011) and therefore it can not be expected that investigations of cortical thickness in populations of different age groups generate similar results.

Regarding the evolution of cortical thickness with age, it is interesting to note that the majority of studies report decreases of thickness with age, which are more accentuated for ASC than for typically developing control groups (Hutsler et al., 2007, Hardan et al., 2009, Wallace et al., 2010, Mak-Fan et al., 2011). This is partially consistent with the results of the current study, which found areas of decreasing cortical thickness with age for the ASC but not the Control group in the left middle frontal gyrus and right medial orbitofrontal gyrus. However, the present study also found regions where there was a decrease in cortical thickness with age for the Control group, but an increase in thickness in the ASC group for the same areas - left and right superior temporal and precentral regions. These latter results are not validated by previous investigations of the evolution of cortical thickness with age in ASC. It is hypothesized that this disparity can possibly be explained by differences in age distributions of the participants recruited for the various studies. Most previous investigations of cortical thickness in ASC recruited participants in a narrow age band (Hardan et al., 2009, Wallace et al., 2010, Mak-Fan et al., 2011), which means they investigated population samples that were good representatives of a given age group. On the other hand, the current study recruited participants across a relatively wide age range, from 16 to 57 years. Despite this wide age band, this was a study with a limited number of participants, and it is possible that the sample size used was not large enough to allow for an accurate statistical representation of the various age groups. In other words, the participants in the present study were too sparsely distributed across a wide age range to allow for a valid longitudinal study of cortical thickness with age to be performed.

Of additional interest to the present discussion is the fact that as mentioned previously, the results of this study did not survive correction for multiple comparisons, unlike many other previous investigations of cortical thickness in ASC (Hyde et al., 2010, Jiao et al., 2010, Wallace et al., 2010, Scheel et al., 2011). This fact, added to the variability of results between the current study and previous investigations, leads to the conclusion that in this case no evidence was found supporting cortical thickness as a structural biomarker in ASC or as an explanatory factor for the signs and symptoms of ASC.

3. AN fMRI INVESTIGATION OF DETECTION OF SEMANTIC INCONGRUITIES IN AUTISM SPECTRUM CONDITIONS

3.1. INTRODUCTION

3.1.1. ASC AND SEMANTIC INCONGRUITIES

As mentioned in Chapter 1, one characteristic group of symptoms of ASC is impairment in language development and processing. Within ASC, people with Asperger's syndrome (AS) or high-functioning autism (HFA) seem to present only mild language disturbances, usually involving subtle deficits in semantical and pragmatical language processing. A characteristic of these deficits, which may underlie the difficulties that people with AS and HFA have in higher language function, could be conceptualized as a difficulty in using associative processes such as context to understand and predict meaning. Difficulty in using context in reading sentences has been demonstrated directly by Frith and Snowling (1983) and also by Happe (1997) who observed that children and adults with HFA failed to use sentence context to determine the correct pronunciation of homographs. Another specific aspect of use of context that seems to be affected in ASC is detection of incongruity - in order to determine if the semantic content of the final word of a sentence is incongruent with the meaning of the rest of the sentence, it is necessary to consider the context of the sentence as a whole. In an adaptation of the paradigm described by Kutas and Hillyard (1980), Ring and colleagues (2007) have shown that people with AS have atypical electrophysiological responses to incongruent final words in written sentences, as indexed by the N400 event related potential (ERP).

3.1.2. EEG AND fMRI IN THE STUDY OF SEMANTIC INCONGRUITIES

Most of the studies investigating brain response to semantic incongruities are EEG studies, in particular ERP studies of the N400 potential - a negative potential, occurring at approximately 400 ms post-stimulus onset. Kutas and Hillyard (1980) were the first to associate the N400 ERP with the neural response to written semantic incongruities. Since then, various investigations have linked the N400 potential with other input modalities, such as spoken words and sign language, line-drawings, pictures and faces (reviewed by Kutas and Federmeier (2011)), making it a strong neural marker for

incongruity. Investigations using intracranial EEG or other image modalities such as fMRI have associated the sources of the N400 ERP with a wide neural network including superior and middle temporal gyrus, inferior temporal cortex and temporo-parietal junction, as well as prefrontal and inferior frontal cortex (Kiehl et al., 2002, Willems et al., 2008, Khateb et al., 2010). Of particular interest to the current investigation is the study of the N400 in the context of language and semantics, and how the amplitude, latency and neural source of this ERP may be affected in developmental disorders such as ASC. In addition to the investigation by Ring and colleagues (2007) mentioned previously, other EEG studies have also found atypical N400 responses to verbal and nonverbal incongruities in adults and children with HFA and/or AS (McCleery et al., 2010, Pijnacker et al., 2010). However no studies had yet investigated the neural response to semantic incongruities in people with ASC using the modality of fMRI.

3.1.3. AIMS OF THE STUDY

The first aim of this study was to investigate differences in the brain's haemodynamic response to semantically incongruent and congruent sentences between ASC and a typically developing control group. In addition to the investigation of the functional anatomy of the response to semantic incongruities in written sentences, the secondary aim of this study was to explore possible modulating effects on this process when the sentences have an emotional content. It was hypothesized that the Control group would present an enhanced response to emotional incongruent sentences when compared to concrete incongruent stimuli, but that this effect would be diminished in the ASC group.

3.2. METHODS

3.2.1. PARTICIPANTS

All participants in this study gave informed written consent. Twelve people with ASC and thirteen typically developing controls were recruited for this study. One of the control participants (the pilot participant for this study) was subjected to a slightly different functional paradigm. This subject was excluded from the analysis. Details on the demographics of the 12 ASC and 12 Control participants

included in this study can be found in Table 3.1. Participants in this study were the same as the ones in the study described in Chapter 2. For more information about participants' characteristics and recruitment please refer to Chapter 2.

Participants Characteristics							
	Controls (n = 12)			ASC (n = 12)			Group Comparison
	Mean	SD	Range	Mean	SD	Range	
Age	34	13	18-57	27	10	16-44	$F_{1,23} = 2.433$; $P = 0.133$
Verbal IQ ^a	120	13	100-136	112	13	86-129	$F_{1,22} = 2.806$; $P = 0.109$
Performance IQ ^b	114	13	96-131	111	17	78-131	$F_{1,17} = 0.149$; $P = 0.705$
Full-Scale IQ ^b	120	12	105-138	113	15	86-132	$F_{1,17} = 1.086$; $P = 0.313$

Table 3.1 – Age, verbal IQ, performance IQ and full-scale IQ for each group; (a) – Verbal IQ score is not available for one of the control participants; (b) – These scores are only available for 9 control participants and 9 ASC participants.

3.2.2. MRI ACQUISITION

MRI images were acquired at the Wolfson Brain Imaging Centre, University of Cambridge, on a 3 Tesla SIEMENS MAGNETOM TrioTim scanner. Functional images were acquired using an EPI-BOLD sequence with voxel size = 3.0 x 3.0 x 4.0 mm, TR = 1100 ms, TE = 30 ms, flip angle = 78°, 21 slices, slice gap = 1 mm.

3.2.3. fMRI TASK

An event-related design was used in this study. The neural basis of detection of semantic incongruities was investigated using syntactically correct 6 to 8 word sentences ending with either a semantically congruent or incongruent word (Ring et al., 2007). 'Concrete' and 'Emotional' sentences were employed in a 2x2 full factorial design with factors 'semantic congruence' (2 levels: Congruent and Incongruent) and 'emotional valence' (2 levels: Concrete and Emotional). 'Emotional' sentences were included to allow the investigation of potential effects of emotional salience on the neural response to semantic congruity / incongruity.

The sentences with a 'Concrete' meaning described aspects of the physical world:

1. Concrete sentence, Congruent final word (CC)
e.g.: The car had a flat tyre.
2. Concrete sentence, Incongruent final word (CI)
e.g.: The fountain pen leaked blue chocolate.

The 'Emotional' sentences ended either with a word describing an emotionally congruent state or a syntactically correct but semantically incongruent word describing an emotional or physical state.

3. Emotional sentence, Congruent final word (EC)

e.g.: The snake hissed and he felt scared.

4. Emotional sentence, Incongruent final word (EI)

e.g.: Scientists predicted an epidemic and she felt hungry.

A 'Baseline' condition consisting of series of 7 words printed in upper or lower case type was also presented. This control condition was a perceptual task, and was introduced in contrast to the semantic tasks 1 to 4.

5. Baseline stimuli

e.g.: umbrella tree road friend card door tile

or

e.g.: MILK SHELF TRAIN PENCIL CHICKEN HAND PARK

In order to develop the sentences in each condition a cloze probability exercise was used. An item's cloze probability is defined by the percentage of individuals that continue a sentence fragment with that item in an offline sentence completion task (DeLong et al., 2005). Concrete and emotional sentences, each with their final word missing, were shown to groups of 8 – 20 people, who were asked to complete each sentence by writing the word that first occurred to them as a likely end to the sentence. For the emotional sentences, words with very close meanings, such as 'afraid' and 'scared' were taken as synonymous. Sixty concrete sentences with the highest cloze probability scores above 90% were selected, and sixty emotional sentences with the highest cloze probability scores above 70% were selected. The mean cloze probability score (the probability of a particular word being chosen to complete a specific sentence (Kutas and Hillyard, 1984)) was 99.8% and 88.4%, for the 'Concrete Congruent' and 'Emotional Congruent' sentences respectively.

The incongruent endings for the concrete sentences were generated by randomly assigning them the original final word from another sentence within the concrete sentence stimulus set. The incongruent endings for the emotional sentences were generated by randomly assigning them words describing physical or emotional states of similar frequency to the original final word (Kucera and Francis, 1967). The 'Emotional Incongruent' sentences were then checked for any possible

accidental semantic congruity, which was addressed by swapping the final word with one originally assigned to another sentence in the EI group. The final word in the concrete and emotional sentences and the words in the Baseline condition were balanced for frequency of use in English (Kucera and Francis, 1967).

Overall, a total of 150 sentences/baseline conditions (30 sentences of each type, 30 baseline conditions) were mixed randomly and presented in 5 blocks (30 sentences/baseline conditions per block). DMDX software (Forster and Forster, 2003) was used to present the conditions visually, one word at a time on a computer screen, in the form of black letters on a white background, following the protocol used by Ring et al. (2007). Participants were instructed to read silently the sentences appearing on the screen in front of them and to answer a question at the end of each sentence. Participants had a practice run of the task on a laptop computer before going into the scanner. Each trial started with a row of X's (XXXX) presented for 300 ms, and then each word was presented for 130 ms, with an inter-word interval of 500 ms. At the end of each sentence the participant was asked 'Was the last word one that you expected?'. In the baseline condition at the end of each series of words participants were asked 'Were the words in capitals?'. The questions were on screen for 1300 ms and participants had 2000 ms to answer 'yes' or 'no' using a button box by their right hand. The inter-trial interval was 800 ms. Each block lasted about 5 min and the participants could have the rest time they needed between blocks. In most cases less than 1 minute was taken. Total scanner acquisition time, including the structural scan, was about 40 minutes per subject.

3.2.4. DATA ANALYSIS

Demographic and behavioural data were analysed using statistical analysis software SPSS Statistics 17.0 (IBM company) with the alpha significance value set at 0.05. To test for differences in behavioural results, a 2-way repeated-measures analysis of variance (ANOVA) was done for accuracy and response time, with group (ASC vs. Controls) as a between-subjects factor, and task (CC, CI, EC, EI and Baseline) as a within-subjects factor. Post-hoc group comparisons of response time and accuracy were done for each condition using a one-way ANOVA. In order to reduce the skewness in the distributions, response time data was transformed using a logarithmic function ($f(x) = \ln(x)$) and proportional accuracy was transformed using an arcsin function ($f(x) = \arcsin(\sqrt{x})$) (McDonald, 2009). The Greenhouse-Geisser adjustment was applied to the degrees of freedom for all analyses (Field, 2009).

Analyses of the functional MRI data were carried out using Statistical Parametric Mapping - SPM software (Wellcome Trust Centre for Neuroimaging, University College London) – version SPM5. Functional images were initially submitted to various pre-processing stages including motion and slice timing correction algorithms (Friston et al., 1995). Motion correction in SPM is done using the 'Realign' tool, which employs a least squares approach and a 6 parameter spatial transformation (rigid body - 3 translational, 3 rotational) to realign a series of scans to a reference scan chosen by the user. For this study a two pass realignment procedure was used, in which scans in a given functional block were initially realigned to the first chronological scan of that block, and then realigned again to the mean of the realigned images. This procedure was repeated for all functional blocks and for each subject before moving on to the slice timing correction routine. Slice timing correction is necessary to correct for temporal mismatch between different slices when an interleaved acquisition sequence is used (i.e. when adjacent slices are not acquired adjacently in time to avoid contamination by residual magnetic gradient fields). Since the signal in each slice is given by a linear combination of sinusoid waves of different frequencies, the slice timing correction routine works by shifting the signal of each slice in time (using a technique called sinc interpolation), realigning it to the first chronological slice of a particular functional block.

After motion and slice timing correction, functional images were coregistered to the structural image of the same subject. Similarly to the realignment algorithm, the coregistration routine utilizes a rigid-body model to adjust functional images to match the orientation of the structural image. As functional and structural images differ so much in spatial resolution, this algorithm makes use of major anatomical landmarks in both images to achieve optimum transformation resorting to an interpolation method.

Functional images were then spatially normalised into standard MNI (Montreal Neurological Institute) space, using ICBM (International Consortium for Brain Mapping) template images included in the SPM software. The normalisation routine uses linear and nonlinear spatial transformations to adjust the images of each subject to the template image, through an interpolation algorithm (trilinear interpolation was used in this study). This normalisation step is essential for inter-subject averaging and comparison in multi-subject studies.

Finally, images were spatially smoothed using a 3D Gaussian kernel with 6 mm full width at half maximum. Spatial smoothing is used to increase signal-to-noise ratio by suppressing high-frequency spatial noise. Additionally it also helps to smooth out the effects of intersubject anatomical and functional variability, improving the conformity of the data to the assumptions that underlie statistical inference procedures applied later during 1st and 2nd level analysis.

The 1st level analysis in SPM follows the pre-processing stages and concerns the analysis of intra-subject functional activation. In the current study the onset times for each type of stimulus were defined for every participant and for each set of scans the 'Concrete Congruent', 'Concrete Incongruent', 'Emotional Congruent', 'Emotional Incongruent' and 'Baseline' conditions were modelled (Figure 3.1). These conditions were specified as covariates in a general linear model and an activation parameter was estimated at each voxel and for each condition. The parameter estimate, derived from the mean least squares fit of the model to the data, reflects the amount of experimental variance attributed to each covariate or condition. The design matrix (see Figure 3.1) is the graphic representation of the general linear model – each column represents a covariate in the model. In this case the covariates are the five experimental conditions and the movement parameters for each subject. Participant movement during image acquisition can affect the signal measured in each voxel and so the movement parameters are included as a covariate in the design matrix, to account for experimental variance that can not be attributed to the experimental conditions.

To compare Congruent and Incongruent responses for Concrete and Emotional sentences four contrasts were created (Figure 3.1):

1. Concrete Congruent > Concrete Incongruent responses
2. Concrete Congruent < Concrete Incongruent responses
3. Emotional Congruent > Emotional Incongruent responses
4. Emotional Congruent < Emotional Incongruent responses

To study effects of differences in sentence type (Emotional or Concrete) and congruence levels (final word of sentence being Congruent or Incongruent) between both groups (ASC, control), two interaction contrasts were also created (Figure 3.1):

5. Concrete Congruent > Concrete Incongruent AND Emotional Congruent < Emotional Incongruent
6. Concrete Congruent < Concrete Incongruent AND Emotional Congruent > Emotional Incongruent

An activation map was generated for each contrast and each individual. Serial correlations were taken into account using the default autoregressive algorithm in SPM. All the contrasts were taken forward to a group analysis (SPM 2nd level analysis) with inter-subject variability being treated as a

random effect. As a result, activation maps were obtained for each group (ASC and Control) and for each contrast. Between group differences were then characterised for key comparisons.

Images were thresholded using the False Discovery Rate (FDR; (Genovese et al., 2002)) with a threshold of $p < 0.05$ at voxel-level. Activations were considered significant only if they had $p_{\text{FDR-corr}} < 0.05$ at cluster level (Forman et al., 1995, Friston et al., 1996, Genovese et al., 2002, Lieberman and Cunningham, 2009). For each contrast, main clusters were tested for the presence of outliers; for a given cluster, a participant's t-value would be considered an outlier if it was more than 2.5*standard deviations (SD) away from the mean.

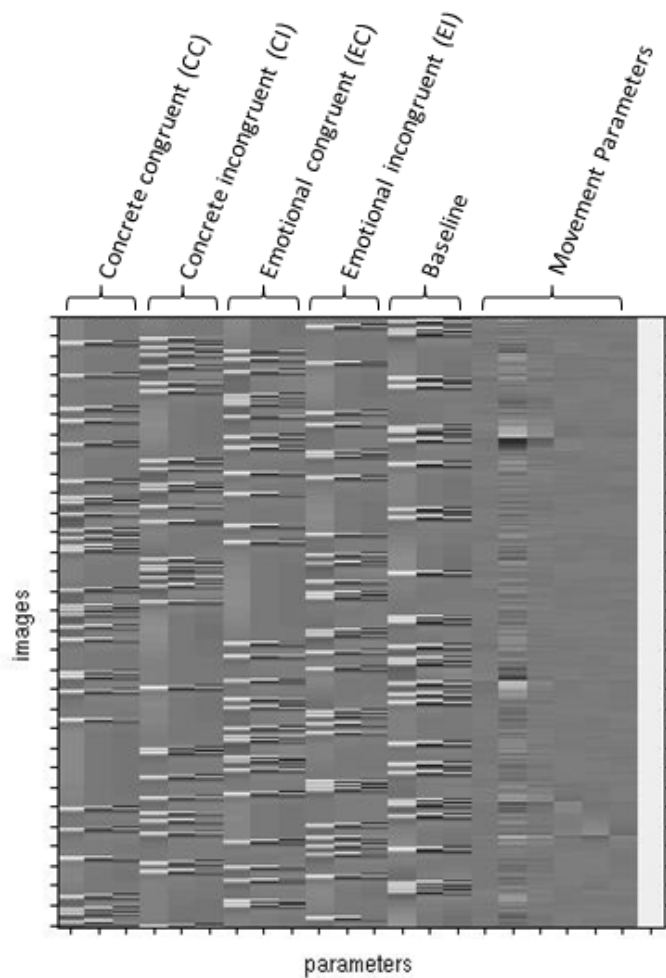
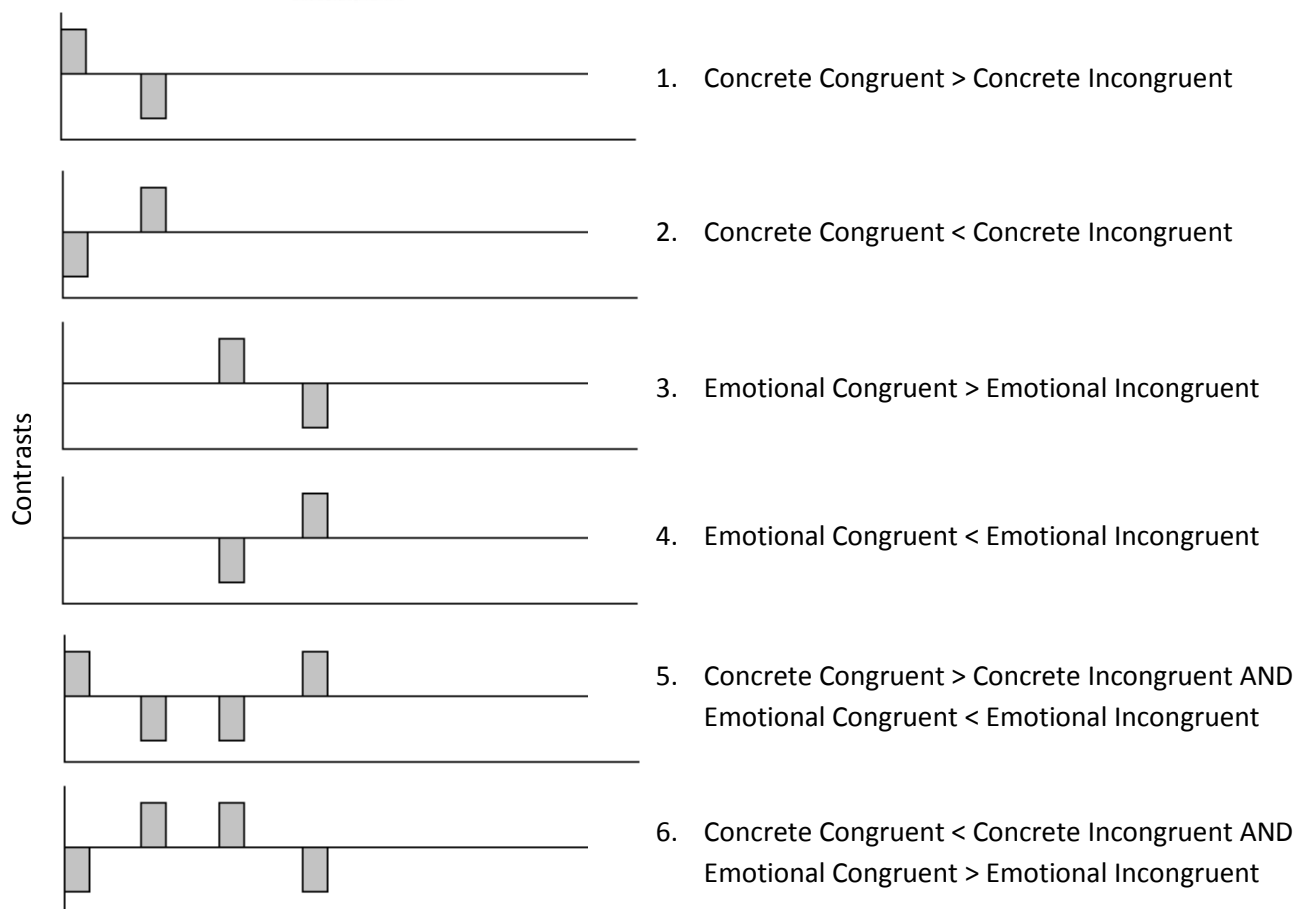


Figure 3.1 – Example of 1st level analysis modelation of experimental conditions (Concrete Congruent, Concrete Incongruent, Emotional Congruent, Emotional Incongruent and Baseline) and movement parameters in a design matrix (right), along with diagrams for the 6 contrasts calculated (below).



3.3. RESULTS

3.3.1. BEHAVIOURAL PERFORMANCE

All participants were able to perform the tasks easily, with accuracy scores well above chance. Response time was not used to distinguish between groups, but rather as a confirmation that both groups were able to respond before the start of the next trial. ANOVA results show no significant differences in response times between groups ($F_{1, 22} = 0.507$, $P = 0.484$). Although there was a significant effect of task ($F_{2.850, 62.696} = 10.085$, $P < 0.0005$) driven by an increased response time for the baseline condition in both groups, no significant group-by-task interaction was observed ($F_{2.850, 62.696} = 2.281$, $P = 0.091$). Details on the response times for each group can be seen in Table 3.2.

Response times (ms)					
Sentence type	Controls (n = 12)		ASC (n = 12)		Group Comparison
	Mean	SD	Mean	SD	
CC	564.56	81.92	633.35	203.16	$F_{1, 23} = 0.407$; $P = 0.530$
CI	570.18	116.88	648.82	239.30	$F_{1, 23} = 0.616$; $P = 0.441$
EC	504.53	130.87	658.18	221.65	$F_{1, 23} = 2.915$; $P = 0.102$
EI	598.52	147.83	637.85	282.90	$F_{1, 23} = 0.000$; $P = 0.989$
Baseline	738.62	136.88	740.70	183.70	$F_{1, 23} = 0.022$; $P = 0.884$

Table 3.2 – Response times for each group and each sentence type. Group comparisons were calculated using a one-way ANOVA.

Regarding accuracy scores, results show a significant group effect ($F_{1, 22} = 5.112$, $P = 0.034$), but no significant effect of task ($F_{3.059, 67.297} = 2.587$, $P = 0.059$) or group-by-task interaction ($F_{3.059, 67.297} = 0.959$, $P = 0.419$). Details on accuracy scores for each group can be found in Table 3.3. Although there are significant differences in accuracy between groups for two conditions (CC and baseline), both groups had mean accuracy scores above 90% in all conditions, showing that they understood and could successfully perform the tasks.

Accuracy (%)					
Sentence type	Controls (n = 12)		ASC (n = 12)		Group Comparison
	Mean	SD	Mean	SD	
CC	99.7	1.0	96.6	3.8	$F_{1, 23} = 11.779$; $P = 0.002$
CI	97.5	2.9	95.0	6.4	$F_{1, 23} = 0.385$; $P = 0.541$
EC	97.0	4.8	91.4	8.7	$F_{1, 23} = 2.254$; $P = 0.147$
EI	98.0	3.8	93.3	8.1	$F_{1, 23} = 1.742$; $P = 0.200$
Baseline	99.2	2.1	93.9	9.5	$F_{1, 23} = 6.322$; $P = 0.020$

Table 3.3 – Accuracy scores for each group and each sentence type. Group comparisons were calculated using a one-way ANOVA.

3.3.2. fMRI FUNCTIONAL ACTIVATION – WITHIN-GROUP CONTRASTS

1. Concrete sentences:

a) Congruent > Incongruent responses (Contrast 1)

No brain areas were identified in which there were greater BOLD responses to Congruent compared to Incongruent stimuli in either study group.

b) Incongruent > Congruent responses (Contrast 2)

In the Control group, there was increased activity for Incongruent relative to Congruent stimuli in the right and left posterior cingulate cortices, right anterior cingulate cortex and left occipitotemporal lobe (Figure 3.2, Table 3.4), $p_{\text{FDR-corr}} < 0.05$ (cluster level). Using a less conservative significance value of $p_{\text{uncorrected}} < 0.001$ (voxel level) the previous pattern of activity extended to the left superior temporal and inferior frontal lobes, as well as right inferior frontal gyrus.

In the ASC group, $p_{\text{FDR-corr}} < 0.05$ (cluster level) revealed areas of increased activity for Incongruent relative to Congruent stimuli located in the left inferior frontal gyrus around Brodmann's areas (BA) 44, 45, 46 and 47, as well as left anterior cingulate cortex and right middle frontal gyrus (Figure 3.2, Table 3.4). When using the less conservative threshold of $p_{\text{uncorrected}} < 0.001$ (voxel level), additional areas of activation were present in posterior regions of the brain. However, these were sparsely distributed and not forming any noticeable clusters.

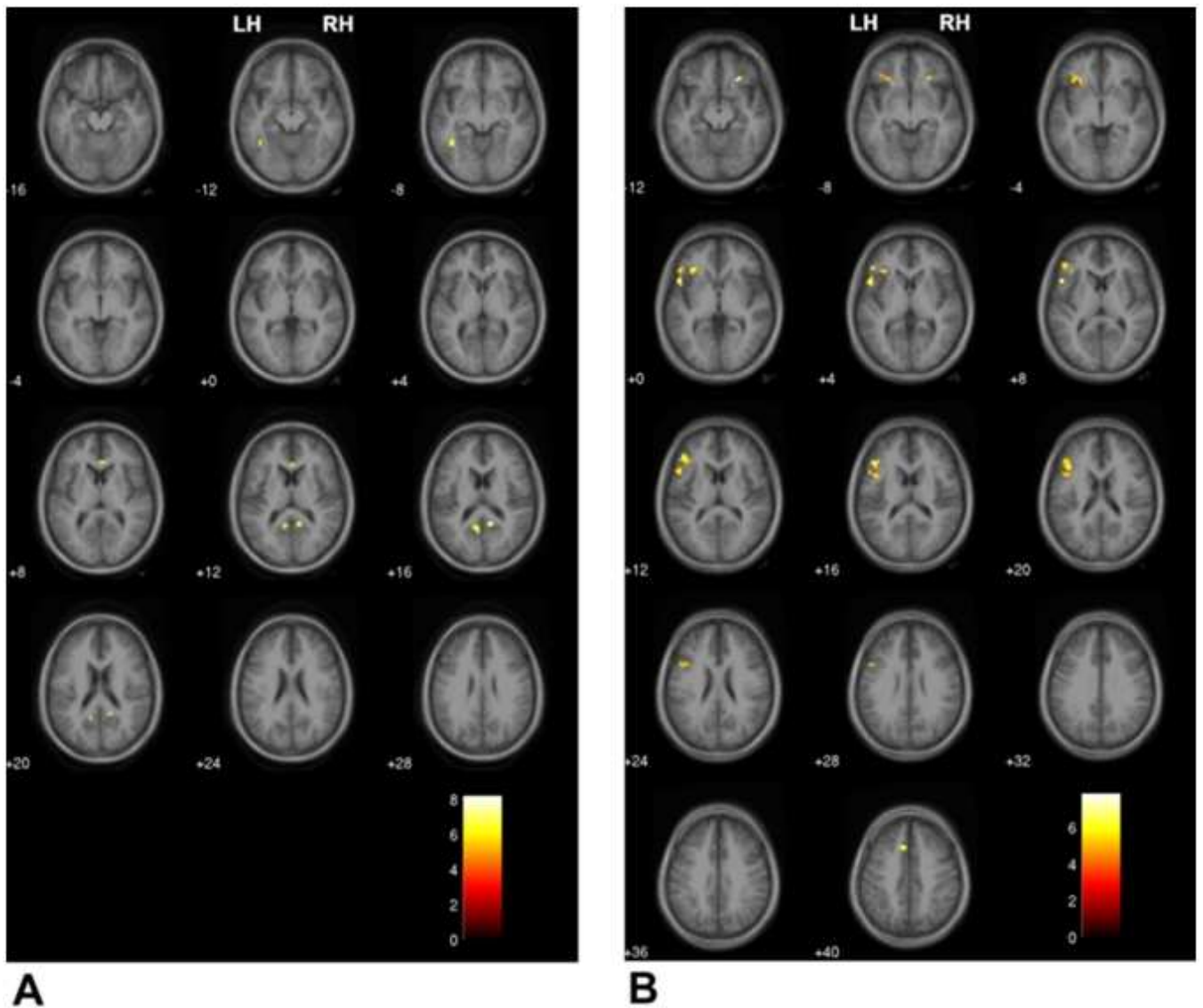


Figure 3.2 – T-maps of increased brain activity to Incongruent compared to Congruent stimuli (Concrete sentences only) in left (LH) and right (RH) hemispheres, for selected axial slices, for Control (A) and ASC (B) participants, at $p_{FDR-corr} < 0.05$ (cluster level); (A) areas of activity can be seen in the left occipitotemporal lobe ($z = -12$, $z = -8$ mm), right anterior cingulate cortex ($z = +4$ to $z = +12$ mm) and right and left posterior cingulate cortices ($z = +12$ to $z = +20$ mm); (B) areas of activity can be seen in the left inferior frontal gyrus ($z = -12$ to $z = +28$ mm), left anterior cingulate cortex ($z = +36$, $z = +40$ mm) and right middle frontal gyrus ($z = -12$, $z = -8$ mm).

Incongruent > Congruent (concrete sentences only)											
Controls											
Set-level P	Cluster-level			Voxel-level				MNI coordinates x, y, z {mm}			Area
	$p_{\text{FDR-corr}}$	k_E	$p_{\text{uncorrected}}$	$p_{\text{FDR-corr}}$	T	Z_{\equiv}	$p_{\text{uncorrected}}$				
5.6×10^{-10}	0.000	10	0.000	0.029	8.21	4.56	0.000	9	-51	16	Right posterior cingulate
	0.005	6	0.001	0.029	7.41	4.35	0.000	3	30	8	Right anterior cingulate
	0.001	9	0.000	0.029	7.23	4.30	0.000	-42	-54	-8	Left occipitotemporal lobe
	0.000	11	0.000	0.029	7.16	4.28	0.000	-6	-60	16	Left posterior cingulate
ASC											
Set-level P	Cluster-level			Voxel-level				MNI coordinates x, y, z {mm}			Area
	$p_{\text{FDR-corr}}$	k_E	$p_{\text{uncorrected}}$	$p_{\text{FDR-corr}}$	T	Z_{\equiv}	$p_{\text{uncorrected}}$				
1.0×10^{-6}	0.000	136	0.000	0.030	7.84	4.47	0.000	-48	27	16	Left inferior frontal gyrus
				0.030	7.56	4.39	0.000	-51	12	4	
				0.030	6.78	4.17	0.000	-33	30	0	
	0.005	13	0.001	0.030	7.47	4.37	0.000	24	27	-12	Right middle frontal gyrus
	0.005	13	0.001	0.030	7.40	4.35	0.000	-9	24	40	Left anterior cingulate

Table 3.4 – T, Z, p FDR-corrected and uncorrected values for voxels and clusters activated more in response to Concrete Incongruent stimuli than to Concrete Congruent stimuli, for each group; Set-level p represents the p value for the whole brain set of voxels and clusters; k_E – number of voxels in a cluster.

2. Emotional sentences:

a) Congruent > Incongruent responses (Contrast 3)

In the Control group, there was increased activity for Congruent relative to Incongruent stimuli in several distinct clusters: posteriorly in the right and left anterior cerebellar lobes and fusiform gyrii (BA 19), more anteriorly, around the right inferior parietal lobule (BA 40) extending to the right insula, left superior temporal gyrus (BA 22) extending to the left putamen and left insula and right and left cingulate gyrus (BA24) (Figure 3.3, Table 3.5). These areas all have $p_{\text{FDR-corr}} < 0.05$ at cluster level. At these levels of significance, in the ASC group, no brain sites were observed to have a greater response to Congruent relative to Incongruent stimuli. However, using a more liberal threshold of $p_{\text{uncorrected}} < 0.001$ (voxel-level) a pattern of increased activity for Congruent relative to Incongruent stimuli was observed, including the right medial superior frontal gyrus, left precentral gyrus and the left anterior cerebellar lobe. The use of the more liberal threshold of $p_{\text{uncorrected}} < 0.001$ (voxel-level) in the Control group results did not change the observed pattern of activated clusters reported above.

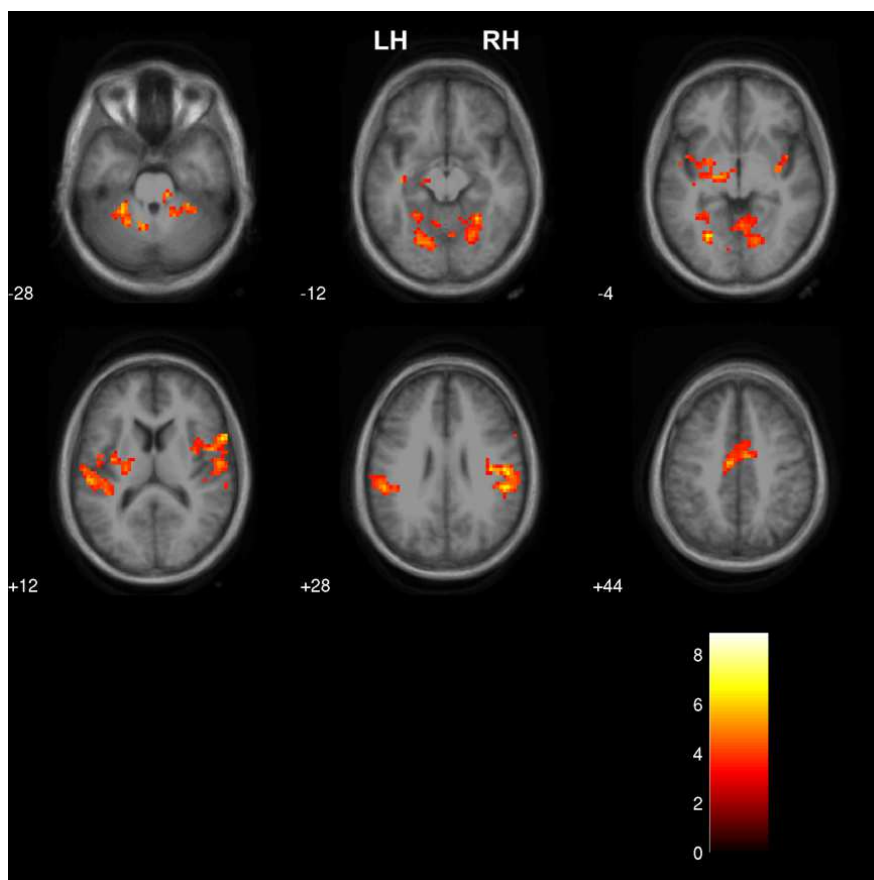


Figure 3.3 – T-maps of increased brain activity for Congruent relative to Incongruent stimuli (Emotional sentences only) in left (LH) and right (RH) hemispheres, for selected axial slices, for Controls, at $p_{\text{FDR-corr}} < 0.05$ (cluster level). Areas of activity can be seen in the right and left anterior cerebellar lobes ($z = -28$ mm), fusiform gyrii ($z = -12$ mm), right inferior parietal lobule ($z = +12$, $z = +28$ mm) extending to right insula ($z = -4$), left superior temporal gyrus ($z = -4$, $z = +12$ mm) extending to left putamen ($z = +12$ mm) and left insula ($z = -4$ mm) and right and left cingulate gyrus ($z = +44$ mm). No areas of activation were observed in the ASC group with $p_{\text{FDR-corr}} < 0.05$ (cluster-level).

Congruent > Incongruent (emotional sentences only)											
Controls											
Set-level	Cluster-level			Voxel-level				MNI coordinates			Area
p	$p_{\text{FDR-corr}}$	k_E	$p_{\text{uncorrected}}$	$p_{\text{FDR-corr}}$	T	Z_{\equiv}	$p_{\text{uncorrected}}$	x, y, z {mm}			
9.8x10 ⁻¹⁵	0.000	367	0.000	0.021	8.86	4.71	0.000	18	-51	-24	Right anterior cerebellar lobe, fusiform gyrus
				0.028	6.01	3.92	0.000	27	-54	-12	
				0.030	5.45	3.72	0.000	12	-33	-28	
	0.000	261	0.000	0.021	8.56	4.64	0.000	-24	-48	-24	Left anterior cerebellar lobe
				0.021	7.43	4.36	0.000	-24	-69	-8	
				0.028	6.51	4.09	0.000	-27	-42	-32	
	0.000	525	0.000	0.021	7.93	4.49	0.000	66	-36	36	Right inferior parietal lobule
				0.021	7.68	4.43	0.000	45	-33	24	
				0.028	6.77	4.17	0.000	51	-18	28	
	0.000	505	0.000	0.022	7.22	4.30	0.000	-48	-3	4	Left superior temporal gyrus, left putamen, left insula
				0.028	5.96	3.90	0.000	-24	-18	8	
				0.028	5.89	3.88	0.000	-57	-27	16	
	0.001	64	0.000	0.028	5.64	3.79	0.000	-6	-12	44	Right and left cingulate gyrus
				0.030	5.10	3.58	0.000	6	-6	44	
				0.039	3.85	3.00	0.001	3	3	44	

Table 3.5 - T, Z, p FDR-corrected and uncorrected values for voxels and clusters activated more in response to Emotional Congruent stimuli than to Emotional Incongruent stimuli, for the Control group (no areas of activation found in the ASC group); Set-level *p* represents the *p* value for the whole brain set of voxels and clusters; *k_E* – number of voxels in a cluster.

b) Incongruent > Congruent responses (Contrast 4)

No brain areas were identified in which there were greater BOLD responses to Incongruent compared to Congruent stimuli in either study group, with $p_{\text{FDR-corr}} < 0.05$ at cluster level. However, for $p_{\text{uncorrected}} < 0.001$ (voxel-level), activity was found in the left inferior frontal gyrus for the Control group only.

3.3.3. fMRI FUNCTIONAL ACTIVATION – BETWEEN-GROUP CONTRASTS

1. Concrete sentences:

a) Congruent > Incongruent responses (Contrast 1)

When making a direct comparison of brain activity between groups, no areas of activation survived multiple comparison correction at $p_{\text{FDR-corr}} < 0.05$ (cluster level). There were also no areas of activation that survived the less conservative threshold of $p_{\text{uncorrected}} < 0.05$ (cluster-level) on parametric maps obtained with $p_{\text{uncorrected}} < 0.005$ (voxel-level).

b) Incongruent > Congruent responses (Contrast 2)

No areas of activation survived multiple comparison correction at $p_{\text{FDR-corr}} < 0.05$ (cluster level). However, using the less conservative threshold of $p_{\text{uncorrected}} < 0.05$ (cluster-level) on parametric maps obtained with $p_{\text{uncorrected}} < 0.005$ (voxel-level), there were areas of increased activity for the ASC group relative to the Control group in the left inferior frontal gyrus (BA 44 and 47), and increased activity for the Control group relative to the ASC group in the left posterior cingulate cortex.

2. Emotional sentences:

a) Congruent > Incongruent responses (Contrast 3)

Once again, no areas of activation survived multiple comparison correction at $p_{\text{FDR-corr}} < 0.05$ (cluster level). Using the more liberal threshold of $p_{\text{uncorrected}} < 0.05$ (cluster-level) on parametric maps obtained with $p_{\text{uncorrected}} < 0.005$ (voxel-level), there was increased activity for the Control group

relative to the ASC group in the left and right anterior cerebellar lobes, the right posterior cerebellar lobe, right inferior parietal lobule and middle temporal gyrus bilaterally.

b) Incongruent > Congruent responses (Contrast 4)

No areas of activation survived multiple comparison correction at $p_{\text{FDR-corr}} < 0.05$ (cluster level). There were also no areas of activation that survived the less conservative threshold of $p_{\text{uncorrected}} < 0.05$ (cluster-level) on parametric maps obtained with $p_{\text{uncorrected}} < 0.005$ (voxel-level).

No outlier t-values were found for any of the main clusters, in any contrast. Analyses of possible interactions between sentence type (Emotional or Concrete), semantic congruence (Congruent or Incongruent) and group (Contrasts 5 and 6) revealed a 3-way interaction, at $p_{\text{uncorrected}} < 0.05$ (cluster level), with stronger activation in the ASC group relative to the Control group in the left inferior frontal gyrus.

3.4. DISCUSSION

The results of this study demonstrate that not only do adults with ASC manifest different patterns of brain activity compared to a neurotypical control group in response to semantically congruent or incongruent final words in written sentences, but that the nature of these differences varies depending on whether the sentences have a concrete or an emotional meaning.

In response to final incongruent, compared to final congruent words, in sentences with a concrete meaning, the Control group presented an increase in neural activity in posterior brain areas, namely posterior cingulate cortex. The ASC group on the other hand showed relatively increased activity for this contrast in the left inferior frontal region (around BA 44, 45, 46, 47). At a lower significance threshold however, the Control group also demonstrated increased activity in the left inferior frontal lobe. This indicates that in the Control group the response to Concrete Incongruent stimuli is relatively weaker in left inferior frontal than in posterior cingulate regions.

Like Kiehl et al. (2002) the current study found no brain areas in which congruent final words elicited a relatively larger response than incongruent final words, and the distribution of left inferior frontal activity observed in both groups in the current study also resembles that reported by those authors in response to incongruent final words. Other studies have also reported activation of the left inferior frontal lobe (Newman et al., 2001, Frishkoff et al., 2004, Just et al., 2004, Harris et al., 2006, Knaus et al., 2008, Binder et al., 2009) and the posterior cingulate cortex (Frishkoff et al., 2004, Harris et al., 2006, Binder et al., 2009) in response to tasks involving semantic processing. The studies by Just et al. (2004) and Harris et al. (2006) are of particular interest, as they investigate different aspects of semantic processing in people with ASC. Harris et al. (2006), in a paradigm involving visual presentation of single words with a request to evaluate the word as either positive or negative, reported that both ASC and Control groups activated, amongst other areas, the left inferior frontal cortex, but with stronger activation in the Control than in the ASC group. In a similar study Just et al. (2004) employed a sentence comprehension task contrasted with fixation, where all the sentences made sense. Like Harris et al. (2006), Just et al. (2004) reported that the ASC group activated left inferior frontal cortex to a smaller extent than the Control group. Hence in both these studies, despite using somewhat different paradigms and contrasts, the participants with ASC demonstrated relatively small left inferior frontal activations when compared to the Control group.

These results seem to be in contrast with the current study's findings of an increased activation of the left inferior frontal gyrus in the ASC group, when compared to the Control group. This discrepancy may be due to fundamental differences in the paradigm used in the current study, where differentiation between Congruent and Incongruent sentences was necessary. In the current study's paradigm, the alternative methods of performing the required task that were utilized by the Controls (i.e. posterior cingulate region in addition to left inferior frontal area) might have not been available to the ASC group, due to impaired connectivity between those two regions, leading to relatively greater inferior frontal gyrus activation in the ASC group. In previous studies (Just et al., 2004, Harris et al., 2006), because of the differing task demands, there may not have been what might be described as the forced dependence on the left inferior frontal gyrus in the ASC group. Hence the current study's results may be considered as complementary to those of Just et al. (2004) and Harris et al. (2006), rather than in opposition to them.

In addition, Harris et al. (2006) report bilateral posterior cingulate activation for concrete words, compared to abstract words, to be stronger in the Control group than the ASC group. A study by Frishkoff et al. (2004) that investigated how activity in brain networks is coordinated over time during semantic processing of incongruities reports brain activity composed of multiple sources,

including sources located in anterior and posterior regions of the cingulate cortex, as well as inferior prefrontal and temporal sources. Of particular relevance to the results of the current study, the authors of that investigation (Frishkoff et al., 2004) suggest that processing in the inferior frontal and prefrontal regions is clearly separable from sources in the temporal and posterior cingulate cortex, and that the time course of the responses points to activity in the posterior cingulate cortex being preceded by activity in inferior frontal and prefrontal regions. Frishkoff et al. (2004) also suggest that the anterior cingulate cortex is one of the first sources to discriminate congruous and incongruous words, and that its activity is sustained over time during processing of semantic incongruities. Also of relevance to the current study's results is the suggestion by Blakemore et al. (1998) that the anterior cingulate cortex, together with posterior cingulate cortex may act as a self-monitoring system in the human brain.

As well as describing temporally separable processes, left inferior frontal and posterior cingulate regions have also been associated with distinct functions in respect to language processing. Activations of left inferior frontal language-related areas have previously been attributed to phonological processing (BA 44), such as silent reading of pseudowords and judging rhyming (Poldrack et al., 1999, Cousin et al., 2007, Heim et al., 2008) and to semantic analysis (BA 45 and 47), such as making a decision about whether or not a word represents a living thing (Poldrack et al., 1999, Gold et al., 2005, Cousin et al., 2007). On the other hand posterior cingulate regions have been proposed to play a role in higher levels of language processing (Binder et al., 2009), working memory (Bledowski et al., 2009) and self-monitoring functions (Blakemore et al., 1998, Vogt et al., 2006). In relation to the results of the current study these observations suggest that those with ASC responded to semantic incongruities with a response more locally associated with the nature of the incongruent words themselves rather than with higher-level associative functions. This may be indicative of impaired connectivity between frontal areas of initial and posterior areas of subsequent higher-processing of language and semantics. This suggestion is compatible with models of impaired 'long-distance' connectivity that have been proposed to underlie aspects of cognitive function in ASC (Belmonte et al., 2004b, Sahyoun et al., 2010). It is also compatible with the results obtained by Monk et al. (2009) showing impairment in connectivity in the resting state default network, specifically weaker connectivity in an ASC group when compared to a Control group, between posterior cingulate cortex and superior frontal regions. The absence of increased activation in these more posterior regions, as observed in the current study, could lead to impaired global processing of language meaning in ASC (Jolliffe and Baron-Cohen, 1999, 2000).

The responses to sentences with emotional meanings differed in both study groups from those manifested in response to the concrete sentences. Although the ASC group activations did not reach the most conservative significance threshold, both groups have shown a pattern of activity corresponding to greater responses to Congruent compared to Incongruent final words. For the Control group activated areas included the left and right anterior cerebellar and fusiform regions and more anteriorly the right inferior parietal lobule, left superior temporal gyrus and left putamen, extending to the insula in both hemispheres. For the ASC group, sub-threshold ($p_{\text{uncorrected}} < 0.001$ voxel-level) activations included right superior medial frontal gyrus, left precentral gyrus and left anterior cerebellar lobe.

Unlike what was hypothesized, in contrast to the Concrete sentences, the Emotional sentences were not associated with significantly increased activations in response to Incongruent final words, but instead with increased activations to Congruent final words. Part of the explanation for this may be that for the Emotional Incongruent sentences the final word was not as unexpected as for the Concrete Incongruent sentences. This suggestion is supported by the observation of lower cloze probabilities, indicating less constrained expectancies, for Emotional Congruent sentences. In addition, event related potential studies have previously reported that N400 ERPs are larger following words that are more unrelated to the expected final word of a sentence (Kutas and Hillyard, 1980, 1984). This may explain why there was only a small (subthreshold) response to Incongruent final words in the Emotional sentences, observed in the Control group in the left inferior frontal gyrus, which may be considered a trace response to semantic incongruity.

It seems plausible that Emotional sentences have been judged by the Controls in terms of whether or not they made sense emotionally, with the activations possibly reflecting an empathic response by the Control group to emotionally congruent sentences. This interpretation is supported by previous studies that point to the existence of a functional relationship between certain areas in the cerebellum and empathic responses (Jackson et al., 2005, Shamay-Tsoory et al., 2005, Schulte-Ruther et al., 2007, Ushida et al., 2008). These studies also suggest the involvement in empathic responses of other brain areas such as medial, superior and inferior frontal lobes, precentral gyrus, inferior parietal and superior temporal regions, as well as anterior insula and inferior occipital lobe, some of which similar to areas activated by the Control (fusiform gyrus, right inferior parietal lobule and left superior temporal gyrus) and the ASC group (at a less conservative statistical threshold - right superior medial frontal gyrus and left precentral gyrus) in the current study. The diminished (less significant and extensive) cerebellar response to emotionally congruent sentences by the ASC group is compatible with clinical and experimental observations that people with ASC are

characterized by an impairment in judging other people's emotions and empathizing with others (Lombardo et al., 2007). It is also in line with previous studies suggesting an association between cerebellar dysfunction or lesion and symptoms of ASC (Bobee et al., 2000, Bauman and Kemper, 2003, Grossberg and Seidman, 2006, Schmahmann et al., 2007).

Whilst there are clear differences in neural activation patterns between the ASC and the Control groups in the current study, the small sample sizes limit the power of the comparisons. It should also be noted that both groups were characterized by relatively wide age and verbal IQ ranges and that overall the Control group performed the behavioural tasks more accurately and more rapidly. However, the behavioural data collected from the participants indicates that both groups understood the tasks and could perform them correctly with high degrees of accuracy. In addition, both groups demonstrated similar response times to the baseline condition, indicating that there were no differences in the speed of motor response to the request to make a decision regarding stimulus type. The significant group differences in accuracy for the Concrete Congruent and Baseline conditions are probably the result of the majority of Control subjects performing at ceiling level, and the participants in the ASC group making a larger, yet still small, number of mistakes. These differences are considered to be not clinically relevant, since the ASC group still presents accuracy scores above 90%. Despite this, it is important to note that although all participants performed adequately in the experimental task, a measure of reading ability was not undertaken, so possible differences in reading ability between groups may have gone unnoticed. Furthermore, during imaging, whilst overall the ASC group moved more within the scanner this movement was not task-related.

In conclusion, the results of this study suggest that adults with AS or HFA activate different brain regions in response to written sentences containing semantic incongruities, when compared to neurotypical controls. Whilst the ASC group manifested brain activation patterns that were distinct from the Control group, it is noted that ASC participants were nevertheless able to distinguish Congruent from Incongruent sentences in both Concrete and Emotional conditions with high degrees of accuracy. This suggests that the alternative processing strategy employed by the ASC group, indexed by less spatially extended neural activation patterns, is nevertheless effective. However, these more spatially restricted activation patterns may indicate impaired integration of neural networks during higher-level language processing, which may be related to the difficulties presented by people with ASC in the use of context to predict meaning and detect incongruities in a sentence.

4. ATYPICAL EEG COMPLEXITY IN AUTISM SPECTRUM CONDITIONS: A MULTISCALE ENTROPY ANALYSIS

4.1. INTRODUCTION

4.1.1. ASC AND FACE PROCESSING

As mentioned in Chapter 1, ASC is characterised, amongst others, by impairments in social interactions such as use of eye contact, engagement in reciprocal interactions and response to the emotional cues of others (American Psychiatric Association, 2000). For this reason, a variety of studies have investigated possible impairments in face processing in ASC (Dawson et al., 2004, Fairhall and Ishai, 2007, Kleinhans et al., 2008, Kliemann et al., 2010, Monk et al., 2010), reporting a variety of findings including impairments in facial discrimination and recognition of facial expressions of emotion, anomalies in gaze processing and memory for facial identity, as well as presence of atypical strategies for face processing including reduced attention to the eyes and use of piecemeal rather than configural strategies in face processing (reviewed by Golarai et al. (2006) and Dawson et al. (2005)). This diversity of atypical findings relating to face processing in ASC is suggestive of a generalized impairment over the range of neural networks involved in facial recognition and processing of facial expressions. A review by Golarai and colleagues (2006) focused on three regions usually implicated in social cognition and face processing: the superior temporal sulcus (STS), fusiform face area (FFA) and the amygdala. That review summarizes numerous behavioural and MRI/fMRI studies describing not only anatomical abnormalities, but also atypical neural activation in these areas in response to a variety of facial stimuli, in individuals with ASC, when compared to typically developing controls. Of particular relevance to the current study, Golarai et al. (2006) reviewed the findings of previous investigations suggesting that specific aspects of face processing such as recognition memory may be impaired in people with ASC, even though evidence shows that visual discrimination among faces may be intact.

Also of significant importance to this thesis are the results of electrophysiological studies of face processing in ASC. Due to their high temporal resolution, EEG recordings are a valuable modality for the study of early and late stages of face processing at the neuronal level. In particular, the N170 is a negative ERP (for a definition of ERP please refer to Chapter 1), well characterised in the normal

population, and that preferentially activates in response to faces. The N170 latency is shortened when faces and eyes are presented alone, and is slowed down by inverted faces or non-facial stimuli (Bentin et al., 1996). The biological source of the N170 is located in the posterior regions of the brain, with the majority of studies reporting the posterior fusiform gyrus as the source of this ERP (Rossion et al., 2003, Deffke et al., 2007), although some investigations have also found evidence supporting the posterior superior temporal sulcus as a source for the N170 (Itier and Taylor, 2004).

Several studies have found atypical N170 patterns in people with ASC (reviewed by Dawson et al. (Dawson et al., 2005)), namely increased N170 latencies when compared to typically developing controls, failure to show a face inversion effect (McPartland et al., 2004), and lack of an attention modulation effect on the N170 (Churches et al., 2010). Regarding other face related ERP components, a study by Dawson and colleagues (2002) has shown that children with ASC, unlike typically developing children, do not show amplitude differentiation to familiar vs. unfamiliar faces as indexed by the P400 ERP.

4.1.2. BRAIN COMPLEXITY IN ASC

In Chapter 1 physiological complexity was introduced as an increasingly recognized novel approach to the investigation of typical and pathological developmental or degenerative states (Costa et al., 2002, 2005, Fallani et al., 2010, Ouyang et al., 2010). Regarding ASC, there are reasons to believe these may be associated with atypical patterns of brain complexity - the wide range of life-long signs and symptoms that characterize ASC suggest an association with atypical functioning at a relatively profound level of brain functioning. In attempting to explain this wide range of features of ASC several explanatory models of brain functioning that suggest disturbances of underlying brain complexity have been proposed, including atypical neural connectivity (Belmonte et al., 2004b, Courchesne and Pierce, 2005b, Just et al., 2007, Barttfeld et al., 2011, Wass, 2011) and disrupted temporal integration of information (Brock et al., 2002, Rippon et al., 2007). Supporting the possibility of atypical functional complexity in ASC it has been observed that, in those without ASC, improved adaptability to cognitive demands is associated with increasing physiological variability reflected by greater scalp EEG complexity (McIntosh et al., 2008, Sitges et al., 2010) and that altered neural connectivity may be associated with atypical signal complexity in schizophrenia (Friston, 1996) and Alzheimer's disease (Jeong, 2004). In addition, a recent study by Bosl et al. (2011) has shown a decrease in resting state EEG complexity in infants at high risk of ASC, when compared to normal controls with low risk of ASC. In the current study, in order to examine whether ASC is

associated with atypical patterns of complexity of brain activity, multiscale entropy (MSE) was employed as a measure of physiological complexity in scalp-recorded EEG data of a group of adults with ASC and a matched group of typically developing controls.

An increase of MSE of brain activity with age has been observed in typical development from childhood to adulthood (McIntosh et al., 2008), and in a study of adults with schizophrenia increased MSE of EEG data has also been observed in fronto-central and parietal regions (Takahashi et al., 2010). On the other hand, age-related response to photic stimulation in typical individuals (Takahashi et al., 2009) and treatment of schizophrenia with antipsychotics have been associated with reduced MSE of brain signals. Regarding degenerative states, Alzheimer's disease has been associated with various patterns of EEG complexity, with earlier studies reporting decreased MSE for this condition (Escudero et al., 2006, Park et al., 2007), whilst more recently Mizuno et al. (2010) reported relatively decreased MSE over smaller time scales but relatively increased MSE at coarser time scales in a group of Alzheimer's patients, possibly reflecting different modulating effects by separate neuropathophysiological mechanisms.

Whilst some MSE studies have analysed EEG data collected during resting states (Escudero et al., 2006, Hornero et al., 2009, Takahashi et al., 2010, Bosl et al., 2011), others have employed activation or stressor tasks to explore responses to stimuli of relevance to a physiological or clinical process of interest (Takahashi et al., 2009, Manor et al., 2010, Sitges et al., 2010). Given the evidence reported above of face processing impairments in people with ASC, the current study analyses EEG signals recorded whilst participants observed images of faces and inanimate objects.

4.1.3. AIMS OF THE STUDY

In this investigation the first aim was to determine whether typically developing controls and a group of people with ASC have similar or differing patterns of MSE of EEG data. The hypothesis was that those with ASC would present atypical patterns of EEG complexity, reflected by significantly different MSE values at coarser time scales compared to controls. Secondly, given the reduced behavioural adaptability observed in ASC (Russo et al., 2007, Thakkar et al., 2008, Foley Nicpon et al., 2010) and the observation that in the general population greater adaptability is associated with higher MSE values (McIntosh et al., 2008), along with findings of reduced complexity in infants at high risk of ASC by Bosl et al. (2011), there was an additional hypothesis that MSE would be reduced over coarser time scales in the ASC group, when compared to MSE in the Control group, during the performance of a visual matching task. To address the question of the extent to which differences in

EEG complexity may relate to group differences in EEG power spectra, a traditional power analysis using the same EEG data was also conducted.

4.2. METHODS

4.2.1. PARTICIPANTS

All participants in this study gave informed written consent. Fifteen patients with ASC and fifteen typical controls were recruited for this study. All ASC participants were diagnosed with ASC by a professional experienced with the diagnosis of ASC based on international criteria (American Psychiatric Association, 2000). Exclusion criteria for ASC participants were uncorrected impairment in eyesight or hand movement, a personal or family history of any psychological or genetic condition apart from ASC or a period of unconsciousness in the last five years. Exclusion criteria for control participants were similar, with the addition of any personal or family history of ASC. All participants were male and right-handed, as measured by the Edinburgh Handedness Inventory (Oldfield, 1971).

Participants were administered the Wechsler Abbreviated Scale of Intelligence (WASI; (Wechsler, 1999) for IQ assessment and the Autism Quotient (AQ; (Baron-Cohen et al., 2001)) for an evaluation of the number of ASC traits. Higher scores on the AQ reflect a greater number of traits indicative of ASC. Not surprisingly the ASC group (Mean = 35, SD = 7) scored significantly higher in the AQ than the Control group (Mean = 16, SD = 7, $F_{1,28} = 57.351$; $P < 0.0005$). Additionally the two study groups were matched for age and IQ. Participants' demographic details and their IQ and AQ scores are presented in Table 4.1.

Participants Characteristics							
	Controls (n = 15)			ASC (n = 15)			Group Comparison
	Mean	SD	Range	Mean	SD	Range	
Age	29	4	21 – 37	31	6	23 – 42	$F_{1,29} = 0.961$; $P = 0.335$
Verbal IQ ^a	114	16	77 – 133	119	11	101 – 134	$F_{1,28} = 1.068$; $P = 0.310$
Performance IQ ^a	119	11	93 – 134	115	14	93 – 132	$F_{1,28} = 0.696$; $P = 0.412$
Full-Scale IQ ^a	119	14	93 – 134	119	13	98 – 136	$F_{1,28} = 0.007$; $P = 0.936$
AQ ^b	16	7	4 – 27	35	7	21 – 46	$F_{1,28} = 57.351$; $P < 0.0005$

Table 4.1 – Age, verbal IQ, performance IQ and full-scale IQ for each group; (a) – IQ scores were not available for one Control participant; (b) Autism Quotient (AQ) scores were not available for one Control participant (different from (a)).

4.2.2. EEG RECORDING

EEG data was acquired as part of an ERP protocol (Churches et al., 2010) using 28 standard scalp electrodes placed in accordance with the International 10-20 System (Klem et al., 1999). Reference was the tip of the nose with ground at Fpz. Eye-movements were monitored using bi-polar channels with electrodes above and below the left eye (vertical electro-oculogram) and 1cm from the outer canthus of each eye (horizontal electro-oculogram). Impedances at all sites were maintained below 5k Ω . EEG data was recorded using a 32-channel Synamps apparatus (Compumedics Neuroscan, Charlotte, NC, USA), at a sampling frequency of 1000 Hz and with a 0.1 to 50 Hz input bandpass filter. The 50 Hz upper limit of the bandpass filter was chosen to attenuate electrical background noise whilst avoiding the use of a notch filter (Escudero et al., 2006, Mizuno et al., 2010, Takahashi et al., 2010). Consistent with previous MSE studies (Escudero et al., 2006, Hornero et al., 2009, Takahashi et al., 2010), the data was not subjected to other pre-processing steps (i.e., notch filtering, artefact removal or data reconstruction algorithms) since this could distort the data and influence the MSE analysis results. Instead artefact free segments of data were visually identified and chosen for analysis.

The EEG was recorded whilst participants performed a face and chair detection task. Participants were seated in a darkened room approximately 60 cm from the computer screen on which the stimuli were presented. Stimuli consisted of 30 pictures of neutral expression faces (15 male, 15 female) and 30 pictures of chairs. Participants viewed two blocks of stimuli between which only the order of the images varied. In each block, all 60 pictures (30 faces, 30 chairs) were presented three times pseudorandomly without immediate repetition. Each image was presented for 500 ms, with an interstimulus interval that varied randomly between 1200 ms and 1400 ms. Thus each block lasted for about 5.5 min. In one of the blocks, the subject's attention was directed to the chairs, and in the other block their attention was directed to the faces pictures. To do this, 10 images of faces (5 male, 5 female) and 10 images of chairs were inserted as immediate repetitions. At the start of each block, participants were asked to attend to one of the categories of stimulus (faces or chairs) and to press a response button whenever they saw an immediate repetition of an image of that category, while ignoring all stimuli in the other category. The purpose of this instruction was to direct the participants' attention to a given category (Figure 4.1). Response times and accuracy were measured for each participant. Each block began with a practice run of ten stimuli and the order of the two blocks, the attended category and the hand used to respond were counterbalanced across participants. Participants rested for approximately 5 minutes between blocks.

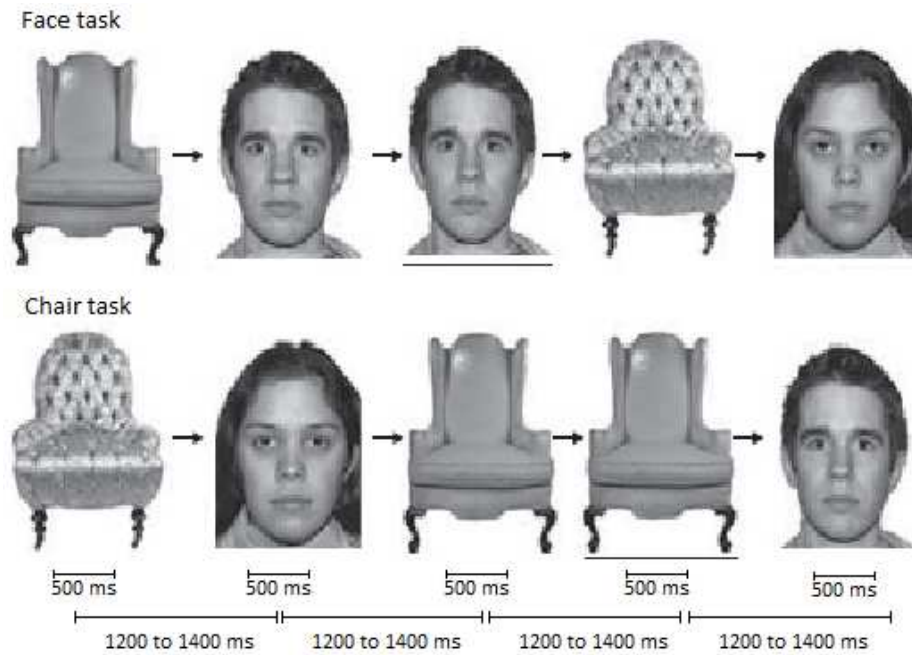


Figure 4.1 – Example of stimuli sequence shown to participants, for both face and chair tasks; underlined stimuli required a button press (adapted from Churches et al. 2010).

4.2.3. SIGNAL ANALYSIS

The first 180 s of EEG recording of all participants during each visual task were extracted for analysis. From these 180 s, segments free of artefacts such as eye movements, blinks, muscle movements or other artefacts were visually identified and selected for analysis. MSE and power analyses were run for each participant for the first 40 000 data points (40 s) of the EEG signal resulting from all the artefact free segments. This is the default number of data points analysed by the MSE algorithm (available at <http://www.physionet.org/physiotools/mse/mse.c>, (Goldberger et al., 2000). Analyses were run separately for the chairs and faces tasks.

There were no significant between group differences in the number of pictures included in the 40 s period chosen for analysis (chair task: Control = 17 (SD = 3), ASC = 16 (SD = 4), $F_{1, 28} = 0.613$, $P = 0.440$; face task: Control = 18 (SD = 3), ASC = 17 (SD = 4), $F_{1, 28} = 0.178$, $P = 0.676$). For all subjects electrodes Fp1, Fp2 and Fz were excessively affected by noise and eye movement artefacts and were removed from the analysis. Additional technical problems affected electrodes F3 and O2 during data acquisition for some participants, and so electrode pairs F3/F4 and O1/O2 were also excluded from the analysis.

4.2.4. MULTISCALE ENTROPY

The MSE method quantifies the complexity of a time-series by calculating the sample entropy (S_E) over several time scales, using a coarse-graining procedure (Costa et al., 2002, 2005).

The S_E is a measure of irregularity of a time-series. Considering an EEG time-series $x = \{x_1, x_2, \dots\}$, S_E can be defined as the negative of the logarithmic conditional probability that two similar sequences of m consecutive data points will remain similar at the next point ($m + 1$) (Richman and Moorman, 2000, Richman et al., 2004):

$$S_E(m, r, N) = -\ln \left(\frac{C_{m+1}(r)}{C_m(r)} \right) \quad (4.1)$$

where

$$C_m(r) = \frac{\{\text{number of pairs } (i, j) \text{ with } |x_i^m - x_j^m| < r, i \neq j\}}{\{\text{number of all probable pairs} = \frac{N - m + 1}{N - m}\}} \quad (4.2)$$

where $|x_i^m - x_j^m|$ denotes the distance between vectors x_i^m and x_j^m , of dimension m , r is the tolerable distance between two vectors (in terms of fraction of the standard deviation of the time-series) and N is the length of the time-series.

Therefore, for more regular series

$$C_{m+1}(r) \approx C_m(r) \Rightarrow \frac{C_{m+1}(r)}{C_m(r)} \rightarrow 1 \Rightarrow S_E(m, r, N) \rightarrow 0 \quad (4.3)$$

On the other hand, for completely irregular time-series

$$C_{m+1}(r) \ll C_m(r) \Rightarrow \frac{C_{m+1}(r)}{C_m(r)} \ll 1 \Rightarrow S_E(m, r, N) \gg 1 \quad (4.4)$$

For MSE analysis, the original EEG time-series $\{x_1, \dots, x_i, \dots, x_N\}$ is coarse-grained into consecutive time-series $\{y^{(\tau)}\}$, each corresponding to a scale factor (SF) τ - first the original time-series is divided into non-overlapping windows of length τ , and then the data points inside each window are averaged, so each coarse-grained time-series is defined by

$$y_j^{(\tau)} = \left(\frac{1}{\tau} \right) \sum_{i=(j-1)\tau+1}^{j\tau} x_i, \quad 1 \leq j \leq \frac{N}{\tau} \quad (4.5)$$

with the length of each coarse-grained time-series being τ times shorter than the length N of the original series. S_E is then calculated for each time-series $\{y^{(\tau)}\}$ to generate the MSE results. Figure 4.2 shows a schematic illustration of the coarse-graining procedure (adapted from Costa et al., 2005).

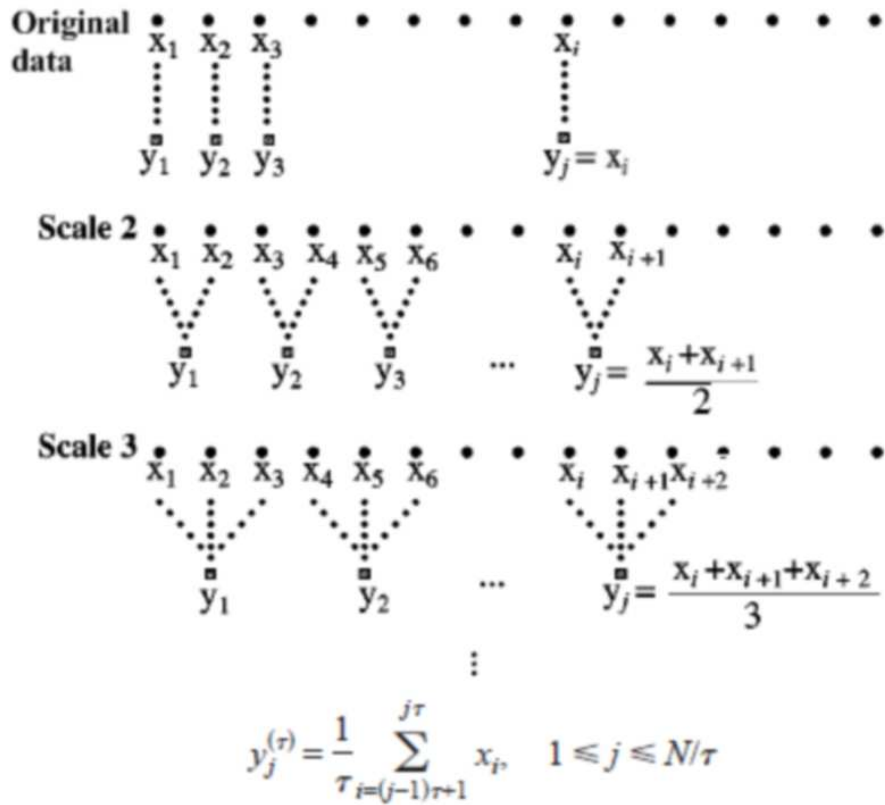


Figure 4.2 - Schematic illustration of the coarse-graining procedure. Adapted from Costa et al. (2005).

Previous studies have shown that S_E has a good statistical validity for $m = 1$ or $m = 2$ and $0.1 \leq r \leq 0.25$ times the SD of the time series (Lake et al., 2002, Richman et al., 2004). In this study values of $m = 2$, $r = 0.15 \cdot \text{SD}$, $N = 40\,000$ data points and 40 scale factors were used, so that for the shortest coarse-grained time-series there were still $N/\tau = 40\,000/40 = 1000$ data points, which is enough to obtain reliable estimation of the S_E value (Richman and Moorman, 2000).

4.2.5. POWER ANALYSIS

It is possible that differences in EEG complexity values are correlated with differences in EEG power spectra between groups (Takahashi et al., 2009). In order to investigate this a conventional power analysis was performed in the first 40 s of artefact free EEG data for each participant. This analysis

was performed using a built in function (pwelch) in MATLAB software (version 7.10.0). This function implements Welch's method to compute the periodogram, optimising the trade-off between frequency resolution and estimation variability of the ensuing spectrum.

To perform the power analysis the data was divided into 8 sections of equal length, each with 50% overlap. Each segment was then windowed with a Hamming window and spectral density (power/frequency) was calculated using a fast Fourier transform (FFT). Four standard band frequencies were studied: theta (4-8 Hz), alpha (8-13 Hz), beta (13-30 Hz) and gamma (30-40 Hz). The relative power at each frequency band was calculated as the power in each frequency band divided by total power across all frequency bands.

4.2.6. STATISTICAL ANALYSIS

Statistical analyses were carried out using SPSS Statistics 17.0 software with the alpha significance value set at 0.05. To test for differences in behavioural results, a 2-way repeated-measures analysis of variance (ANOVA) was done for accuracy and response time, with group (ASC vs. Controls) as a between-subjects factor, and task (chairs vs. face) as a within-subjects factor. Group comparisons of accuracy and response time were done for each task using a one-way ANOVA. In order to reduce the skewness in the distributions, response time data was transformed using a logarithmic function ($f(x) = \ln(x)$) and proportional accuracy was transformed using an arcsin function ($f(x) = \arcsin(\sqrt{x})$) (McDonald, 2009).

Distribution normality of MSE values was confirmed by use of the Kolmogorov-Smirnov normality test and examination of skewness and kurtosis values, for each electrode and each group. To test for group differences in complexity a 4-way repeated-measures ANOVA was performed, with group (ASC vs. Controls) as a between-subjects factor, and task (chair vs. face), SF (τ : 40 scales) and electrode (21 electrodes: C3, C4, Cp3, Cp4, F7, F8, Fc3, Fc4, Ft7, Ft8, P3, P4, P7, P8, T7, T8, Tp7, Tp8, Cz, Oz, Pz) as within-subjects factors.

To test for group differences in EEG power spectra a 4-way repeated-measures ANOVA was used, with group as a between-subjects factor, and task, electrode and frequency band (4 frequency bands: theta, alpha, beta, gamma) as within-subjects factors. The Greenhouse-Geisser adjustment (Field, 2009) was applied to the degrees of freedom for all analyses and the Bonferroni correction was applied for all post-hoc tests.

4.3. RESULTS

4.3.1. BEHAVIOURAL PERFORMANCE

Regarding accuracy, there was no significant group-by-task interaction ($F_{1, 28} = 3.661$, $P = 0.066$) or effect of group ($F_{1, 28} = 2.409$, $P = 0.132$), but there was a significant effect of task ($F_{1, 28} = 4.898$, $P = 0.035$) with higher accuracy for the chairs than for the faces task, across both groups. Regarding response time, no significant effects of group ($F_{1, 28} = 1.214$, $P = 0.280$) or task ($F_{1, 28} = 0.606$, $P = 0.443$) were observed. The group-by-task interaction was also non-significant ($F_{1, 28} = 0.740$, $P = 0.397$). Further details on the participants' accuracy and response times can be found in Table 4.2.

Behavioural Results					
	Controls (n = 15)		ASC (n = 15)		Group comparison
	Mean	SD	Mean	SD	
Chair task:					
Accuracy (out of 10)	9.73	0.59	9.60	0.91	$F_{1, 29} = 0.071$; $P = 0.791$
Response time (ms)	479.01	83.43	514.10	70.47	$F_{1, 29} = 1.907$; $P = 0.178$
Face task:					
Accuracy (out of 10)	9.73	0.46	8.80	1.47	$F_{1, 29} = 4.566$; $P = 0.041$
Response time (ms)	493.12	88.46	515.34	84.36	$F_{1, 29} = 0.572$; $P = 0.456$

Table 4.2 – Accuracy (out of 10) and response times (in ms) for both tasks, for each group.

4.3.2. MSE ANALYSIS

The results of the MSE analysis show a main effect of group in which the sample entropy was higher across all scale factors in the Control group (Mean = 1.33, SD = 0.23) than in the ASC group (Mean = 1.12, SD = 0.29, $F_{1, 28} = 4.859$, $P = 0.036$). This was qualified by a significant group-by-scale factor (SF) interaction ($F_{1.936, 54.195} = 4.914$, $P = 0.012$). This interaction arises from a difference between groups in sample entropy curves profiles, when collapsing across task and electrode, i.e. the curves for each group have different characteristics, starting together for both groups but with different slopes for higher SF, as can be seen for example in the graphs for electrode T7 in Figure 4.5. Specifically in this study, relative to the Control group, there is a decrease in the values of sample entropy in the ASC group as the SF increases (see Figures 4.3 and 4.4 reflecting group differences in sample entropy for increasing SF in each task). Although the difference between groups is not noticeable for smaller SF, the curves for both groups become distinguishable for higher SF, representing greater group differences in sample entropy at higher SF. It is this difference in curve profile between groups for smaller and higher SF that drives the significant group-by-SF interaction found (Figure 4.5).

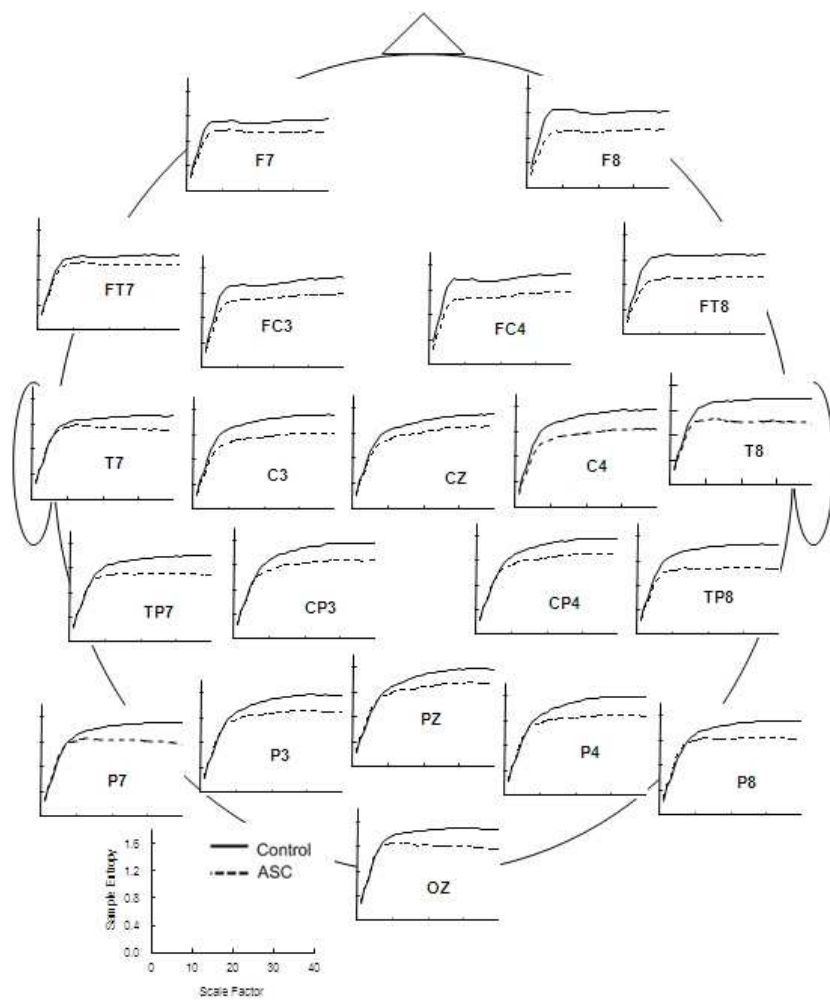


Figure 4.3 - Sample entropy by scale factor (SF) graphs for the chairs task, for each electrode, for each group (full line – Control group, dashed line – ASC group).

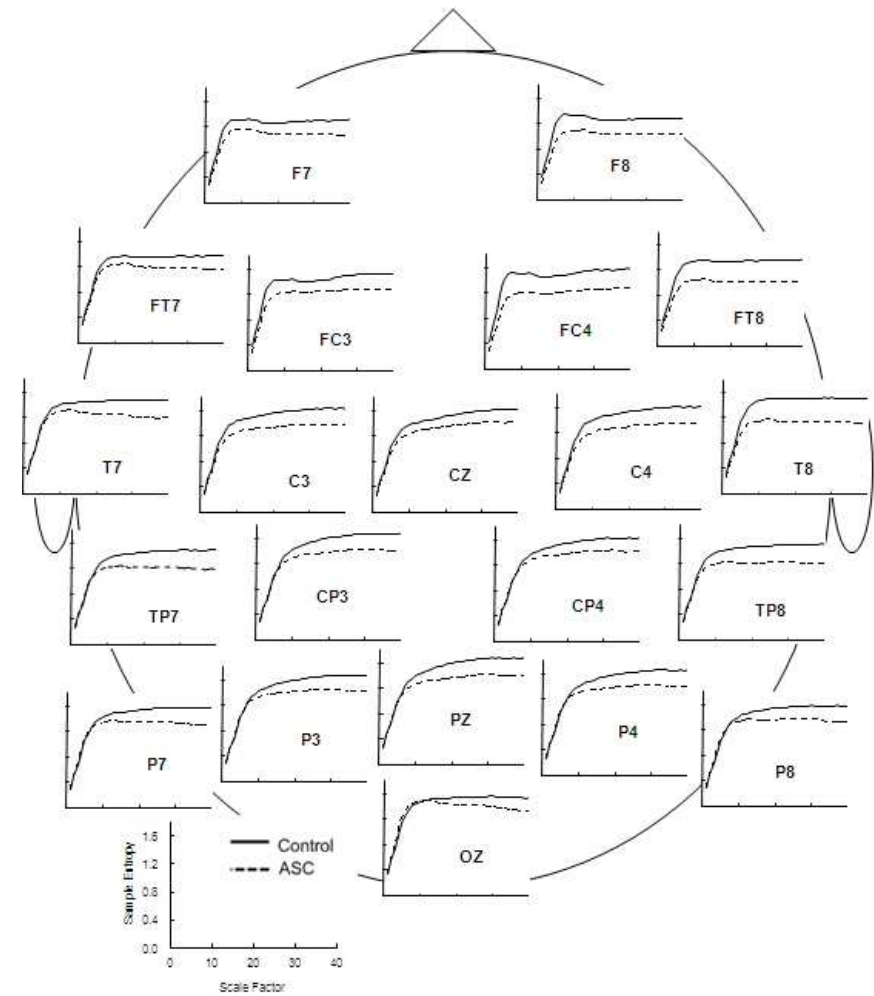


Figure 4.4 - Sample entropy by scale factor (SF) graphs for the faces task, for each electrode, for each group (full line – Control group, dashed line – ASC group).

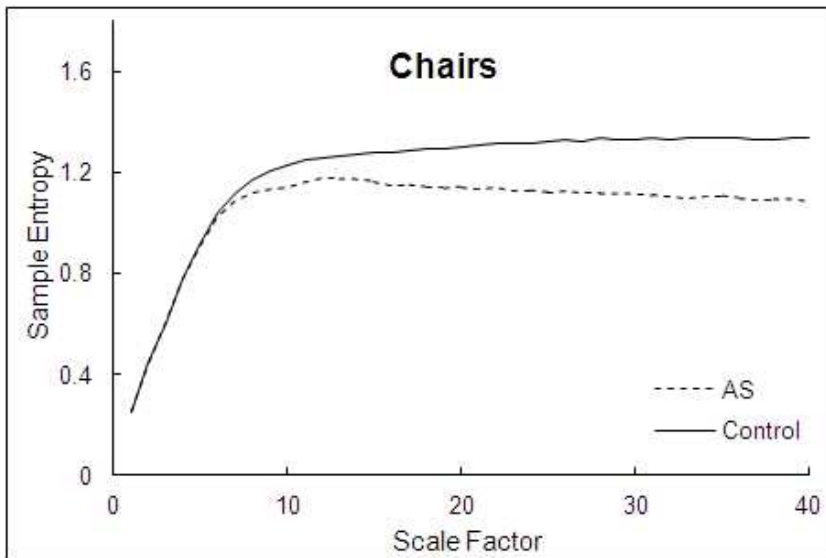
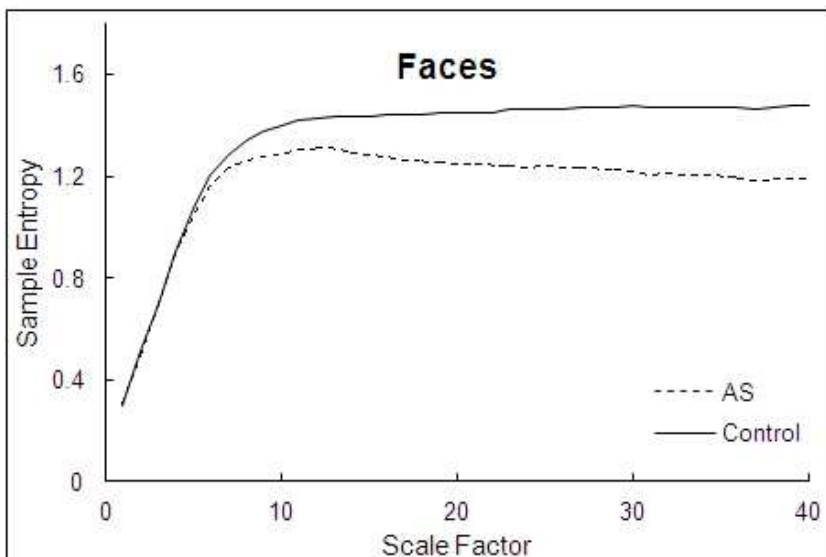


Figure 4.5 - Sample entropy by scale factor (SF) graphs for electrode T7, for both chairs and faces task. Group differences in curve slope for higher scale factors give rise to a significant group-by-scale factor interaction.



The results also showed a significant main effect of task ($F_{1, 28} = 6.719$, $P = 0.015$), with higher entropy associated with the faces (Mean = 1.28, SD = 0.31) than the chairs task (Mean = 1.17, SD = 0.29), across both groups. However, there was no significant interaction between task and participant group ($F_{1, 28} = 0.067$, $P = 0.797$).

A significant group-by-SF-by-electrode interaction ($F_{7.637, 213.829} = 4.262$, $P < 0.0005$) was also found. Although independence of measurement cannot be assumed for each electrode, this interaction was explored further in a post-hoc 2-way ANOVA (group-by-SF) for each electrode, to investigate differences in group-by-SF interactions between distant regions of the cortex. These results are shown in Table 4.3.

Group-by-SF ANOVA	
Electrode	Group-by-SF Interaction
C3	$F_{1.982, 55.502} = 4.432$; $P = 0.017$
C4	$F_{1.799, 50.360} = 3.629$; $P = 0.038$
Cp3	$F_{1.832, 51.293} = 6.405$; $P = 0.004$
Cp4	$F_{1.675, 46.897} = 5.071$; $P = 0.014$
F7	$F_{2.465, 69.023} = 1.060$; $P = 0.363$
F8	$F_{2.174, 60.870} = 1.160$; $P = 0.323$
Fc3	$F_{2.306, 64.560} = 1.467$; $P = 0.237$
Fc4	$F_{2.207, 61.805} = 1.730$; $P = 0.183$
Ft7	$F_{2.265, 63.432} = 1.267$; $P = 0.291$
Ft8	$F_{1.915, 53.609} = 3.085$; $P = 0.056$
P3	$F_{1.692, 47.378} = 6.047$; $P = 0.007$
P4	$F_{1.641, 45.941} = 8.268$; $P = 0.002$ *
P7	$F_{1.997, 55.927} = 7.748$; $P = 0.001$ *
P8	$F_{1.659, 46.445} = 6.844$; $P = 0.004$
T7	$F_{2.246, 62.875} = 4.806$; $P = 0.009$
T8	$F_{1.742, 48.780} = 5.028$; $P = 0.013$
Tp7	$F_{2.234, 62.542} = 8.217$; $P < 0.0005$
Tp8	$F_{2.092, 58.584} = 6.930$; $P = 0.002$ *
Cz	$F_{1.873, 52.452} = 2.153$; $P = 0.129$
Pz	$F_{1.579, 44.206} = 5.691$; $P = 0.010$
Oz	$F_{1.756, 49.158} = 5.843$; $P = 0.007$

Table 4.3 - Group-by-scale factor (SF) interaction significance values for each electrode site. Electrode sites in bold showed a significant ($P \leq 0.05$) group-by-SF interaction; electrode sites marked by * showed a significant ($P \leq 0.05$) group-by-SF interaction after Bonferroni correction ($P_{\text{corrected}} = P_{\text{uncorrected}} * 21$ electrode sites).

A significant group-by-SF interaction was found in electrode sites C3, C4, Cp3, Cp4, T7, T8, Tp7, Tp8, P3, P4, P7, P8, Pz and Oz, as shown in Figure 4.6. After correcting for multiple statistical testing using the Bonferroni correction ($P_{\text{corrected}} = P_{\text{uncorrected}} \times 21$ electrodes), a significant group-by-SF interaction was still evident in electrodes Tp7, Tp8, P7 and P4 (Figure 4.6). These group-by-SF interactions should not be confused with between group differences in mean sample entropy, calculated from the average of sample entropy values across scale factors for each group.

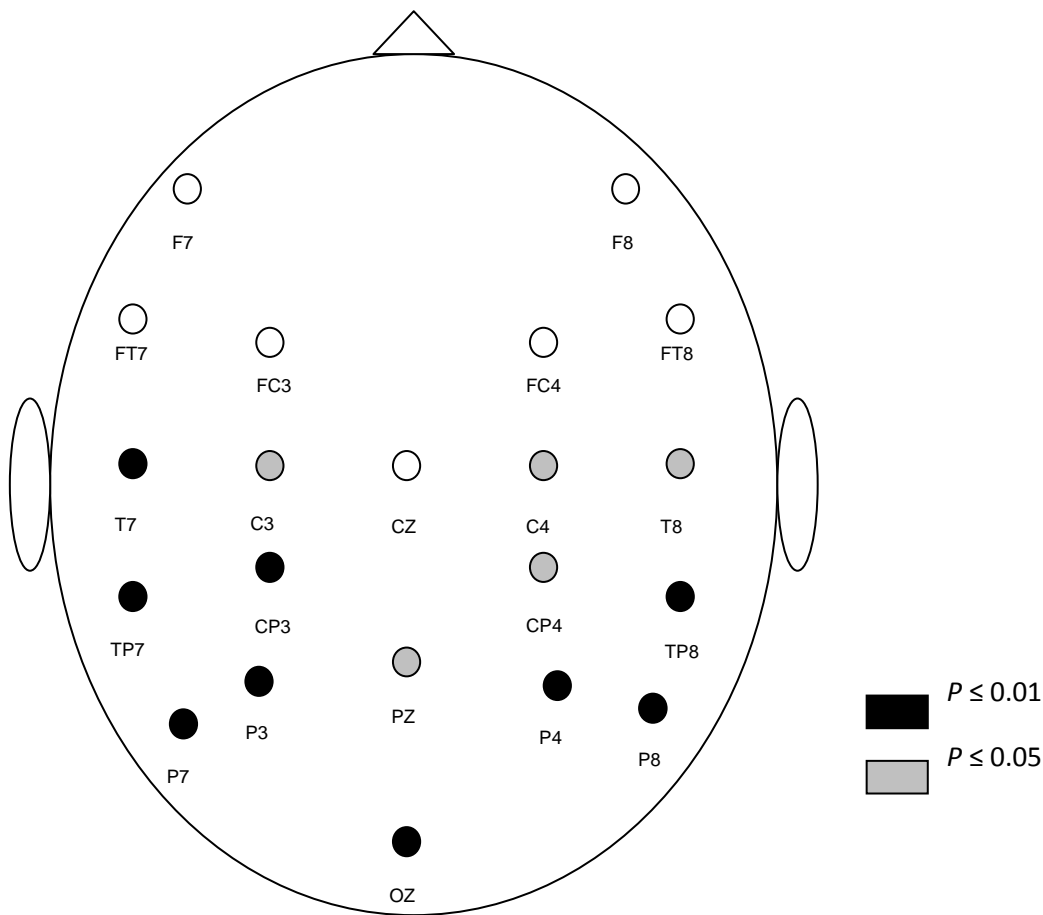


Figure 4.6 – Electrodes that presented a significant group-by-scale factor (SF) interaction. For electrode sites shaded gray, the group-by-SF interaction was significant at $P \leq 0.05$, whilst for electrode sites shaded black, this interaction was significant at $P \leq 0.01$. Group-by-SF interactions remained significant ($P \leq 0.05$) after Bonferroni correction ($P_{\text{corrected}} = P_{\text{uncorrected}} \times 21$ electrode sites) at electrode sites Tp7, P7, Tp8 and P4.

4.3.3. POWER ANALYSIS

No significant effects of group ($F_{1, 28} = 1.895$, $P = 0.180$) or task ($F_{1, 28} = 0.082$, $P = 0.776$) were found. Group-by-frequency band ($F_{1.949, 54.584} = 1.545$, $P = 0.223$) and task-by-frequency band ($F_{2.170, 60.765} = 2.074$, $P = 0.131$) interactions were also not significant.

4.4. DISCUSSION

The present study found reduced sample entropy in EEG signals acquired during a visual matching task in people with ASC, relative to controls, at higher SF, as indexed by a significant group-by-SF interaction. This interaction reflects a difference in curve behaviour which serves as an index for measuring signal

complexity - systems with higher complexity will present higher values of sample entropy, sustained over increasing values of SF (Costa et al., 2002, 2005). This is due to the fact that values of sample entropy sustained over increasing values of SF suggest the existence of a power-law scaling property, which is a characteristic of nonlinearity and intrinsic complexity in physiological systems (Takahashi et al., 2009). These results support the hypothesis that the complexity of electrical brain activity is reduced in people with ASC, possibly in association with relatively reduced long-range temporal correlations in brain activity (Takahashi et al., 2009) in response to the visual task employed in this study.

Concerning power analysis, whilst some investigations report findings of atypical EEG power in people with ASC when compared to typically developing controls (Oberman et al., 2005, Isler et al., 2010, Leveille et al., 2010), others present no evidence of EEG power differences between these two groups (Raymaekers et al., 2009). The lack of significant differences in EEG power spectra between groups or tasks in the current study establishes a distinction between complexity measures and power spectrum analysis; changes in complexity values were not a reflection of changes in EEG power spectra. This is in accordance with previous studies reporting the absence of abnormal patterns in EEG power spectra in individuals with ASC (Milne et al., 2009, Raymaekers et al., 2009).

ASC have long been associated with atypical patterns of neural connectivity (Belmonte et al., 2004b, Courchesne and Pierce, 2005b, Just et al., 2007, Barttfeld et al., 2011, Wass, 2011). Given the findings of previous research demonstrating that changes in local complexity may be related to changes in brain connectivity (Friston, 1996, Sakalis et al., 2008), it can be hypothesized that the findings of the current study may be associated with atypical neural connectivity in ASC. Supporting this hypothesis is the work by Bosl et al. (2011), showing a pattern of reduced EEG complexity for infants at high-risk of ASC, at early stages of brain development (6 to 24 months). Those authors considered that local neural connectivity, which undergoes rapid changes during early brain development, may be reflected in variations of EEG signal complexity at these early stages, suggesting the possibility of EEG complexity being used in the future as a biomarker for ASC risk. However, for their analysis Bosl et al. (2011) employ classification algorithms to data acquired from infants at risk of ASC (by virtue of having an older sibling with a diagnosis of ASC), but provide no information on the proportion of infants receiving a formal diagnosis of ASC in later years. Additionally, issues of sensitivity and specificity not addressed by those authors suggest that the development of a biomarker for ASC may not be readily achieved.

Nevertheless the results of the current study can be considered complementary to those reported by Bosl et al. (2011) - whilst their findings indicated decreased complexity in resting state EEG in infants at risk of developing an ASC, the current study demonstrates the presence of reduced EEG complexity in adults with a confirmed diagnosis of ASC, relative to typical controls, supporting the hypothesis that EEG

complexity, as an index for neural processing of information and neural connectivity, is sensitive to the presence of an autistic condition.

As previously described in Chapter 1 of this thesis, electrical activity measured in a single scalp electrode may not have its origin in the cortex area directly underneath the electrode (Picton et al., 2000), so it is not possible to localize the differences observed in this study as arising from any specific cortical regions. However, volume conduction issues that affect source analysis are likely to have a smaller influence between distant cortical regions, and so a crude estimation of source location (in terms of frontal, temporal, parietal or occipital lobes) is still possible. In the current study a post-hoc analysis of the significant group-by-SF-by-electrode interaction was performed to explore the variation of group-by-SF interactions with cortical region. The results of this analysis suggest that the differences between groups are more evident in temporo-parietal and occipital regions of the cortex (Figure 4.6), areas known to subserve integrative functions during the processing of visual information (Belmonte et al., 2004b). These results are also in accordance with those of functional imaging studies of visuospatial processing in ASC, where differences in brain activity have been found between ASC and typically developing controls in the temporo-parietal junction and occipital regions of the cortex (Di Martino and Castellanos, 2003, Billington et al., 2008, Sahyoun et al., 2010). In addition, an earlier ERP analysis of the EEG data included in the current study demonstrated that the N170 ERP face response in posterior sites (P7 and P8) was less modulated by attention in the participants with ASC than in a neurotypical control group (Churches et al., 2010). This observation is compatible with the suggestion that the current MSE results may reflect a decrease in integrative capacity in the participants with ASC. Also of interest is the report by Bosl et al. (2011), who compared resting state EEG complexity of infants at high risk and low risk of ASC, of a pattern of reduced complexity for infants at high risk of ASC particularly in frontal regions of the brain. This is in contrast to the findings of the current study, in which group differences in EEG complexity were greater in posterior brain regions, during the performance of a visual matching task likely to involve temporo-parietal brain regions (Corbetta et al., 1993, Schultz et al., 2000, Deffke et al., 2007). This suggests that EEG complexity, as indexed by MSE measures, may be a marker for local disturbances in task-specific processing of information as well as for more non-specific associations of pervasive developmental disorders.

As well as potentially reflecting task-related neuronal activity, the results of the current study suggest the possibility that MSE may also be sensitive to how demanding a task is. In support of this proposition, it was noted that the face task was performed, across both groups, a little less accurately than the chair task, whilst at the same time, although overall entropy levels were lower in the ASC group, the analysis

revealed an increase in complexity of the EEG signal for the face task relative to the chair task, across both study groups. It is therefore possible that the decreased accuracy observed reflected increased difficulty of the faces task compared to the chairs task, and that the increase in MSE during performance of the face task was a reflection of brain response to greater task demands associated with attending to faces compared to non-face objects. It should be noted however that this possible interpretation of these facts is speculative and limited by the absence of a direct correlation between MSE indices and behavioural task performance. The nature of the tasks is an additional confound, in that while both required visual matching, the more 'difficult' task involved faces whilst the easier task involved chairs. In addition, subjective ratings of the perceived difficulty of the two tasks by the participants are not available. All these issues should be explored during future research in this topic.

However, the variation of MSE with task found in the present study is in line with the conclusion reported by Takahashi et al. (2009), who interpreted higher MSE values following photic stimulation in their healthy younger participants as reflecting the cortical response to the stimuli, and the decrease in MSE values for the elderly group as representative of an attenuated cortical response to photic stimulation. Thus, whilst in the current study those with ASC manifested overall lower entropy than the Control group, this group difference was not differentially modulated by the precise nature of the visual task and the ASC group, like the controls, responded to the faces with an increase in EEG complexity. A possible implication of these results is that the widely recognised atypical social and communication behaviours that characterise ASC are not the result of isolated disturbances in selective brain functions. Rather, they may reflect an overall change in brain functioning but since social, emotional and language functions make greater demands on neural networks and on relationships between neural networks (Minshew and Williams, 2007), these behaviours may be particularly vulnerable to deficits in integrative capacity.

Regarding the methods employed in this study, it is important to note that several approaches can be used to examine auto-correlations in complex physiological time series including the Hurst exponent (Lai et al., 2010), power spectral density analysis, the rate of moment convergence and MSE methods. In a comparison of these four approaches, Crevecoeur et al. (2010) concluded that MSE was the most appropriate method for examining long-range correlations in time series with more than 512 points - in the current study time series comprising a total of 40 000 points were examined, with a minimum of 1000 points for the shortest coarse-grained time-series.

Regarding task, although some MSE studies have investigated physiological complexity in resting conditions (Escudero et al., 2006, Hornero et al., 2009, Takahashi et al., 2010), others have employed activation or stressor tasks to explore complexity responses to stimuli or clinical processes of interest

(Takahashi et al., 2009, Sitges et al., 2010). Whilst there have been no MSE studies so far analysing resting state EEG from adults with a confirmed diagnosis of ASC, the results of the present study, together with those of Bosl et al. (2011), seem to suggest that the pattern of group differences observed in the current study is related to the fact that EEG signal was recorded during a visual task. However, this should be confirmed by future MSE studies of EEG data in ASC using resting state EEG data. If future studies confirm MSE measures as indexing task-specific patterns of EEG complexity, this might provide a new tool for the investigation of the temporal organization of neural networks subserving specific cognitive processes, and their possible perturbation in neurocognitive disorders.

Overall, the results of this study show a significant difference in complexity between the ASC and the Control group. Particularly, results show that there is a decrease in EEG complexity in the ASC group, when compared to the Control group, in occipital and parietal regions of the cortex. This supports the model of an inherent alteration in neuronal integration of information in people with ASC, in response to a visual matching task, which may be associated with relatively reduced long-range temporal correlations in EEG and atypical neural connectivity in people with ASC.

5. INTERHEMISPHERIC FUNCTIONAL CONNECTIVITY IN AUTISM

SPECTRUM CONDITIONS: AN EEG STUDY USING WAVELET COHERENCE

TRANSFORM

5.1. INTRODUCTION

5.1.1. COHERENCE AND CONNECTIVITY

As mentioned in Chapter 1 of this thesis, coherence is a tool commonly used in the analysis of neurophysiological signals. It computes the correlation between the spectral properties of two signals by measuring the level of synchronisation between signals generated by different cell populations (Lachaux et al., 2002, Nunez and Srinivasan, 2006). High coherence values reflect greater signal synchronisation and hence greater functional integration due to either direct cortico-cortical connections or indirect cortical-subcortical-cortical connections (Nunez and Srinivasan, 2006).

Coherence between signals from different EEG electrodes has traditionally been calculated using a Fast Fourier Transform (FFT) to determine the power in selected frequency bands across a large period of time. Whilst this method can deliver some insight into the connectivity between different brain regions, there is a serious limitation to the use of FFT in coherence analysis – given that coherence is calculated over a relatively long time period (usually one second), this methodology is incapable of providing information about the temporal structure of coherence (Lachaux et al., 2002). As previously discussed in Chapter 1 high temporal resolution is the great advantage that EEG has over other imaging methodologies and knowledge of the time points at which coherence is heightened or reduced is essential for an understanding of complex brain dynamics (Lachaux et al., 2002). At the practical level, a method of analysing coherence at different time points will allow for the analysis of coherence related to the perception of specific stimuli, rather than during a period of rest (Murias et al., 2007, Coben et al., 2008, Barttfeld et al., 2011) or sleep (Leveille et al., 2010).

A procedure called event-related coherence was developed to study the time course of coherence following a specific stimulus. In this method, the coherence between two signals is calculated for a given latency t post-stimulus onset, for each trial. Final values of coherence are then computed by averaging coherence measures across all trials (Rappelsberger et al., 1994, Lachaux et al., 2002). Although this

technique provides better temporal resolution than simple coherence, it assumes stationarity of cortical activity across trials, an assumption that has not yet been validated (Lachaux et al., 2002).

Another technique for the analysis of coherence as a function of time is Wavelet Transform Coherence (WTC) (Lachaux et al., 2002). This algorithm performs a time-frequency analysis of coherence by transforming the original signals using a wavelet function (mother wavelet) with a characteristic time t and frequency f . One of the most popular choices for mother wavelet is the Morlet wavelet. The wavelet coherence between two signals can then be calculated for any time-frequency bin, hence generating coherence values for the entire time-frequency spectrum and allowing for the analysis of coherence related to particular events in time, such as the presentation of sensory stimuli. WTC is similar to short-term Fourier coherence analysis (e.g. event-related coherence) in the way that both use a function in a time window to transform the original signals. However, in short-term Fourier analysis, the size of this time-window is fixed, which limits the frequency resolution of the coherence calculation. In WTC, the size of the time window is adapted to the frequency of the original signals, resulting in a more accurate time-frequency resolution (Lachaux et al., 2002). More details on the properties of the wavelet function and the WTC algorithm can be found in the Methods section of this chapter.

5.1.2. COHERENCE AND CONNECTIVITY IN ASC

As mentioned in Chapter 1 the connectivity model is one of the most commonly cited explanatory models of atypical brain functioning in ASC. According to this model, atypical patterns of functional connectivity between neural networks in the ASC brain, including increased short-range connectivity and decreased long-range connectivity, may act as a neurological substrate for the full range of observed behavioural and cognitive characteristics of ASC (Brock et al., 2002, Belmonte et al., 2004a, Belmonte et al., 2004d, Courchesne and Pierce, 2005c, Rippon et al., 2007) (for recent reviews see Neul, 2011, Wass, 2011).

Evidence to support the connectivity model comes from multiple methods of neuroanatomical and neurofunctional measurement. Several studies have shown abnormal trajectories of brain growth in ASC, more specifically faster growth in the first years of life followed by a premature cessation of growth (Lainhart et al., 1997a, Courchesne et al., 2001a, Courchesne et al., 2003a, for review see Courchesne and Pierce, 2005a). It is considered that this growth pathology in the first years of life disrupts development of neural circuitry that is essential for higher order social, language and cognitive functions (Courchesne and Pierce, 2005a). Of particular interest to the current study are the findings of thinning of the corpus callosum in ASC (Courchesne et al., 1993, Hughes, 2007) - according to previous

investigations (Chung et al., 2004, Boger-Megiddo et al., 2006, Vidal et al., 2006) white matter density appears to be decreased in the genu, rostrum and splenium of the corpus callosum in people with ASC, reflecting decreased interhemispheric connectivity in this group, relative to typically developing controls. Diffusion Tensor Imaging has also shown decreased white matter integrity and connectivity in ASC (Haueisen et al., 2002, Barnea-Goraly et al., 2004b, Lee et al., 2007, Sundaram et al., 2008, Sahyoun et al., 2010). Another technique, Dynamic Causal Modeling, has revealed decreased functional connectivity in ASC during tasks involving the extrapolation of the affective meaning of abstract shapes (Castelli et al., 2002) and real actions (Grezes et al., 2009), as well as the perception of emotionally expressive faces (Monk et al., 2010). Moving from functional imaging in vivo to cytoarchitectural analysis of brain samples, it has been shown that ASC is associated with narrower minicolumns and decreased inter-column spacing in frontal and temporal areas (Casanova and Trippe, 2009). These anatomical alterations are likely to disrupt formation of long-range connections between neural networks, consequently impairing systems involved in top-down control and integration of information (Casanova and Trippe, 2009). Finally, the analysis of EEG signals has provided evidence of long-range functional underconnectivity along with short-range over-connectivity in ASC as reflected by atypical EEG signal coherence when compared to typically developing controls (Barttfeld et al., 2011).

In Chapter 4 of this thesis a study of EEG complexity has shown evidence of decreased signal complexity in parietal and occipital sites in individuals with ASC, when compared to typically developing controls, suggesting decreased neural connectivity in these regions for the ASC group (Catarino et al., 2011). Additionally, two other ASC models - the weak central coherence model (Frith, 1989) and the executive dysfunction model (Pennington and Ozonoff, 1996) - are based on observations suggesting an aetiological role for decreased neural connectivity in ASC (Just et al., 2004), particularly with frontal regions (Koshino et al., 2008).

Regarding coherence specifically, studies using standard coherence algorithms have found evidence of decreased intrahemispheric coherence in ASC between frontal and other scalp sites along with increased coherence within frontal and temporal (Murias et al., 2007), lateral frontal (Barttfeld et al., 2011) and occipital sites (Leveille et al., 2010). Decreased interhemispheric coherence in ASC has been found across frontal, parietal (Coben et al., 2008) and occipital sites (Isler et al., 2010). All these reports performed their analysis in EEG data of subjects during resting state or sleep, with the exception of Isler et al. (2010) who have run their analysis in EEG recordings of individuals receiving visual flash stimulation. Their results are suggestive of atypical interhemispheric coherence in ASC, when compared to typical controls, in response to visual stimuli.

5.1.3. AIMS OF THE STUDY

The first aim of the current study was to test the hypothesis of reduced interhemispheric coherence in ASC, arising out of earlier anatomical (Chung et al., 2004, Boger-Megiddo et al., 2006, Vidal et al., 2006) and functional (Coben et al., 2008, Isler et al., 2010) reports of decreased interhemispheric connectivity in people with this condition. Particularly, taking into consideration the results of Isler et al. (2010) suggestive of atypical interhemispheric coherence in ASC in response to visual stimuli, the current study aimed to test the hypothesis that participants with ASC would, during the performance of a visual recognition task, manifest reduced interhemispheric coherence compared to a group of matched controls. An additional advantage of this approach is that coherence is calculated between signals measured by electrodes located on different brain hemispheres, reducing the influence of volume conduction issues previously described in Chapters 1 and 4 of this thesis.

Secondly, this study aimed to investigate variations of interhemispheric coherence with task for each group. A social (visual recognition of faces) and a non-social (recognition of chairs) task were included in the current study. Given the social difficulties that characterize ASC, along with evidence from previous research showing impairment in the visual processing of faces in people with ASC (Dawson et al., 2005, Golarai et al., 2006, Kleinhans et al., 2008), it was hypothesized that whilst the Control group would present differences in interhemispheric coherence between the faces and the chairs task, such differentiation would not be seen for the ASC group.

Finally, the present study aimed to take advantage of the temporal and frequency specificity of the WTC approach to ascertain whether there are time-frequency specific effects on group differences in coherence related to task and brain location (coarsely defined as frontal, temporal, parietal and occipital lobes).

5.2. METHODS

The dataset used for this study was the same as the one used for the study described in Chapter 4.

5.2.1. PARTICIPANTS

All participants in this study gave informed written consent. Fifteen patients with ASC and fifteen typical controls were recruited for this study. Participants in this study were the same as the ones in the study described in Chapter 4. Further details on participant recruitment criteria can be found in Chapter 4.

As mentioned in Chapter 4, participants were administered the Wechsler Abbreviated Scale of Intelligence (WASI; (Wechsler, 1999) for IQ assessment and the Autism Quotient (AQ; (Baron-Cohen et al., 2001)) for an evaluation of the number of ASC traits. Participants' demographic details and their IQ and AQ scores are presented in Table 4.1.

5.2.2. EEG RECORDING

Details on the parameters used for EEG data acquisition can be found in Chapter 4. The EEG was recorded whilst participants performed a face and chair detection task. More details on these tasks can also be found in Chapter 4.

5.2.3. SIGNAL ANALYSIS

EEG epochs were extracted from artefact free sections of the EEG recordings using the SCAN software package (Compumedics, Neuroscan), for two distinct tasks – for the face task, epochs chosen included those where a picture of a face was presented, when the subjects' attention was directed to faces; for the chair task, selected epochs included those where a picture of a chair was presented, when the subjects' attention was directed to chairs. Motion and eye blink artifacts were identified visually and epochs affected by these (from the initial number of 90) were excluded from the analysis. Despite this, the number of epochs included in the analysis did not differ significantly between groups (mean ASC = 162 (SD = 16), mean Control = 163 (SD = 16), $F_{1, 29} = 0.016$, $p = 0.901$) or task (Chair task: mean ASC = 81 (SD = 9), mean Control = 80 (SD = 9), $F_{1, 29} = 0.183$, $p = 0.672$; Face task: mean ASC = 81 (SD = 8), Mean Control = 83 (SD = 7), $F_{1, 29} = 0.569$, $p = 0.457$). The time-bin for each epoch was 0 to 400 ms post-stimulus presentation. The WTC algorithm, with a Morlet wavelet length of 4 cycles, was applied to each epoch separately, with coherence values being calculated for each time point (resolution of 1 ms) and for a range of frequency values between 5 and 40 Hz (frequency resolution varying between approximately 0.5 Hz for the lowest frequencies and 2 Hz for the highest frequencies). Coherence maps for the entire time-frequency space (0 ms to 400 ms post-stimulus onset, 5 Hz to 40 Hz) were calculated by averaging coherence values across all epochs. Analyses were run separately for the chairs and for the faces tasks. Electrodes Fp1, Fp2 and Fz were excessively affected by eye movement artefacts and were removed from the analysis. Technical problems affected electrodes F3 and O2 during data acquisition for some participants. Therefore electrode pairs F3/F4 and O1/O2 were also excluded from the analysis.

Statistical group and task comparisons were undertaken for available interhemispheric electrode pairs: F7-F8, FT7-FT8, T7-T8, TP7-TP8 and P7-P8. These pairs were included based on previous reports of atypical interhemispheric neural connectivity in people with ASC, in the context of visual or face processing tasks (Coben et al., 2008, Churches et al., 2010, Isler et al., 2010).

5.2.4. WAVELET TRANSFORM COHERENCE

Let x and y be two stationary signals. Let S_{xx} and S_{yy} denote the autospectral densities (i.e. the Fourier transform of the autocorrelation function) of x and y respectively, and S_{xy} the cross-spectral density between x and y . The coherence between waveforms x and y can then be defined, at the frequency of interest f , as (Lachaux et al., 2002):

$$\varrho(f) = \frac{|S_{xy}(f)|}{[S_{xx}(f) \cdot S_{yy}(f)]^{\frac{1}{2}}} \quad (5.1)$$

However, this theoretical value of coherence can only be computed for waveforms of infinite duration. In real situations, with finite time-series, the coherence value is computed through approximation – the finite time-series x and y are divided into N overlapping segments, x_j and y_j , $j = 1, \dots, N$. Each segment is multiplied by a weighting function (e.g.: Hamming window), and for each weighted segment the discrete Fourier coefficients are computed:

$$\tilde{x}_j(f) = \int x_j(t) e^{-i2\pi f t} dt \quad (5.2)$$

$$\tilde{y}_j(f) = \int y_j(t) e^{-i2\pi f t} dt \quad (5.3)$$

For each segment, the cross-spectrum coefficient is calculated:

$$c_j(f) = \tilde{x}_j(f) \cdot \tilde{y}_j^*(f) \quad (5.4)$$

The cross-spectral density estimation is defined by the average of the coefficients c_j over the N segments:

$$S_{xy}(f) \approx \tilde{S}_{xy}(f) = \frac{1}{N} \sum_{j=1}^N c_j(f) = \frac{1}{N} \sum_{j=1}^N \tilde{x}_j(f) \cdot \tilde{y}_j^*(f) \quad (5.5)$$

The same approximation can be done for the autospectral densities:

$$\tilde{S}_{xx}(f) = \frac{1}{N} \sum_{j=1}^N \tilde{x}_j(f) \cdot \tilde{x}_j^*(f) \quad (5.6)$$

$$\tilde{S}_{yy}(f) = \frac{1}{N} \sum_{j=1}^N \tilde{y}_j(f) \cdot \tilde{y}_j^*(f) \quad (5.7)$$

leading to an estimation of coherence defined as

$$\tilde{q}(f) = \frac{|\tilde{S}_{xy}(f)|}{[\tilde{S}_{xx}(f) \cdot \tilde{S}_{yy}(f)]^{\frac{1}{2}}} \quad (5.8)$$

However, most physiological signals are non-stationary, and in this case methods based on simple Fourier analysis are inadequate – the weighted segments would correspond to multiple sub-processes with different spectral properties, and averaging the spectral estimates of these segments would be meaningless (Lachaux et al., 2002).

In an attempt to improve the temporal resolution of coherence calculations, and to be able to study the time-course of coherence, alternative algorithms were created. One example is event related coherence (ERC), an algorithm usually employed to investigate the time course of coherence of cortical activity following a sensory stimulus. In ERC, for original signals x and y , a weighted segment centered around a latency t post stimulus onset ($t \pm \delta$) is extracted for each trial. If there are N trials, the discrete Fourier coefficients and the cross-spectrum coefficients are calculated for each trial (equations 5.2 to 5.4). An estimation of coherence for the latency t will be obtained by averaging the cross-spectrum coefficients over the N trials and then using these values to calculate the cross and autospectral densities (equations 5.5 to 5.8).

In ERC the spectral densities are not averaged over time and so the problem of non-stationarity is mitigated. It is however, replaced by the problem of the assumption of stationarity across trials. As already mentioned in the Introduction of this chapter, this assumption has not yet been validated (Rappelsberger et al., 1994, Lachaux et al., 2002).

As ERC, wavelet coherence transform (WTC) analysis mitigates the problem of temporal non-stationarity by providing a time-frequency analysis of the coherence between two signals x and y . The advantage of WTC when compared to ERC is that whilst ERC uses a time-window of fixed size as a weighting function, in WTC the size of the time window is adapted to the frequency of the original signals, resulting in better time-frequency resolution (Lachaux et al., 2002).

In WTC analysis, each signal x and y is wavelet transformed, i.e. multiplied by a weighting wavelet function, which is a complex valued function with zero average. Although there are many wavelet functions (e.g. Paul, Mexican hat, Meyer), one of the most commonly used for computing coherence in physiological signals, and also the one used in the current study, is the Morlet wavelet. The Morlet wavelet, consisting of the product of a sinusoidal wave at frequency f and a Gaussian function centered at time τ and with standard deviation σ ($\sigma \propto \frac{1}{f}$), can be defined as (Lachaux et al., 2002):

$$\Psi_{\tau,f}(u) = \sqrt{f} e^{i2\pi f(u-\tau)} e^{-\frac{(u-\tau)^2}{\sigma^2}} \quad (5.9)$$

Due to the fact that the standard deviation of the Gaussian function is inversely proportional to frequency f , the wavelet will be narrower in time the higher the frequency, i.e. the temporal resolution of the coherence estimate improves when frequency increases.

The wavelet transform of a given signal x at time τ and frequency f is therefore given by:

$$W_x(\tau, f) = \int_{-\infty}^{+\infty} x(u) \cdot \Psi_{\tau,f}^*(u) du \quad (5.10)$$

From this one can define the wavelet auto and cross-spectral density, respectively, as

$$SW_{xx}(t, f) = \int_{t-\frac{\delta}{2}}^{t+\frac{\delta}{2}} W_x(\tau, f) \cdot W_x^*(\tau, f) d\tau \quad (5.11)$$

and

$$SW_{xy}(t, f) = \int_{t-\frac{\delta}{2}}^{t+\frac{\delta}{2}} W_x(\tau, f) \cdot W_y^*(\tau, f) d\tau \quad (5.12)$$

Analogous to ordinary Fourier-based coherence, wavelet coherence between signals x and y is defined at time t and frequency f by:

$$WCo(t, f) = \frac{|SW_{xy}(t, f)|}{[SW_{xx}(t, f) \cdot SW_{yy}(t, f)]^{\frac{1}{2}}} \quad (5.13)$$

where $WCo(t, f)$ takes values between 0 (no coherence) and 1 (maximum coherence), and the time resolution of the estimated coherence is inversely proportional to the frequency in which it is computed (Lachaux et al., 2002, Klein et al., 2006).

5.2.5. STATISTICAL ANALYSIS

Statistical analyses were carried out using SPSS Statistics v17.0 software and the statistical analysis package R. The alpha significance values were set at 0.05.

To test for differences in behavioural results, a 2-way repeated-measures analysis of variance (ANOVA) was done for accuracy and response time, with group (ASC vs. Control) as a between-subjects factor, and task (chairs vs. faces) as a within-subjects factor. In order to reduce the skewness in the distributions, response time data was transformed using a logarithmic function ($f(x) = \ln(x)$) and proportional accuracy was transformed using an arcsin function ($f(x) = \arcsin(\sqrt{x})$).

Statistical software package R was used to run Mann-Whitney analyses over the full time-frequency range (36 frequency points (ranging from 5 to 40 Hz) by 401 time points (ranging from 0 to 400 ms post-stimulus onset)), to assess significant differences in WTC values between groups (ASC vs. Control) and tasks (chairs vs. faces), for all electrode pairs (F7-F8, FT7-FT8, T7-T8, TP7-TP8 and P7-P8). This approach is consistent with previous studies applying the WTC algorithm to the analysis of EEG data (Klein et al., 2006). Additionally, correction for multiple comparisons was performed using a False Discovery Rate (FDR) algorithm implemented using the R software package. Significant group differences are presented in time-frequency maps, where p-values smaller than 0.05 are represented in a grey scale. The Greenhouse-Geisser adjustment was applied to the degrees of freedom for all analyses (Field, 2009).

5.3. RESULTS

5.3.1. BEHAVIOURAL PERFORMANCE

Regarding accuracy, there was no significant group-by-task interaction or effect of group, but there was a significant effect of task with higher accuracy for the chairs than for the faces task, across both groups. Regarding response time, no significant effects of group or task were observed and the group-by-task interaction was also non-significant. Further details on the participants' accuracy, response times and statistical analysis can be found in section 4.3.1 and Table 4.2.

5.3.2. WTC ANALYSIS

Mann-Whitney analyses of interhemispheric coherence revealed various patterns of significant group differences. There were patterns of significantly decreased coherence for the ASC group when compared to the Control group, for both tasks (chairs and faces) and for all the electrode pairs studied, at $p_{\text{uncorrected}} < 0.05$ (Figures 5.1 and 5.2). Across both tasks this relatively decreased coherence in the ASC group was observed largely for frequencies below about 13 Hz and, except at the parietal electrode pair, only at times later than about 150 ms post stimulus onset. After correcting for multiple comparisons, group differences in interhemispheric coherence remained significant at $p_{\text{FDR-corrected}} < 0.05$ for one electrode pair (T7-T8) and for the faces task only. These group differences remained significant ($p_{\text{FDR-corrected}} < 0.05$) for a time-frequency window around 300 ms post-stimulus onset and between 7 and 10 Hz (Figure 5.3).

No regions of increased coherence for the ASC group when compared to the Control group were found, for any task or electrode pair, at $p_{\text{uncorrected}} < 0.05$.

Regarding within-group task comparisons at $p_{\text{uncorrected}} < 0.05$, whilst the Control group presented differences in interhemispheric coherence between faces and chairs tasks at various electrode pairs (increased coherence for chairs relative to faces at electrode pair TP7-TP8, decreased coherence for chairs relative to faces at electrode pairs FT7-FT8, TP7-TP8, P7-P8), such differences were only seen for one electrode pair in the ASC group (decreased coherence for chairs relative to faces at electrode pair T7-T8) (Figures 5.4 and 5.5). No within-group differences in coherence between tasks survived correction for multiple comparisons at $p_{\text{FDR-corrected}} < 0.05$.

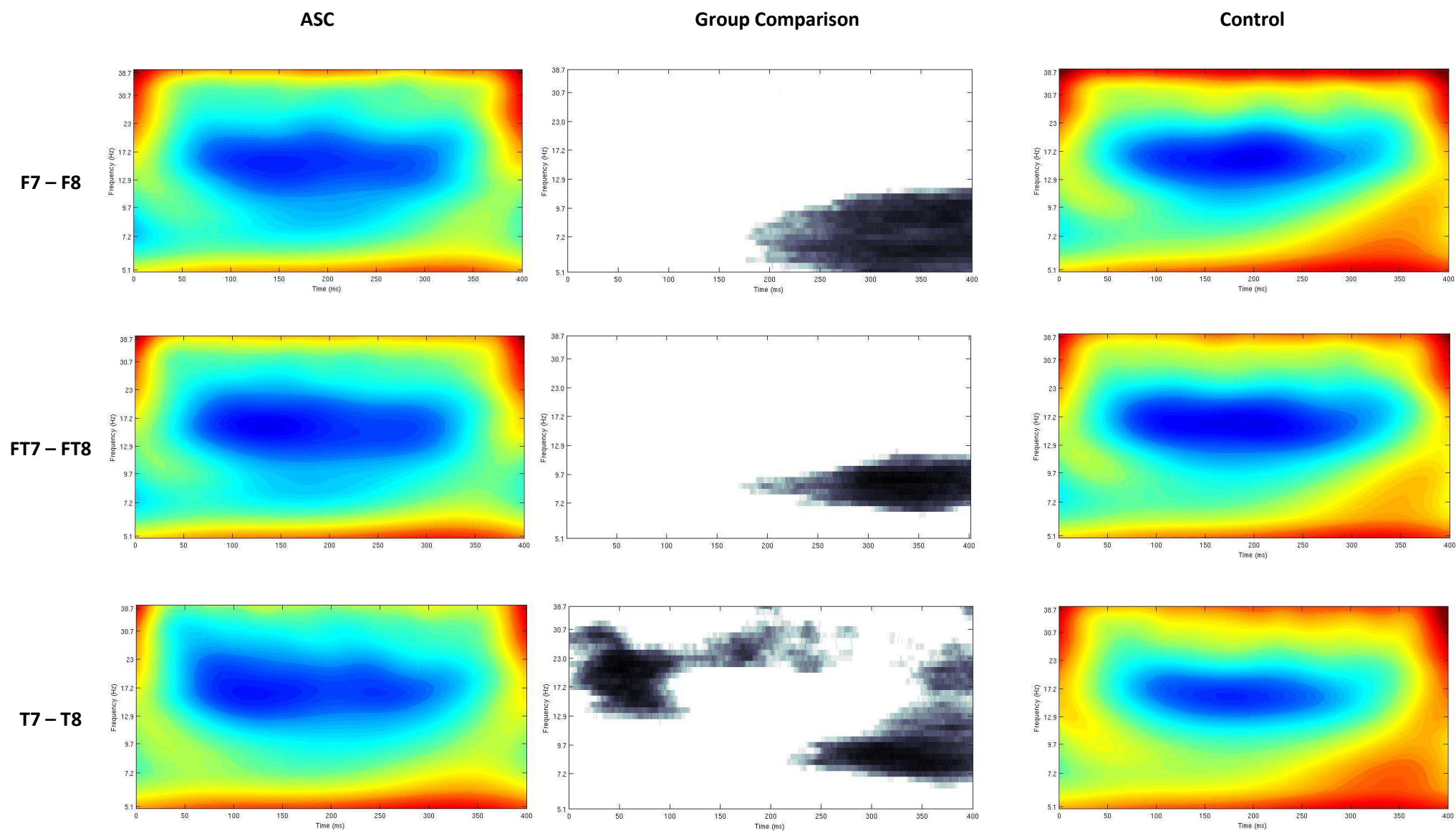


Figure 5.1 – (continues on next page)

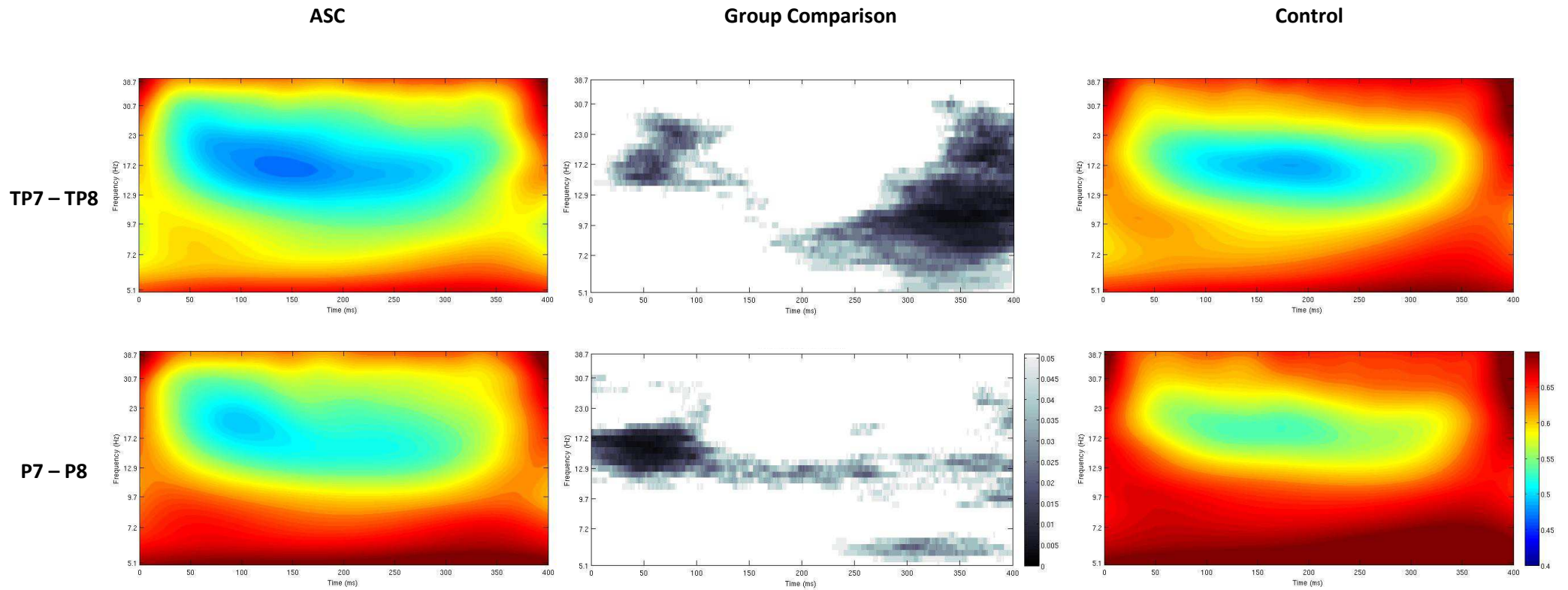


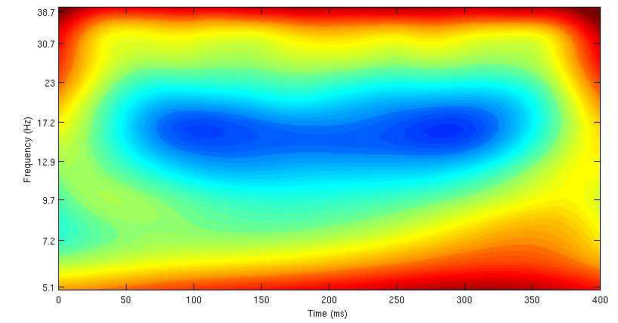
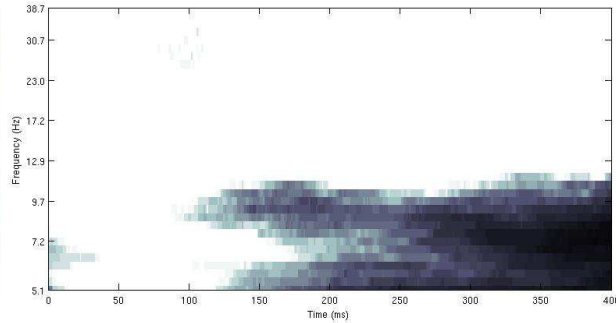
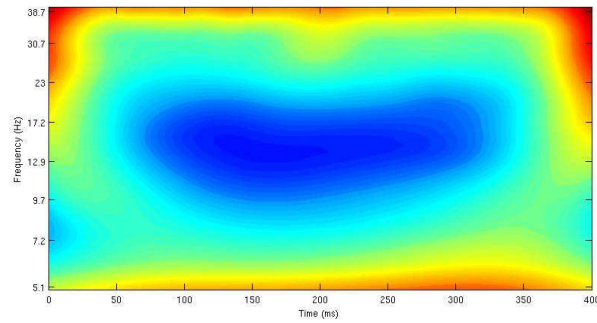
Figure 5.1 – Statistical group comparison of interhemispheric coherence for the chairs task, not corrected for multiple comparisons - the coloured graphs represent values of wavelet coherence for the *chairs* task, for every time-frequency point and for each group (ASC: left column, Control: right column) and each pair of electrodes (different rows); areas in blue represent regions of low coherence in the time-frequency spectrum, whilst areas in red represent regions of high coherence. The graphs in the middle column represent the statistical group comparison for each electrode pair; areas shaded grey represent regions of the time-frequency spectrum where there is a significant decrease of coherence for the ASC group when compared to the Control group, at p (uncorrected) < 0.05 . No areas were found where there was a significant increase in coherence for the ASC group when compared to the Control group.

ASC

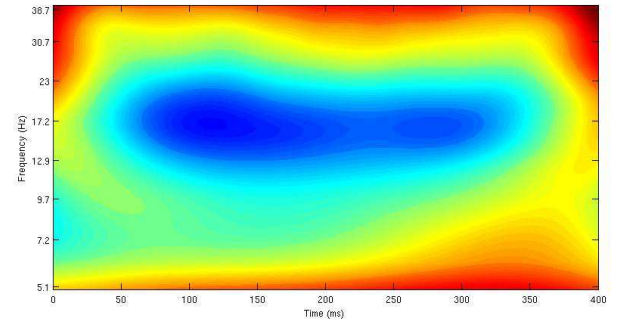
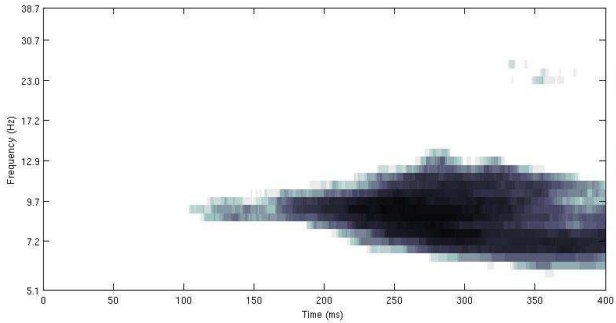
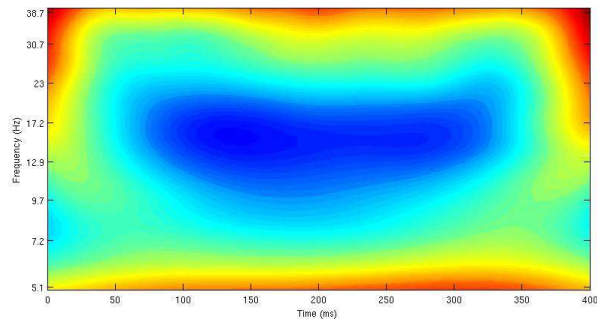
Group Comparison

Control

F7 – F8



FT7 – FT8



T7 – T8

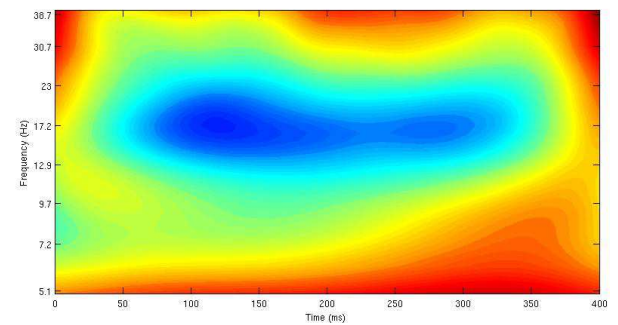
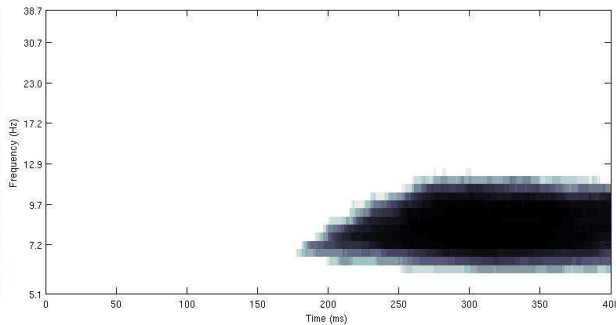
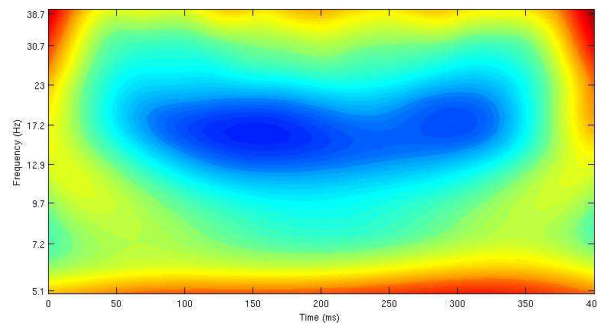


Figure 5.2 – (continues on next page)

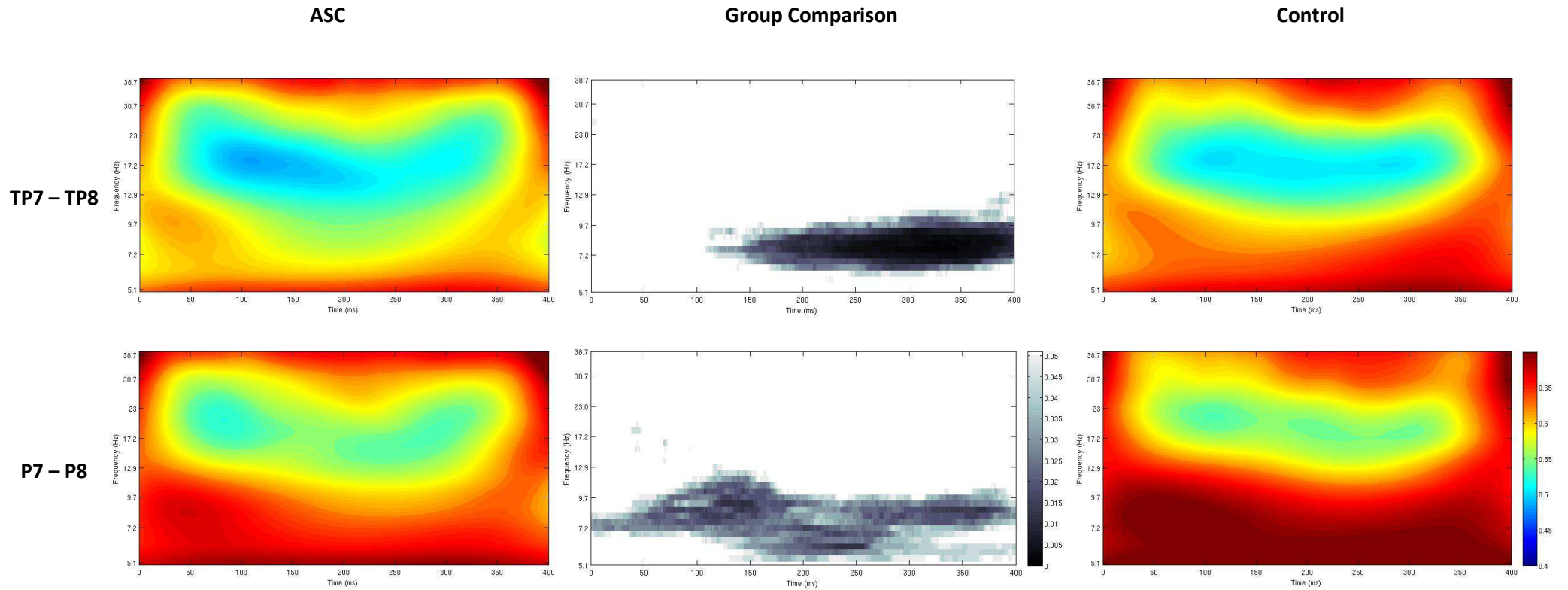


Figure 5.2 – Statistical group comparison of interhemispheric coherence for the faces task, not corrected for multiple comparisons - the coloured graphs represent values of wavelet coherence for the *faces* task, for every time-frequency point and for each group (ASC: left column, Control: right column) and each pair of electrodes (different rows); areas in blue represent regions of low coherence in the time-frequency spectrum, whilst areas in red represent regions of high coherence. The graphs in the middle column represent the statistical group comparison for each electrode pair; areas shaded grey represent regions of the time-frequency spectrum where there is a significant decrease of coherence for the ASC group when compared to the Control group, at p (uncorrected) < 0.05 . No areas were found where there was a significant increase in coherence for the ASC group when compared to the Control group.

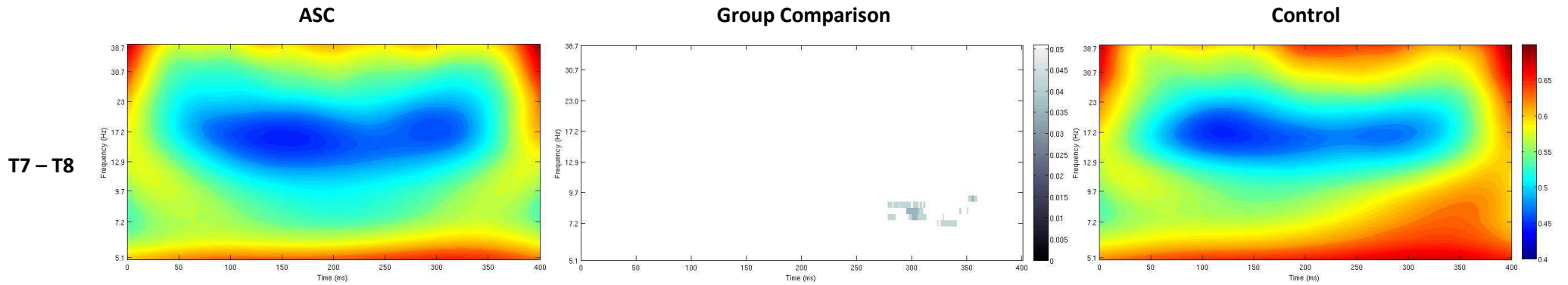


Figure 5.3 – Statistical group comparison of interhemispheric coherence, corrected for multiple comparisons using the False Discovery Rate (FDR) algorithm - the coloured graphs represent values of wavelet coherence for the *faces* task, for every time-frequency point, for each group (ASC: left column, Control: right column) and for electrode pair T7-T8; areas in blue represent regions of low coherence in the time-frequency spectrum, whilst areas in red represent regions of high coherence. The graph in the middle represents the FDR-corrected statistical group comparison for electrode pair T7-T8; areas shaded grey represent regions of the time-frequency spectrum where there is a significant decrease of coherence for the ASC group when compared to the Control group, at p (FDR-corrected) < 0.05 . No areas were found where there were significant group differences after FDR correction for any other electrode pairs or task.

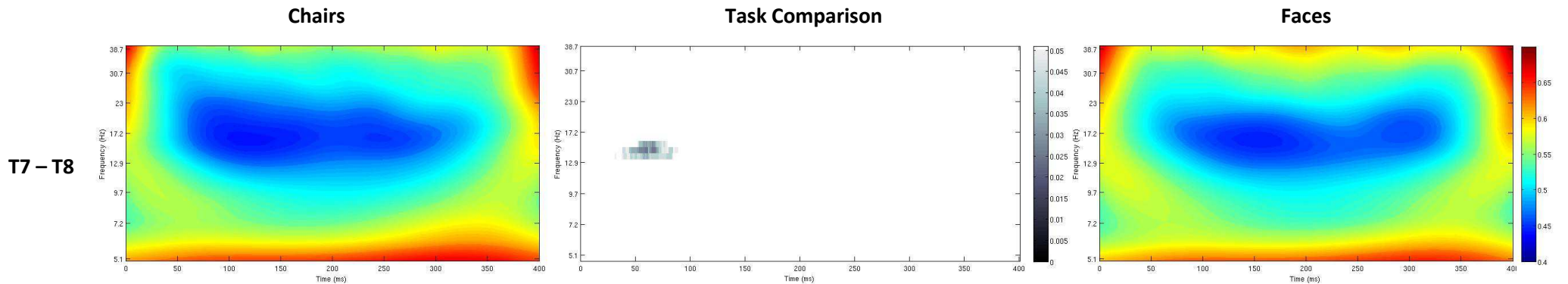


Figure 5.4 - Statistical task comparison of interhemispheric coherence for the ASC group, not corrected for multiple comparisons - the coloured graphs represent values of wavelet coherence for the ASC group, for every time-frequency point, for each task (Chairs: left column, Faces: right column) and for electrode pair T7-T8; areas in blue represent regions of low coherence in the time-frequency spectrum, whilst areas in red represent regions of high coherence. The graph in the middle represents the statistical task comparison for electrode pair T7-T8; areas shaded grey represent regions of the time-frequency spectrum where there is a significant decrease of coherence for the chairs task when compared to the faces task, at p (uncorrected) < 0.05 . For the ASC group, no areas of significant differences in coherence between tasks were found for any other electrode pairs.

Chairs coherence < Faces coherence

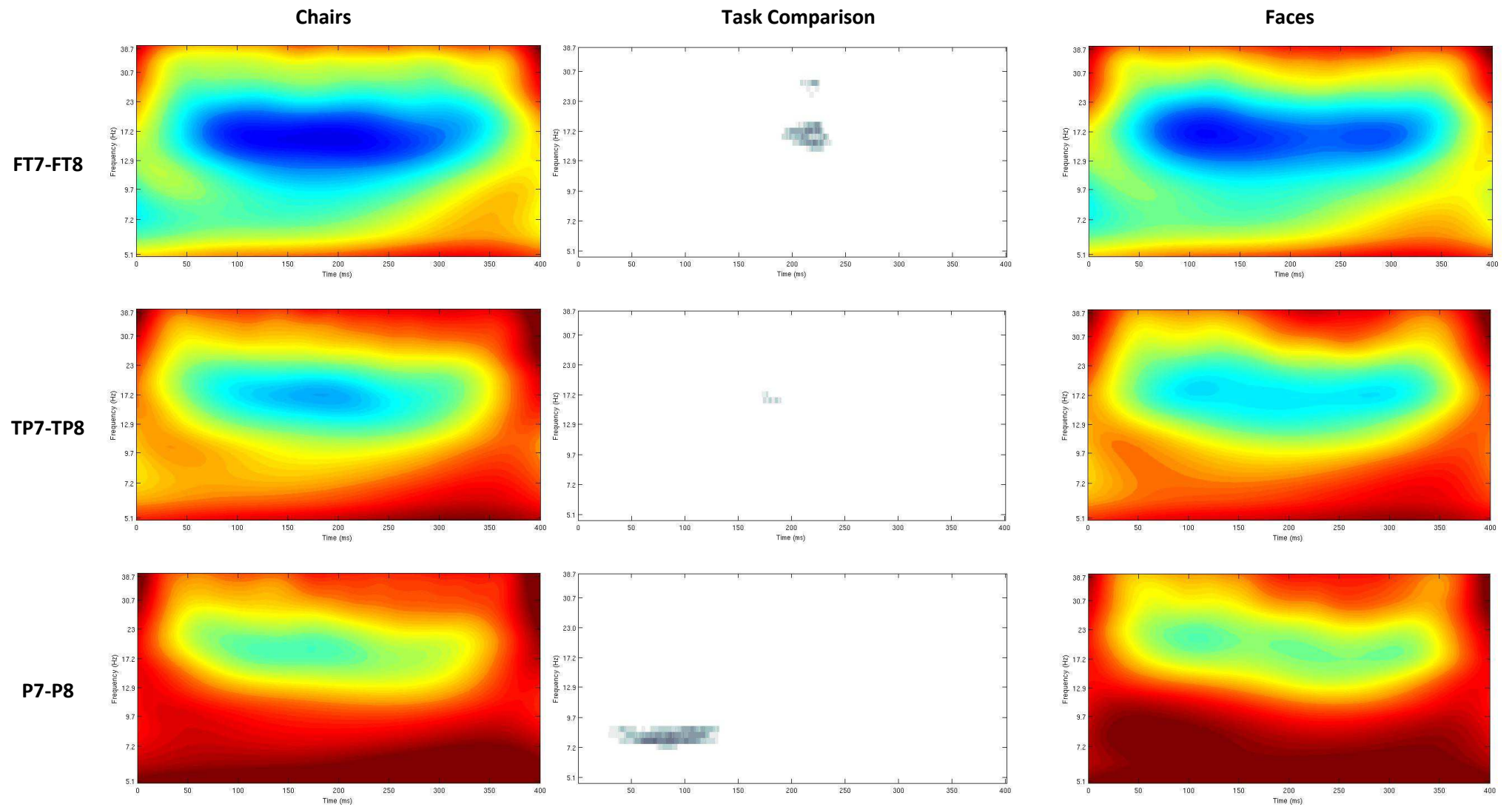


Figure 5.5 – (continues on next page)

TP7-TP8

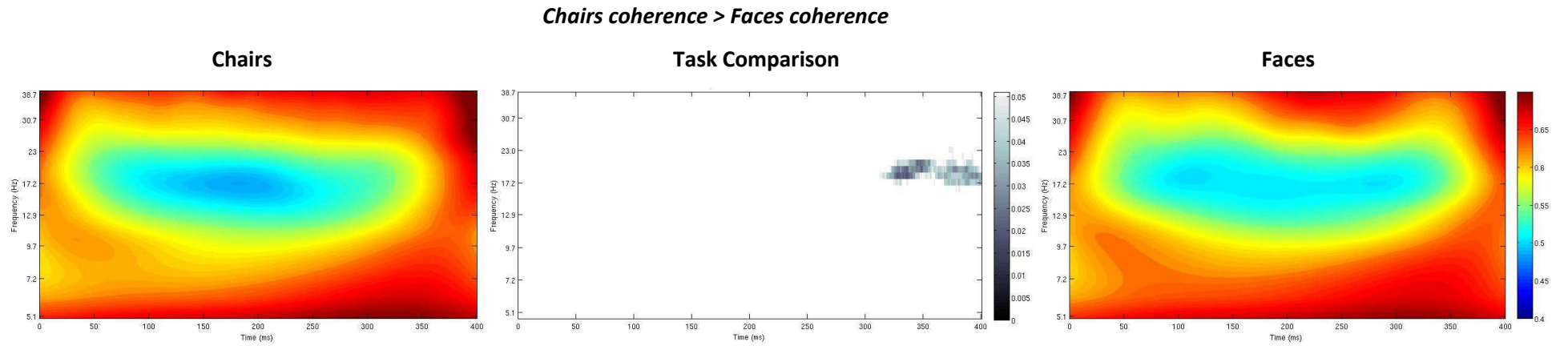


Figure 5.5 - Statistical task comparison of interhemispheric coherence for the Control group, not corrected for multiple comparisons - the coloured graphs represent values of wavelet coherence for the *Control* group, for every time-frequency point and for each task (Chairs: left column, Faces: right column), for different electrode pairs (each row) and directions (decreased coherence for chairs task relative to faces task on first three rows, increased coherence for chairs relative to faces task on last row); areas in blue represent regions of low coherence in the time-frequency spectrum, whilst areas in red represent regions of high coherence. The graphs in the middle column represents the statistical task comparison for different electrode pairs; areas shaded grey represent regions of the time-frequency spectrum where there is a significant difference in coherence between the chairs and the faces task, at p (uncorrected) < 0.05 . For the Control group, no areas of significant differences in coherence between tasks were found for any other electrode pairs.

5.4. DISCUSSION

Coherence is an important tool for the study of complex cortical network dynamics and temporal fluctuations in the coupling between neural signals. Previous studies have shown that measures of coherence reflect patterns of cortical connectivity in the brain and that decreased values of coherence are associated with reduced connectivity between distant neural networks (Nunez et al., 1997, Isler et al., 2010).

The results of the present study show a widespread and consistent reduction in interhemispheric coherence in the ASC group compared to the Control group, during both visual tasks employed. These group differences are spread across the entire time-frequency spectrum, though they are more pronounced at frequencies lower than about 13 Hz and generally after around 150 ms post-stimulus onset (Figures 5.1 and 5.2). It is hypothesized that these results are indicative of an overall impairment in functional interhemispheric connectivity during visual processing in people with ASC. This hypothesis is supported by previous reports of decreased structural and functional interhemispheric connectivity in ASC (Chung et al., 2004, Boger-Megiddo et al., 2006, Vidal et al., 2006, Neul, 2011, Wass, 2011).

In addition, the tasks employed in this study involved object categorization, in the sense that participants needed to decide whether each presented image was of a chair or a human face. There is evidence that object categorization may be impaired in people with ASC (Klinger and Dawson, 1995, Gastgeb et al., 2006, Soulieres et al., 2007). It is also interesting to note that superordinate distinctions in object categorization can occur relatively soon after stimulus presentation and Van Rullen and Thorpe (2001) reported electrophysiological differences associated with superordinate categorical differences (e.g. animals vs. vehicles), peaking between 200 and 250 ms post-stimulus onset in typical controls. Similarly, Curran et al. (2002) have reported event-related potentials (ERP) data indicating that feature analysis (supporting the process of finding similarities that bind object exemplars into categories) precedes later processing stages associated with recognition of specific objects. Hence, it can be hypothesized that the relatively reduced coherence manifested in the current study by the participants with ASC from around 150 ms is related to atypical performance in this categorisation task.

Consistent with this proposal, studies of the time-frequency responses of healthy members of the general population to visual stimuli, including houses and faces, have shown that these responses could be explained by amplitude increases maximal in the 5 to 15 Hz frequency band, between 100 and 200 ms post-stimulus onset (Rousselet et al., 2007, Tang et al., 2008).

These reported frequencies are similar to the ones at which the participants with ASC display decreased interhemispheric coherence in the current study. The paradigms employed by Rousselet et al. (2007) and Tang et al. (2008) differ significantly from the one used in the current study, and neither explored coherence of EEG activity between different electrode sites. Nevertheless, it is interesting to consider their results in the context of the present study, where most group differences in interhemispheric coherence are found in a frequency band below around 13 Hz – it can be hypothesized that the differences in coherence observed in the current study may be related to differences in brain activity associated with structural encoding of the observed images, as part of their initial categorization as either faces or chairs.

Observation of Figures 5.1 and 5.2 also seems to indicate that during the chair task but not the face task, there is also relatively decreased interhemispheric coherence in the ASC group earlier in the response window (less than 200 ms post-stimulus onset), at higher frequencies (> 13 Hz), in more posterior regions of the cortex. Whilst this observation is interesting, these group differences do not survive correction for multiple comparisons and without additional group-by-task interactions analyses further discussions on the interpretation of these findings would be speculative. Informed by the methods of previous WTC analysis of EEG data (Klein et al., 2006) and taking into account the small sample size of the current data set, in the current study it was decided to run the statistical analysis in a non-parametric context. In this case, group-by-task interaction analyses are not trivial to perform, and algorithms for non-parametric interaction analyses are still under development (Sawilowsky, 1990, Leys and Schumann, 2010).

Whilst there are clear differences in interhemispheric coherence between the ASC and the Control groups in this study, the small sample sizes limit the power of the comparisons. Additionally, it is also important to note that due to the size of the data matrices being analysed in this study (36 frequency points by 401 time points giving a total of 14 436 data points) standard methods for correction for multiple comparisons, such as Bonferroni, could not be applied. However, despite the fact that previous studies using WTC for the analysis of EEG data do not correct for multiple comparisons (Klein et al., 2006), it is recognized that care must be taken when interpreting uncorrected statistical results and although in the current study significant group differences are seen in well defined time-frequency clusters, increasing

the likelihood of these differences being meaningful (Forman et al., 1995), correction for multiple comparisons was still performed.

The multiple comparisons problem for such a large data set must be carefully considered. As mentioned above, conservative methods such as Bonferroni correction are not suitable as they lead to a high number of type II (false-negative) errors. However, the absence of any type of correction leads to the presence of type I (false-positive) errors. Less conservative methods such as False Discovery Rate correction (FDR; (Genovese et al., 2002)) are commonly used in the statistical analysis of functional neuroimaging data, usually comprising hundreds of thousands of data points, and so FDR was considered an adequate choice for the current study. It is important to note however, that as highlighted in a review on type I and type II error concerns in neuroimaging research (Lieberman and Cunningham, 2009), even FDR correction may be overly conservative when dealing with small effects. In this review Lieberman and Cunningham (2009) suggest systematic meta-analyses as an alternative approach in dealing with type I and type II errors, given that these errors will not replicate across multiple studies, unlike truly significant effects.

In the present study the only group difference that survives FDR correction is an area of decreased coherence for the ASC relative to the Control group, for electrode pair T7-T8 in the faces task. This area is located at around 300 ms post-stimulus onset, on a frequency band between 7 and 10 Hz. It is interesting to note that temporal sites have previously been associated with visual processing of faces, albeit at earlier post-stimulus onset times (Bentin et al., 1996, Tang et al., 2008). The measures used in these investigations differ from the one used in the current study, in that the former are measures of localized brain activity indexed by ERP components and the latter is a measure of interhemispheric coherence. Nevertheless, these previous investigations provide evidence that temporal regions are functionally involved in facial processing, and it can be hypothesized that the group differences identified in the present study reflect atypical face processing in people with ASC, indexed by decreased interhemispheric coherence between temporal sites in this group.

As pointed out by Srinivasan et al. (2007), moderate to large EEG coherence can also arise from volume conduction effects. However, in the current study, the finding of specific time-frequency regions surviving FDR correction suggests that group differences in interhemispheric coherence are not simply the result of differences in magnitude of volume conduction between the two groups, but represent a difference in genuine source coherence. It is also important to note that although group differences surviving FDR correction are quite limited,

considering the small population size of the current study and taking into account the review by Lieberman and Cunningham (2009) mentioned above, it is possible that in this case the FDR correction may have been overly conservative, and that other equally important small effects are being missed.

Decreased interhemispheric coherence in ASC has been reported in previous studies (Coben et al., 2008, Isler et al., 2010). Isler and colleagues (2010) found decreased interhemispheric synchrony in children with ASC, when compared to typically developing children, in occipital lobes, in and below the theta frequency band (< 8 Hz), during a visual stimulation task. In an investigation of resting state EEG coherence in children with ASC, Coben et al. (2008) found evidence of decreased interhemispheric delta (0 to 4 Hz) and theta (4 to 8 Hz) coherences in frontal regions, as well as decreased delta, theta and alpha (< 13 Hz) interhemispheric coherences in temporal areas of the cortex. Coben et al. (2008) also report a decrease in delta, theta and beta (< 8 Hz and 13 to 30 Hz) interhemispheric coherences in parietal regions of the brain. Although the paradigms and population samples of the current study and those of Isler et al. (2010) and Coben et al. (2008) are not directly comparable in that the current study was an investigation of task related coherence in adults and the others examined resting state and visual flash evoked coherence in children, all studies investigated a variety of brain regions and frequency bands, and the results of the current study can be considered as supported by and complementary to those of Isler et al. (2010) and Coben et al. (2008). Additionally, the investigation of functional brain coherence using other modalities confirms that decreased interhemispheric connectivity in people with ASC is a consistent finding (Anderson et al., 2011, Dinstein et al., 2011) - in a resting state MRI study that recruited individuals with and without ASC from late childhood to early adulthood, Anderson et al. (2011) found evidence of impaired interhemispheric connectivity in ASC in sensorimotor cortex, anterior insula, fusiform gyrus, superior temporal gyrus and superior parietal lobule, whilst Dinstein et al. (2011) investigated interhemispheric coherence in toddlers with ASC using MRI, and reported decreased interhemispheric connectivity in putative language areas such as superior temporal gyrus.

The present study investigated task-related interhemispheric coherence during visual perception of chairs or faces in cortical regions including frontal, temporal and parietal areas. These disparate regions are likely to have been involved in a variety of different components of the task, from visual processing to visual categorization learning (Haxby et al., 2000, Ishai et al., 2000, Seger et al., 2010). The relatively extensive analysis of coherence performed in the

current study, over a time-frequency range from 5 to 40 Hz and 1 to 400 ms post-stimulus onset, supports the conclusion that interhemispheric connectivity in ASC is impaired not only in posterior regions but also in frontal and temporal regions of the cortex, in similarity to the results of the resting state studies of Coben et al. (2008), Dinstein et al. (2011) and Anderson et al. (2011). In addition, the use of the WTC approach enabled evidence to be gathered suggesting that it was in lower frequency bands that group differences in EEG responses to the tasks were concentrated. Previous studies have shown evidence relating low frequency theta and alpha synchronization with top-down working memory processes, subserving functional integration over multiple neural networks (von Stein and Sarnthein, 2000, Tsoneva et al., 2011). The visual matching task included in the current study can be considered to involve working memory processes (Owen et al., 2005, Tsoneva et al., 2011), and it is hypothesized that the decrease in low frequency coherence in the ASC group reflects atypical neural connectivity that results in an impairment of integration of information across neural networks. Additionally, previous studies have suggested the existence of a relation between the size and distance of a neural interaction and the frequency of the neural synchronization. In particular, it has been reported that lower frequency oscillations seem to be associated with larger neuronal assemblies and long range connectivity (Nunez et al., 1999, Nunez, 2000, von Stein and Sarnthein, 2000, Buzsaki and Draguhn, 2004, Broyd et al., 2009). The results of the present study are complementary to these reports, and show further evidence supporting theories of impaired long-range connectivity in ASC (Belmonte et al., 2004a, Belmonte et al., 2004d, Neul, 2011, Wass, 2011). The present results suggest that interhemispheric connectivity in ASC is widely atypical, and it is hypothesized that this may have greater implications for tasks that require integration of information over neural networks spread across both cortical hemispheres.

As can be seen in Figures 5.4 and 5.5, some differences were found in within-group interhemispheric coherence between the chairs and the faces task, for both groups. Differences in coherence between tasks were not constrained to a particular region of the time-frequency map, occurring at both early (50 ms) and late (300 ms) post-stimulus onset times, from lower (7 Hz) to higher (23 Hz) frequencies. These differences were significant at a larger number of electrode pairs for the Control group than for the ASC group, possibly reflecting an impairment in task differentiation in people with ASC relative to typically developing controls. This is consistent with previous investigations showing impairments in object categorization and face processing in people with ASC (Dawson et al., 2005, Gastgeb et

al., 2006, Soulieres et al., 2007, Kleinhans et al., 2008). It is important to note that although within-group differences in coherence between tasks were found, these were not as significant as the group differences represented in Figures 5.1 and 5.2, and did not survive correction for multiple comparisons. This may be related to the behavioural results of this study, showing an absence of significant group differences in task performance in terms of speed and accuracy of image recognition. However, behavioural results also show that across both groups, the face task was performed a little less accurately than the chair task. This task effect in accuracy was driven by relatively lower accuracy for the ASC group in the face task, reflected in a group-by-task interaction that approached significance ($F_{1, 28} = 3.661$, $p = 0.066$). Despite this, both the ASC and the Control groups performed the tasks with high degrees of accuracy and close to ceiling level (Table 4.2) and the trend observed in the group-by-task interaction is probably the result of the majority of Control subjects performing at ceiling level, and the participants in the ASC group making a larger, yet still small, number of mistakes. These differences are considered to be not clinically relevant, as the ASC group still presents accuracy scores of around 90% for the face task. The paradigm used in the current study may thus not have been sufficiently demanding to detect possible group differences in task performance or task differences in coherence. Further research is recommended to examine potential correlations between specific cognitive or behavioural functions and atypical patterns of interhemispheric coherence in people with ASC. Additionally, future investigations using the WTC algorithm should seek to improve power of their analyses by involving larger population sizes and correcting for multiple comparisons using FDR or similar methods.

In conclusion, the results of the current study support the potential value of WTC in examining the time-frequency microstructure of task-related interhemispheric EEG coherence in people with ASC. Specifically, using WTC, it has been shown that interhemispheric coherence is reduced in people with ASC, in a time and frequency specific manner, during visual perception and categorization of both social and inanimate stimuli, and that this reduction in coherence is widely dispersed across the brain.

6. GENERAL DISCUSSION

6.1. UNIFYING MODELS OF ASC

As described in Chapter 1 of this thesis, ASC are a set of pervasive neurodevelopmental conditions currently defined by a triad of impairments in social interaction, communications and behavioural flexibility (American Psychiatric Association, 2000, Brock et al., 2002). The definition and diagnosis of ASC is based purely on developmental and behavioural observations, and for this reason ASC were first investigated by behavioural psychology. However, scientific and technological advances through the decades have prompted a very large number of neuroanatomical, neurofunctional, biochemical and genetic investigations that have attempted to identify the cognitive and neurobiological causes behind the behavioural features presented by people with ASC. A full integration of results from these various domains is necessary to form a unifying theory of ASC, yet currently ASC research is still a fragmented field and there is little coherence of results across studies. In fact, in their review published in 2004, Belmonte and colleagues (2004b) describe ASC research as a *'fragmented tapestry stitched from differing analytical threads and theoretical patterns'*. These authors propose that the unification of these different levels of analysis may provide therapeutic targets for the treatment and prevention of ASC.

A variety of unifying models of ASC have been proposed throughout the years. One of the earlier ones, the executive dysfunction model, suggested that certain characteristics of ASC, such as lack of behavioural flexibility, may be explained by an impairment in executive function (Hughes et al., 1994) - executive function describes a set of mental operations that enable an individual to disengage from the immediate context and guide their behaviour based on mental models or future goals. It has been proposed that an impairment in executive function in ASC could also account for the social and communication deficits that characterise this condition, as explained by a loss of executive control within communication (Hughes et al., 1994). However, this model is not complete and fails to explain certain characteristics of ASC, such as the ability to appreciate the fallibility of concrete concepts like photographs and drawings, but not of abstract concepts and beliefs (Charman and Baron-Cohen, 1992). A different hypothesis, proposing that ASC is characterised by a deficit in the ability to attribute mental states to oneself and to others, could explain these differences (Baron-Cohen et al.,

1985). This hypothesis, known as the model of impaired theory of mind, accounts for the various socialisation, imagination and communication difficulties presented by people with ASC (Baron-Cohen et al., 1985, Frith and Happe, 1994). However, similarly to the executive dysfunction model, the impaired theory of mind model is not complete as it fails to explain certain ASC features such as restrictive range of interests and lack of behavioural flexibility (Frith and Happe, 1994).

6.1.1. ATYPICAL NEURAL CONNECTIVITY IN ASC

The weak central coherence model, another unifying model of ASC introduced by Frith (1989), proposes that ASC can be characterized by a reduction in contextual integration of information, with a bias towards local rather than global processing. In 2002, Brock and colleagues (2002) proposed a link between weak central coherence and a deficit in temporal binding in ASC - the binding problem describes the question of how different brain regions interact and consequently how information is integrated in the brain (Brock et al., 2002). The temporal binding solution to the binding problem suggests that neurons responding to different properties of the same object could be associated through a temporal correlation of their firing patterns (Singer et al., 1997, Brock et al., 2002). Brock et al. (2002) hypothesized that the features of ASC associated with weak central coherence could be the result of impaired integration of information over specialized local neural networks, caused by a deficit in temporal binding potentially associated with an impairment in neural connectivity. This hypothesis is the base for the connectivity model, another unifying theory of ASC proposing that the symptoms presented by people with this condition may be caused by atypical neural connectivity. These impairments in neural connectivity may account for deficits in executive function and difficulties in representation of mental states, and this model could be argued to underpin both the executive dysfunction and theory of mind models previously described.

Although neural underconnectivity in ASC was first reported in 1988 by Horwitz and colleagues (1988), it was only years later that connectivity was proposed as a unifying theoretical framework for ASC (Brock et al., 2002, Belmonte et al., 2004b, Just et al., 2004). Based on the results of their fMRI investigation of executive function and corpus callosum morphometry in ASC, Just et al. (2004) proposed that altered cognition in ASC is caused by reduced intracortical connectivity, resulting in a deficit of integration of information across distinct cortical regions. Belmonte et al. (2004b) extended this model, based on evidence from their own and other investigations (Rubenstein and Merzenich, 2003, Belmonte et al., 2004c), and hypothesized

that local over-connectivity may develop concurrently to global underconnectivity in ASC. Furthermore, these authors proposed a theory of high physical but low computational connectivity in ASC, in which strongly connected regions in the ASC brain are not sufficiently delimited or differentiated, causing a lack of development of computationally meaningful long range connections.

The investigations carried out in this thesis are supportive of the atypical connectivity model of ASC. Of special significance is the fact that the convergent evidence presented in this thesis was acquired through both novel and classical analysis techniques - the innovative MSE and WTC analysis, described in Chapters 4 and 5, present a new set of results supporting the connectivity model of ASC, whilst classical methods such as fMRI and power analysis provide confirmation of results from previous investigations. Most importantly, by employing a variety of algorithms for the analysis of neuroimaging and neurophysiological data, this thesis provides some degree of unification of different levels of analysis, a step in ASC research deemed essential by Belmonte et al. (2004b). Of additional interest, the results presented in this thesis seem to consistently support theories of medium and long range underconnectivity in ASC, but provide no evidence supporting theories of local overconnectivity in ASC. Results indicative of local overconnectivity in ASC would be, for example, patterns of increased complexity or increased coherence of EEG signals for the ASC compared to the Control group. The absence of such results is consistent with a recent review by Wass (2011), where the author notes that evidence towards the model of increased short range connectivity in ASC is limited and often contradictory, in opposition to what is observed for the underconnectivity model.

6.1.2. LIMITATIONS OF THE DATASETS USED IN THIS THESIS

Additionally to the points mentioned above, a further strength of the research carried out in the context of this thesis is that despite the numerous analyses performed, only two different sets of participants were recruited, one for the functional and structural MRI analysis, and another for the EEG based studies. This is particularly important considering the potential confounding effect of group heterogeneity discussed in Chapter 2 (Anagnostou and Taylor, 2011). However, although using data from the same sample to perform different analyses can eliminate confounding effects related to group heterogeneity, it can also be considered a weakness. The small size of the population samples recruited for this thesis (12 to 15 individuals per group) might mean that these are not representative of the wider population,

and for maximal value, the findings reported in this thesis would have to be reproduced for a different population sample.

An additional weakness of the results described in this thesis is the absence of significant group-by-task interactions, for all the behavioural data analyses performed. Although this absence is not in line with predictions made based on the weak central coherence model, these results are not unexpected given that all ASC individuals recruited were at the high-functioning end of the autism spectrum. As hypothesized by Brock et al. (2002), individuals with high-functioning autism do not have such a severe deficit in neural connectivity, hence global integration is less affected and impairments in connectivity are only reflected behaviourally for high complexity tasks. This hypothesis is in line with the proposition made in Chapter 4 that social, emotional and language functions, because they make greater demands on neural networks and on relationships between neural networks, are more vulnerable to impairments in neural connectivity. In this case, as indicated by accuracy results in Chapters 3 and 4, both ASC and Control groups performed the tasks at ceiling level, and it is possible that the tasks included in this thesis were not sufficiently difficult to generate significant group-by-task effects.

The next three sections of this discussion will summarize the results of each of the studies performed in the context of this thesis, with particular emphasis on the implications of those results on the connectivity model of ASC.

6.2. fMRI MEASURES OF CONNECTIVITY IN ASC

In Chapter 3 an fMRI investigation showed that individuals with ASC activate different brain regions compared to neurotypical controls when detecting semantic incongruities in written sentences. The results of this study showed that, in response to semantic incongruities, the ASC group activated mainly frontal areas (particularly left inferior temporal lobe), whilst activation in the Control group included areas over all regions of the cortex, such as posterior and anterior cingulate cortices and occipitotemporal lobe. These spatially restricted patterns of activation observed in the ASC group when compared to the Control group are suggestive of impaired integration of information over distant neural networks and an indication of reduced long range neural connectivity in ASC. The temporal binding deficit hypothesis of ASC proposed by Brock et al. (2002) seems to support this interpretation – the authors highlight the

importance of global integration of information in sentence processing, defending that a deficit in temporal binding between distant neural regions could result in individual words being processed out of their wider context. This proposition is supported by previous studies showing unimpaired processing of individual words (Frith and Snowling, 1983, Eskes et al., 1990), but impaired sentence comprehension in ASC (Frith and Snowling, 1983, Jolliffe and Baron-Cohen, 2000).

Various previous studies have investigated functional connectivity using fMRI, employing a variety of tasks previously shown to be performed suboptimally in ASC such as those involving sentence comprehension (Just et al., 2004), action planning (Villalobos et al., 2005) and working memory (Koshino et al., 2005). In a whole brain analysis of functional connectivity using fMRI, Welchew and colleagues (2005) have shown evidence of atypical connectivity involving the medial temporal lobe in a group of individuals with ASC. These authors assessed whole brain functional connectivity during the performance of a task involving the incidental visual processing of fearful facial expressions. They used a technique known as multidimensional scaling, which derives from principal component analysis (Welchew et al., 2002).

Principal component analysis (PCA) and similarly the independent component analysis (ICA) algorithms perform a correlation analysis by converting data series into a set of orthogonal or independent variables. Assaf and colleagues (2010), in an fMRI investigation of neural connectivity in ASC, used ICA to compare resting state functional connectivity in the default mode network (a set of structures whose activity is thought to be associated with resting-state and self-referential modes of the brain) between a group of individuals diagnosed with ASC and a group of typically developing controls. Their results show a pattern of decreased functional connectivity in the ASC group compared to the control group, involving default mode network core areas.

Another algorithm commonly used in the study of neural connectivity is seed based correlation analysis, which consists of calculating correlation coefficients between time series originating from two or more anatomically well defined regions of interest. This technique has been applied in previous investigations of functional connectivity in ASC, revealing various patterns of decreased connectivity in ASC, comparative to neurotypical controls (Just et al., 2004, Koshino et al., 2005, Villalobos et al., 2005).

Most importantly, the analysis of the results from these previous investigations demonstrates that findings from both activation and resting state fMRI studies are suggestive of atypical

patterns of functional connectivity in ASC, supporting the results of the fMRI study described in Chapter 3 of this thesis.

6.2.1. LIMITATIONS ON THE INTERPRETATION OF THE fMRI STUDY DESCRIBED IN CHAPTER 3

Despite the fact that the results of the fMRI investigation performed in the context of this thesis are suggestive of reduced long range neural connectivity in ASC, it is important to note that no direct connectivity analysis was performed in the study described in Chapter 3. The main aim of that study was to investigate atypical patterns of brain activation in response to semantic stimuli in individuals with ASC. The suggestion that the findings of the current fMRI study are indicative of impaired long range connectivity in ASC is based on results from group averaged data, making it difficult to define anatomical regions of interest on which to run a post-hoc connectivity analysis. In order to confirm the previous suggestion, a hypothesis driven investigation of functional connectivity in semantic processing would be necessary, which would involve extracting time-series from anatomically well defined regions of interest during stimuli presentation, followed by a connectivity analysis using PCA/ICA or seed based correlation algorithms on an individual basis.

6.3. EEG MEASURES OF CONNECTIVITY IN ASC

Chapter 4 of this thesis described an investigation of neurophysiological signal complexity in ASC. Its results demonstrated consistent patterns of reduced complexity of EEG data in a group of individuals with ASC, relative to a group of neurotypical controls. These results are indicative of an alteration in neuronal integration in people with ASC, which may be associated with reduced long-range temporal correlations and atypical neural connectivity. However, although past investigations have suggested that changes in local complexity may be related to brain connectivity (Friston, 1996, Sakalis et al., 2008), it is important to note that no direct measure of neural connectivity was performed in the investigation described in Chapter 4.

Connectivity studies in EEG data usually employ algorithms for computing EEG signal coherence. In fact, the majority of EEG investigations of neural connectivity in ASC consist of coherence analysis (Murias et al., 2007, Coben et al., 2008, Isler et al., 2010, Leveille et al.,

2010, Mathewson et al., 2012, Sheikhan et al., 2012). The coherence analysis performed in the context of this thesis, described in Chapter 5, showed evidence of decreased interhemispheric coherence for the ASC group when compared to the Control group. Although these results are consistent with some of the investigations cited above (Murias et al., 2007, Coben et al., 2008, Isler et al., 2010, Leveille et al., 2010), other past studies present contradictory evidence of increased coherence for individuals with ASC relative to controls (Murias et al., 2007, Leveille et al., 2010, Sheikhan et al., 2012), with the absence of group differences in coherence also being reported (Mathewson et al., 2012).

As reported in Chapter 2, there are a variety of factors that can account for heterogeneity of results in ASC research. Apart from methodological issues such as variations in the algorithms and paradigms (e.g. resting state, sleep or active task) employed in each investigation, another important factor that may influence consistency of results across studies is sample heterogeneity - differences in diagnostic methods used to identify patients (e.g. ADOS/ADI), participants' age group and correlation of results with IQ are all possible confounds (Anagnostou and Taylor, 2011). For the particular case of EEG coherence in ASC, a key factor to take into consideration is the age of the populations recruited for each study, with some studies investigating neural connectivity in children (Coben et al., 2008, Isler et al., 2010, Sheikhan et al., 2012) and others running their analysis in adults (Murias et al., 2007, Leveille et al., 2010, Mathewson et al., 2012). Early stages of brain development involve significant anatomical changes that may be associated with changes in neural connectivity (Huttenlocher, 1990, Power et al., 2010, Vogel et al., 2010). Therefore, differing or even conflicting results from connectivity investigations across different age groups are not only unsurprising, but to be expected. A larger longitudinal study of EEG coherence in ASC would be necessary to investigate variations of coherence with age and clarify discrepancies amongst past studies' results.

It is important to note that in the current thesis both linear (WTC) and nonlinear (MSE) approaches were used for the analysis of EEG data. A wide range of measures can be employed in the study of neural connectivity and complexity, and although the majority of them provide qualitatively equivalent results (Quiñero et al., 2002), different measures have different sensitivities - in an evaluation of different measures of functional connectivity, David and colleagues (2004) highlight the fact that despite being able to provide a rapid and straightforward characterisation of connectivity, linear measures such as coherence are insensitive to the nonlinear components of electrophysiological signals. These authors conclude that the research of functional connectivity in electrophysiological data is far from

trivial, suggesting the combined use of both linear and nonlinear analysis as a more appropriate and balanced approach (David et al., 2004).

6.4. ANATOMICAL MEASURES OF CONNECTIVITY IN ASC

Regarding anatomy, early brain overgrowth and increased brain volume in children with ASC are presently the strongest anatomical findings for this condition (Lainhart et al., 1997b, Courchesne et al., 2001b, Courchesne et al., 2003b, Belmonte et al., 2004b). It has been proposed that this overgrowth influences the normal development of cortical connectivity, by interfering with the processes of synaptogenesis, apoptosis and myelination that peak at a young age (Courchesne and Pierce, 2005b). Of particular interest to the results of this thesis is the hypothesis proposed by Brock and colleagues (2002), which suggests that reduced neural integration resulting from limited growth of long-range connections and excessive pruning of these connections could be reflected as attenuated EEG coherence in ASC. This hypothesis is consistent with the results presented in Chapter 5 of reduced interhemispheric EEG coherence for the ASC group relative to the Control group.

The direct measurement of anatomical connectivity is not a trivial problem. Diffusion tensor imaging (DTI), a technique commonly used in structural connectivity studies, offers the possibility of measuring white matter tracts (an index for neural connectivity), but provides no evidence of synaptic connections or neuronal origin of pathways (Rippon et al., 2007). Despite this, numerous studies have used DTI for the study of neural connectivity in ASC, consistently presenting evidence of abnormal white matter integrity in this group (Barnea-Goraly et al., 2004a, Cheung et al., 2009, Jou et al., 2011, Lo et al., 2011, Weinstein et al., 2011). Diffusion tensor images were not acquired in the context of this thesis, and so it was not possible to confirm the findings of these previous investigations. Instead, an anatomical analysis of cortical thickness in a group of individuals with ASC and a group of typically developing controls was performed. Evidence of a correlation between structural connectivity (as measured by DTI) and cortical thickness has been shown in previous research (Phillips et al., 2011, Koch et al., 2012) - in an anatomical investigation of cortical networks involved in language processing, Phillips et al. (2011) have shown evidence of a positive correlation between arcuate fasciculus fractional anisotropy (an index for anterior-posterior neural connectivity), as measured by DTI, and cortical thickness of anterior and posterior language areas and surrounding cortices.

Complementary to these results are the findings of Koch et al. (2012), reporting a significant correlation between disrupted white matter connectivity in superior temporal cortex and diminished cortical thickness in posterior cingulate cortex, in a cohort of individuals with schizophrenia.

The analysis of cortical thickness performed in the context of the current thesis and described in Chapter 2, provided no evidence supporting cortical thickness as an explanatory factor for ASC symptomatology. This may be due to numerous reasons described in detail in Chapter 2 such as the wide age range of the population studied. Nevertheless, future research investigating a possible correlation between white matter integrity and cortical thickness in ASC could provide interesting results, and potentially clarify the relation between structural and functional connectivity findings in ASC.

6.5. LIMITATIONS OF THE CONNECTIVITY THEORY IN ASC AND FUTURE PERSPECTIVES

It has been almost a decade since Belmonte et al. (2004b) and Just et al. (2004) proposed that impaired neural connectivity may be the cause for the signs and symptoms of ASC. Presently, the potential of the connectivity model as a unifying theory for ASC is widely recognized (Rippon et al., 2007). However, despite the existence of many structural and functional findings supporting the connectivity model, there is little if any direct evidence towards it, and these accounts remain just an hypothesis (Rippon et al., 2007). One particularly important factor to take into consideration is the definition of connectivity - through the years a variety of techniques and algorithms have been employed to measure different indicators of neural connectivity, such as effective connectivity, white matter tracts, fractional anisotropy, coherence, amongst others. However, although the results from these different analyses may be correlated, they are not necessary co-referential (e.g.: anatomical connectivity as measured by fractional anisotropy vs. functional connectivity as measured by coherence algorithms). In current research, neural connectivity can only be described through a set of measures that account for its different aspects, and defining a generalized direct measure of connectivity is not a trivial problem. As noted by Wass (2011) describing connectivity through a single measure gets intrinsically more complicated when both global and local connectivity have to be taken into consideration. However, defining a single measure of connectivity is not necessarily a central problem in ASC research - in his review, Wass (2011) highlights the relation of causality between aberrant neural development (abnormally fast brain growth at

an early age) and impaired connectivity as a more important factor to take into consideration, emphasizing the need for longitudinal studies addressing this question.

It is difficult to judge what place impaired connectivity should take in the current understanding of ASC - is it a primary problem, or a downstream feature resulting from disrupted system performance? In his review, Wass (2011) notes that not all individuals with ASC present disrupted connectivity and highlights the fact that the majority of investigations report group averages only, potentially obscuring information about within-group heterogeneity. Related to this is the high degree of overlap between ASC and other conditions such as Rett's syndrome or fragile X syndrome, not only terms of symptomatology but also in reports of atypical neural connectivity (Belmonte et al., 2004b, Percy, 2011). It is important that future investigations address this issue - clarification of the reasons behind this overlap would be an important step towards understanding the causes and implications of impaired neural connectivity in ASC and other conditions (Belmonte et al., 2004b, Wass, 2011).

In light of this, newly developed neural modelling techniques such as graph theory may prove valuable in ASC research. In graph theory, neural systems are abstractly defined as a set of nodes and interconnecting edges (Bassett and Bullmore, 2006, Bullmore and Bassett, 2011). Topological and geometrical measures can be extracted from these modeled graphs to inform research on structural and functional neural connectivity of the human brain. Despite being a relatively recent model, graph theory has already been applied in a few investigations of functional connectivity in ASC (Pollonini et al., 2010, Dennis et al., 2011, Tsiaras et al., 2011). These studies show promising results that not only support the atypical connectivity model of ASC, but also suggest a potential added value of graph measures as biomarkers for ASC.

6.6. CONCLUSIONS

This thesis presents a set of results which are congruent with the atypical connectivity model of ASC. The fact that all the levels of analysis consistently show evidence of impaired neural connectivity in ASC highlights the importance of the unification of results in ASC research (Table 6.1).

As described in previous sections of this discussion, the current state of the art in ASC research is fundamentally made of fragmented small scale studies focused on a narrow research question, which often generates inconsistent results across studies.

In this thesis, as summarized in Table 6.1., a variety of algorithms and analyses were employed to study various aspects of brain function and anatomy in ASC. Although no conclusions can be drawn from the anatomical study, all the functional investigations provided direct or indirect evidence supporting the atypical neural connectivity model of ASC.

This provides some level of unification in ASC research but most importantly, the work of this thesis demonstrates the pressing need for future large scale longitudinal studies, encompassing a variety of analyses performed on data acquired from a cohort of individuals with well defined demographics, a well characterized diagnosis of ASC and covering a wide age range, from infancy to late adulthood. Such investigations would employ analyses similar to the ones used in the current thesis and their results would allow for stronger conclusions to be drawn in regards to explanatory models of ASC, consequently leading the field of ASC research into a better defined line of investigation.

Summary of results				
Chapter	Modality	Measure	Results	Implications for the connectivity model
2	MRI	Cortical thickness	No significant group differences.	None.
3	fMRI	Functional activation	ASC group presented more spatially restricted functional activation patterns, when compared to the Control group.	Spatially restricted neural activation patterns may suggest decreased neural connectivity for the ASC group. Results may indirectly support the connectivity model.
4	EEG	Multiscale entropy	ASC group presented decreased multiscale entropy values (indexing neurophysiological complexity) when compared to the Control group.	Neurophysiological complexity may be directly related to neural connectivity. Results are indicative of decreased neural connectivity for the ASC group, indirectly supporting the connectivity model.
5	EEG	Wavelet based coherence	ASC group presented patterns of decreased interhemispheric coherence when compared to the Control group.	EEG signal coherence is a measure of neural connectivity. Results demonstrate a reduction of neural connectivity for the ASC group and directly support the connectivity model.

Table 6.1 – Summary of methods and results of the different studies performed in the context of this thesis.

REFERENCES

- Abrahams BS, Geschwind DH (2008) Advances in autism genetics: on the threshold of a new neurobiology. *Nat Rev Genet* 9:341-355.
- Adams JB, Romdalvik J, Ramanujam VM, Legator MS (2007) Mercury, lead, and zinc in baby teeth of children with autism versus controls. *J Toxicol Environ Health A* 70:1046-1051.
- American Psychiatric Association (2000) Diagnostic and statistical manual of mental disorders : DSM-IV-TR. Washington, DC: American Psychiatric Association.
- Anagnostou E, Taylor MJ (2011) Review of neuroimaging in autism spectrum disorders: what have we learned and where we go from here. *Mol Autism* 2:4.
- Anderson JS, Druzgal TJ, Froehlich A, DuBray MB, Lange N, Alexander AL, Abildskov T, Nielsen JA, Cariello AN, Cooperrider JR, Bigler ED, Lainhart JE (2011) Decreased interhemispheric functional connectivity in autism. *Cereb Cortex* 21:1134-1146.
- Anticevic A, Repovs G, Barch DM (2011) Emotion Effects on Attention, Amygdala Activation, and Functional Connectivity in Schizophrenia. *Schizophr Bull*.
- Assaf M, Jagannathan K, Calhoun VD, Miller L, Stevens MC, Sahl R, O'Boyle JG, Schultz RT, Pearlson GD (2010) Abnormal functional connectivity of default mode sub-networks in autism spectrum disorder patients. *Neuroimage* 53:247-256.
- Atladdottir HO, Thorsen P, Ostergaard L, Schendel DE, Lemcke S, Abdallah M, Parner ET (2010) Maternal infection requiring hospitalization during pregnancy and autism spectrum disorders. *J Autism Dev Disord* 40:1423-1430.
- Barnea-Goraly N, Kwon H, Menon V, Eliez S, Lotspeich L, Reiss AL (2004a) White matter structure in autism: preliminary evidence from diffusion tensor imaging. *Biol Psychiatry* 55:323-326.
- Barnea-Goraly N, Kwon H, Menon V, Eliez S, Lotspeich L, Reiss AL (2004b) White matter structure in autism: Preliminary evidence from diffusion tensor imaging. *Biol Psychiatry* 55:323-326.
- Baron-Cohen S, Leslie AM, Frith U (1985) Does the autistic child have a "theory of mind"? *Cognition* 21:37-46.
- Baron-Cohen S, Wheelwright S, Skinner R, Martin J, Clubley E (2001) The autism-spectrum quotient (AQ): evidence from Asperger syndrome/high-functioning autism, males and females, scientists and mathematicians. *J Autism Dev Disord* 31:5-17.
- Barttfeld P, Wicker B, Cukier S, Navarta S, Lew S, Sigman M (2011) A big-world network in ASD: dynamical connectivity analysis reflects a deficit in long-range connections and an excess of short-range connections. *Neuropsychologia* 49:254-263.
- Bassett DS, Bullmore E (2006) Small-world brain networks. *Neuroscientist* 12:512-523.
- Bauman ML, Kemper TL (2003) The neuropathology of the autism spectrum disorders: what have we learned? *Novartis Found Symp* 251:112-122; discussion 122-118, 281-197.
- Belmonte M, Allen G, Beckel-Mitchener A, Boulanger L, Carper R, Webb SJ (2004a) Autism and abnormal development of brain connectivity. *J Neurosci* 24:9228-9231.
- Belmonte MK, Allen G, Beckel-Mitchener A, Boulanger LM, Carper RA, Webb SJ (2004b) Autism and abnormal development of brain connectivity. *J Neurosci* 24:9228-9231.
- Belmonte MK, Cook EH, Jr., Anderson GM, Rubenstein JL, Greenough WT, Beckel-Mitchener A, Courchesne E, Boulanger LM, Powell SB, Levitt PR, Perry EK, Jiang YH, DeLorey TM,

- Tierney E (2004c) Autism as a disorder of neural information processing: directions for research and targets for therapy. *Mol Psychiatry* 9:646-663.
- Belmonte MK, Cook Jr EH, Anderson GM, Rubenstein JLR, Greenough WT, Beckel-Mitchener A, Courchesne E, Boulanger LM, Powell SB, Levitt PR, Perry EK, Jiang YH, DeLorey TM, Tierney E (2004d) Autism as a disorder of neural information processing: Directions for research and targets for therapy. *Molecular Psychiatry* 9:646-663.
- Ben Bashat D, Kronfeld-Duenias V, Zachor DA, Ekstein PM, Hendler T, Tarrasch R, Even A, Levy Y, Ben Sira L (2007) Accelerated maturation of white matter in young children with autism: a high b value DWI study. *Neuroimage* 37:40-47.
- Benau EM, Morris J, Couperus JW (2011) Semantic Processing in Children and Adults: Incongruity and the N400. *J Psycholinguist Res.*
- Bentin S, Allison T, Puce A, Perez E, McCarthy G (1996) Electrophysiological Studies of Face Perception in Humans. *J Cogn Neurosci* 8:551-565.
- Billington J, Baron-Cohen S, Bor D (2008) Systemizing influences attentional processes during the Navon task: an fMRI study. *Neuropsychologia* 46:511-520.
- Binder JR, Desai RH, Graves WW, Conant LL (2009) Where is the semantic system? A critical review and meta-analysis of 120 functional neuroimaging studies. *Cereb Cortex* 19:2767-2796.
- Blakemore SJ, Rees G, Frith CD (1998) How do we predict the consequences of our actions? A functional imaging study. *Neuropsychologia* 36:521-529.
- Bledowski C, Rahm B, Rowe JB (2009) What "works" in working memory? Separate systems for selection and updating of critical information. *J Neurosci* 29:13735-13741.
- Bobee S, Mariette E, Tremblay-Leveau H, Caston J (2000) Effects of early midline cerebellar lesion on cognitive and emotional functions in the rat. *Behav Brain Res* 112:107-117.
- Boger-Megiddo I, Shaw DW, Friedman SD, Sparks BF, Artru AA, Giedd JN, Dawson G, Dager SR (2006) Corpus callosum morphometrics in young children with autism spectrum disorder. *J Autism Dev Disord* 36:733-739.
- Bosl W, Tierney A, Tager-Flusberg H, Nelson C (2011) EEG complexity as a biomarker for autism spectrum disorder risk. *BMC Medicine* 9:18.
- Brock J, Brown CC, Boucher J, Rippon G (2002) The temporal binding deficit hypothesis of autism. *Dev Psychopathol* 14:209-224.
- Broyd SJ, Demanuele C, Debener S, Helps SK, James CJ, Sonuga-Barke EJ (2009) Default-mode brain dysfunction in mental disorders: a systematic review. *Neurosci Biobehav Rev* 33:279-296.
- Bullmore ET, Bassett DS (2011) Brain graphs: graphical models of the human brain connectome. *Annu Rev Clin Psychol* 7:113-140.
- Burbach JP, van der Zwaag B (2009) Contact in the genetics of autism and schizophrenia. *Trends Neurosci* 32:69-72.
- Buzsaki G, Draguhn A (2004) Neuronal oscillations in cortical networks. *Science* 304:1926-1929.
- Carroll LS, Owen MJ (2009) Genetic overlap between autism, schizophrenia and bipolar disorder. *Genome Med* 1:102.
- Casanova M, Trippe J (2009) Radial cytoarchitecture and patterns of cortical connectivity in autism. *Philos Trans R Soc Lond B Biol Sci* 364:1433-1436.
- Castelli F, Frith C, Happé F, Frith U (2002) Autism, asperger syndrome and brain mechanisms for the attribution of mental states to animated shapes. *Brain* 125:1839-1849.

- Catarino A, Churches O, Baron-Cohen S, Andrade A, Ring H (2011) Atypical EEG complexity in autism spectrum conditions: A multiscale entropy analysis. *Clin Neurophysiol*.
- Chang C, Glover GH (2010) Time-frequency dynamics of resting-state brain connectivity measured with fMRI. *Neuroimage* 50:81-98.
- Charman T, Baron-Cohen S (1992) Understanding drawings and beliefs: a further test of the metarepresentation theory of autism: a research note. *J Child Psychol Psychiatry* 33:1105-1112.
- Chen CH, Suckling J, Lennox BR, Ooi C, Bullmore ET (2011) A quantitative meta-analysis of fMRI studies in bipolar disorder. *Bipolar Disord* 13:1-15.
- Cheung C, Chua SE, Cheung V, Khong PL, Tai KS, Wong TK, Ho TP, McAlonan GM (2009) White matter fractional anisotropy differences and correlates of diagnostic symptoms in autism. *J Child Psychol Psychiatry* 50:1102-1112.
- Chung MK, Dalton KM, Alexander AL, Davidson RJ (2004) Less white matter concentration in autism: 2D voxel-based morphometry. *Neuroimage* 23:242-251.
- Chung MK, Robbins SM, Dalton KM, Davidson RJ, Alexander AL, Evans AC (2005) Cortical thickness analysis in autism with heat kernel smoothing. *Neuroimage* 25:1256-1265.
- Churches O, Wheelwright S, Baron-Cohen S, Ring H (2010) The N170 is not modulated by attention in autism spectrum conditions. *Neuroreport* 21:399-403.
- Claus S, Leijten F, Kallansee P, Klepper J, Lopes da Silva FH, Ronner H, Velis D, Viergever MA, Kalitzin S (2009) An electro-encephalogram beta gap after induction with diazepam: a localization method in epileptogenic lesions. *Clin Neurophysiol* 120:1235-1244.
- Coben R, Clarke AR, Hudspeth W, Barry RJ (2008) EEG power and coherence in autistic spectrum disorder. *Clin Neurophysiol* 119:1002-1009.
- Corbetta M, Miezin FM, Shulman GL, Petersen SE (1993) A PET study of visuospatial attention. *J Neurosci* 13:1202-1226.
- Costa M, Goldberger AL, Peng CK (2002) Multiscale entropy analysis of complex physiologic time series. *Phys Rev Lett* 89:068102.
- Costa M, Goldberger AL, Peng CK (2005) Multiscale entropy analysis of biological signals. *Phys Rev E Stat Nonlin Soft Matter Phys* 71:021906.
- Courchesne E, Carper R, Akshoomoff N (2003a) Evidence of Brain Overgrowth in the First Year of Life in Autism. *Journal of the American Medical Association* 290:337-344.
- Courchesne E, Carper R, Akshoomoff N (2003b) Evidence of brain overgrowth in the first year of life in autism. *JAMA* 290:337-344.
- Courchesne E, Karns CM, Davis HR, Ziccardi R, Carper RA, Tigue ZD, Chisum HJ, Moses P, Pierce K, Lord C, Lincoln AJ, Pizzo S, Schreibman L, Haas RH, Akshoomoff NA, Courchesne RY (2001a) Unusual brain growth patterns in early life in patients with autistic disorder - An MRI study. *Neurology* 57:245-254.
- Courchesne E, Karns CM, Davis HR, Ziccardi R, Carper RA, Tigue ZD, Chisum HJ, Moses P, Pierce K, Lord C, Lincoln AJ, Pizzo S, Schreibman L, Haas RH, Akshoomoff NA, Courchesne RY (2001b) Unusual brain growth patterns in early life in patients with autistic disorder: an MRI study. *Neurology* 57:245-254.
- Courchesne E, Pierce K (2005a) Brain overgrowth in autism during a critical time in development: Implications for frontal pyramidal neuron and interneuron development and connectivity. *International Journal of Developmental Neuroscience* 23:153-170.

- Courchesne E, Pierce K (2005b) Why the frontal cortex in autism might be talking only to itself: local over-connectivity but long-distance disconnection. *Curr Opin Neurobiol* 15:225-230.
- Courchesne E, Pierce K (2005c) Why the frontal cortex in autism might be talking only to itself: local over-connectivity but long-distance disconnection. *Current Opinion in Neurobiology* 15:225-230.
- Courchesne E, Press GA, Yeung-Courchesne R (1993) Parietal lobe abnormalities detected with MR in patients with infantile autism. *AJR Am J Roentgenol* 160:387-393.
- Courchesne E, Redcay E, Morgan JT, Kennedy DP (2005) Autism at the beginning: microstructural and growth abnormalities underlying the cognitive and behavioral phenotype of autism. *Dev Psychopathol* 17:577-597.
- Cousin E, Peyrin C, Pichat C, Lamalle L, Le Bas JF, Baciou M (2007) Functional MRI approach for assessing hemispheric predominance of regions activated by a phonological and a semantic task. *Eur J Radiol* 63:274-285.
- Crevecoeur F, Bollens B, Detrembleur C, Lejeune TM (2010) Towards a "gold-standard" approach to address the presence of long-range auto-correlation in physiological time series. *J Neurosci Methods* 192:163-172.
- Cuffin BN (1998) EEG dipole source localization. *IEEE Eng Med Biol Mag* 17:118-122.
- Curran T, Tanaka JW, Weiskopf DM (2002) An electrophysiological comparison of visual categorization and recognition memory. *Cogn Affect Behav Neurosci* 2:1-18.
- Dale AM, Fischl B, Sereno MI (1999) Cortical surface-based analysis. I. Segmentation and surface reconstruction. *Neuroimage* 9:179-194.
- David O, Cosmelli D, Friston KJ (2004) Evaluation of different measures of functional connectivity using a neural mass model. *Neuroimage* 21:659-673.
- Dawson G, Carver L, Meltzoff AN, Panagiotides H, McPartland J, Webb SJ (2002) Neural correlates of face and object recognition in young children with autism spectrum disorder, developmental delay, and typical development. *Child Dev* 73:700-717.
- Dawson G, Webb SJ, Carver L, Panagiotides H, McPartland J (2004) Young children with autism show atypical brain responses to fearful versus neutral facial expressions of emotion. *Dev Sci* 7:340-359.
- Dawson G, Webb SJ, McPartland J (2005) Understanding the nature of face processing impairment in autism: insights from behavioral and electrophysiological studies. *Dev Neuropsychol* 27:403-424.
- De Martino B, Harrison NA, Knafo S, Bird G, Dolan RJ (2008) Explaining enhanced logical consistency during decision making in autism. *J Neurosci* 28:10746-10750.
- Deffke I, Sander T, Heidenreich J, Sommer W, Curio G, Trahms L, Lueschow A (2007) MEG/EEG sources of the 170-ms response to faces are co-localized in the fusiform gyrus. *Neuroimage* 35:1495-1501.
- DeLong KA, Urbach TP, Kutas M (2005) Probabilistic word pre-activation during language comprehension inferred from electrical brain activity. *Nat Neurosci* 8:1117-1121.
- Dennis EL, Jahanshad N, Rudie JD, Brown JA, Johnson K, McMahon KL, de Zubicaray GI, Montgomery G, Martin NG, Wright MJ, Bookheimer SY, Dapretto M, Toga AW, Thompson PM (2011) Altered Structural Brain Connectivity in Healthy Carriers of the Autism Risk Gene, CNTNAP2. *Brain Connect* 1:447-459.

- Di Martino A, Castellanos FX (2003) Functional neuroimaging of social cognition in pervasive developmental disorders: a brief review. *Ann N Y Acad Sci* 1008:256-260.
- Dinstein I, Pierce K, Eyer L, Solso S, Malach R, Behrmann M, Courchesne E (2011) Disrupted neural synchronization in toddlers with autism. *Neuron* 70:1218-1225.
- Dziuk MA, Gidley Larson JC, Apostu A, Mahone EM, Denckla MB, Mostofsky SH (2007) Dyspraxia in autism: association with motor, social, and communicative deficits. *Dev Med Child Neurol* 49:734-739.
- Egaas B, Courchesne E, Saitoh O (1995) Reduced size of corpus callosum in autism. *Arch Neurol* 52:794-801.
- Emerich DM, Creaghead NA, Grether SM, Murray D, Grasha C (2003) The comprehension of humorous materials by adolescents with high-functioning autism and Asperger's syndrome. *J Autism Dev Disord* 33:253-257.
- Escudero J, Abasolo D, Hornero R, Espino P, Lopez M (2006) Analysis of electroencephalograms in Alzheimer's disease patients with multiscale entropy. *Physiol Meas* 27:1091-1106.
- Eskes GA, Bryson SE, McCormick TA (1990) Comprehension of concrete and abstract words in autistic children. *J Autism Dev Disord* 20:61-73.
- Fairhall SL, Ishai A (2007) Effective connectivity within the distributed cortical network for face perception. *Cereb Cortex* 17:2400-2406.
- Fallani FdV, Costa LdF, Rodriguez FA, Astolfi L, Vecchiato G, Toppi J, Borghini G, Cincotti F, Mattia D, Salinari S, Isabella R, Babiloni F (2010) A graph-theoretical approach in brain functional networks. Possible implications in EEG studies. *Nonlinear Biomed Phys* 4 Suppl 1:S8.
- Feng ZY (2003) Analysis of rat electroencephalogram during slow wave sleep and transition sleep using wavelet transform. *Sheng Wu Hua Xue Yu Sheng Wu Wu Li Xue Bao (Shanghai)* 35:741-746.
- Field AP (2009) *Discovering statistics using SPSS : (and sex, drugs and rock 'n' roll)*. Los Angeles: SAGE Publications.
- Fischl B, Dale AM (2000) Measuring the thickness of the human cerebral cortex from magnetic resonance images. *Proc Natl Acad Sci U S A* 97:11050-11055.
- Fischl B, Sereno MI, Dale AM (1999) Cortical surface-based analysis. II: Inflation, flattening, and a surface-based coordinate system. *Neuroimage* 9:195-207.
- Foley Nicpon M, Doobay AF, Assouline SG (2010) Parent, teacher, and self perceptions of psychosocial functioning in intellectually gifted children and adolescents with autism spectrum disorder. *J Autism Dev Disord* 40:1028-1038.
- Forman SD, Cohen JD, Fitzgerald M, Eddy WF, Mintun MA, Noll DC (1995) Improved assessment of significant activation in functional magnetic resonance imaging (fMRI): use of a cluster-size threshold. *Magn Reson Med* 33:636-647.
- Forster KI, Forster JC (2003) DMDX: a windows display program with millisecond accuracy. *Behav Res Methods Instrum Comput* 35:116-124.
- Freeman WJ (1992) Tutorial on neurobiology: from single neuron to brain chaos. *International Journal of Bifurcation and Chaos* 2:451-482.
- Freitag CM, Kleser C, Schneider M, von Gontard A (2007) Quantitative assessment of neuromotor function in adolescents with high functioning autism and Asperger Syndrome. *J Autism Dev Disord* 37:948-959.

- Frishkoff GA, Tucker DM, Davey C, Scherg M (2004) Frontal and posterior sources of event-related potentials in semantic comprehension. *Brain Res Cogn Brain Res* 20:329-354.
- Friston KJ (1996) Theoretical neurobiology and schizophrenia. *Br Med Bull* 52:644-655.
- Friston KJ, Frith CD, Frackowiak RS, Turner R (1995) Characterizing dynamic brain responses with fMRI: a multivariate approach. *Neuroimage* 2:166-172.
- Friston KJ, Holmes A, Poline JB, Price CJ, Frith CD (1996) Detecting activations in PET and fMRI: levels of inference and power. *Neuroimage* 4:223-235.
- Frith U (1989) A new look at language and communication in autism. *Br J Disord Commun* 24:123-150.
- Frith U, Happe F (1994) Autism: beyond "theory of mind". *Cognition* 50:115-132.
- Frith U, Snowling M (1983) Reading for meaning and reading for sound in autistic and dyslexic children. *Brit J Dev Psychol* 1:329-342.
- Fruhholz S, Jellinghaus A, Herrmann M (2011) Time course of implicit processing and explicit processing of emotional faces and emotional words. *Biol Psychol*.
- Gastgeb HZ, Strauss MS, Minshew NJ (2006) Do individuals with autism process categories differently? The effect of typicality and development. *Child Dev* 77:1717-1729.
- Genovese CR, Lazar NA, Nichols T (2002) Thresholding of statistical maps in functional neuroimaging using the false discovery rate. *Neuroimage* 15:870-878.
- Gidley Larson JC, Mostofsky SH (2006) Motor deficits in autism. In: *Autism: A Neurological Disorder of Early Brain Development* (Tuchman, R. and Rapin, I., eds), pp 231-247; London: MacKeith Press.
- Glass L. MMC (1992) *From Clocks to Chaos: The Rhythms of Life*. Princeton: Princeton University Press.
- Golarai G, Grill-Spector K, Reiss AL (2006) Autism and the development of face processing. *Clin Neurosci Res* 6:145-160.
- Gold BT, Balota DA, Kirchoff BA, Buckner RL (2005) Common and dissociable activation patterns associated with controlled semantic and phonological processing: evidence from FMRI adaptation. *Cereb Cortex* 15:1438-1450.
- Goldberger AL, Amaral LA, Glass L, Hausdorff JM, Ivanov PC, Mark RG, Mietus JE, Moody GB, Peng CK, Stanley HE (2000) PhysioBank, PhysioToolkit, and PhysioNet: components of a new research resource for complex physiologic signals. *Circulation* 101:E215-220.
- Grezes J, Wicker B, Berthoz S, de Gelder B (2009) A failure to grasp the affective meaning of actions in autism spectrum disorder subjects. *Neuropsychologia* 47:1816-1825.
- Grossberg S, Seidman D (2006) Neural dynamics of autistic behaviors: cognitive, emotional, and timing substrates. *Psychol Rev* 113:483-525.
- Guye M, Bettus G, Bartolomei F, Cozzone PJ (2010) Graph theoretical analysis of structural and functional connectivity MRI in normal and pathological brain networks. *MAGMA* 23:409-421.
- Haller S, Bartsch AJ (2009) Pitfalls in FMRI. *Eur Radiol* 19:2689-2706.
- Happe F (1997) Central coherence and theory of mind in autism: reading homographs in context. *British Journal of Developmental Psychology* 15:1-12.
- Hardan AY, Jou RJ, Keshavan MS, Varma R, Minshew NJ (2004) Increased frontal cortical folding in autism: a preliminary MRI study. *Psychiatry Res* 131:263-268.

- Hardan AY, Libove RA, Keshavan MS, Melhem NM, Minshew NJ (2009) A preliminary longitudinal magnetic resonance imaging study of brain volume and cortical thickness in autism. *Biol Psychiatry* 66:320-326.
- Hardan AY, Minshew NJ, Mallikarjunn M, Keshavan MS (2001) Brain volume in autism. *J Child Neurol* 16:421-424.
- Hardan AY, Muddasani S, Vemulapalli M, Keshavan MS, Minshew NJ (2006) An MRI study of increased cortical thickness in autism. *Am J Psychiatry* 163:1290-1292.
- Harms MB, Martin A, Wallace GL (2010) Facial emotion recognition in autism spectrum disorders: a review of behavioral and neuroimaging studies. *Neuropsychol Rev* 20:290-322.
- Harris GJ, Chabris CF, Clark J, Urban T, Aharon I, Steele S, McGrath L, Condouris K, Tager-Flusberg H (2006) Brain activation during semantic processing in autism spectrum disorders via functional magnetic resonance imaging. *Brain Cogn* 61:54-68.
- Haswell CC, Izawa J, Dowell LR, Mostofsky SH, Shadmehr R (2009) Representation of internal models of action in the autistic brain. *Nat Neurosci* 12:970-972.
- Haueisen J, Tuch DS, Ramon C, Schimpf PH, Wedeen VJ, George JS, Belliveau JW (2002) The influence of brain tissue anisotropy on human EEG and MEG. *Neuroimage* 15:159-166.
- Haxby JV, Hoffman EA, Gobbini MI (2000) The distributed human neural system for face perception. *Trends Cogn Sci* 4:223-233.
- Hazlett HC, Poe M, Gerig G, Smith RG, Provenzale J, Ross A, Gilmore J, Piven J (2005) Magnetic resonance imaging and head circumference study of brain size in autism: birth through age 2 years. *Arch Gen Psychiatry* 62:1366-1376.
- Hazlett HC, Poe MD, Gerig G, Styner M, Chappell C, Smith RG, Vachet C, Piven J (2011) Early brain overgrowth in autism associated with an increase in cortical surface area before age 2 years. *Arch Gen Psychiatry* 68:467-476.
- Heim S, Eickhoff SB, Amunts K (2008) Specialisation in Broca's region for semantic, phonological, and syntactic fluency? *Neuroimage* 40:1362-1368.
- Hitoglou M, Ververi A, Antoniadis A, Zafeiriou DI (2010) Childhood autism and auditory system abnormalities. *Pediatr Neurol* 42:309-314.
- Hodge SM, Makris N, Kennedy DN, Caviness VS, Jr., Howard J, McGrath L, Steele S, Frazier JA, Tager-Flusberg H, Harris GJ (2010) Cerebellum, language, and cognition in autism and specific language impairment. *J Autism Dev Disord* 40:300-316.
- Hornero R, Abasolo D, Escudero J, Gomez C (2009) Nonlinear analysis of electroencephalogram and magnetoencephalogram recordings in patients with Alzheimer's disease. *Philos Transact A Math Phys Eng Sci* 367:317-336.
- Horwitz B, Rumsey JM, Grady CL, Rapoport SI (1988) The cerebral metabolic landscape in autism. Intercorrelations of regional glucose utilization. *Arch Neurol* 45:749-755.
- Hughes C, Russell J, Robbins TW (1994) Evidence for executive dysfunction in autism. *Neuropsychologia* 32:477-492.
- Hughes JR (2007) Autism: the first firm finding = underconnectivity? *Epilepsy Behav* 11:20-24.
- Hutsler JJ, Love T, Zhang H (2007) Histological and magnetic resonance imaging assessment of cortical layering and thickness in autism spectrum disorders. *Biol Psychiatry* 61:449-457.
- Huttenlocher PR (1990) Morphometric study of human cerebral cortex development. *Neuropsychologia* 28:517-527.

- Hyde KL, Samson F, Evans AC, Mottron L (2010) Neuroanatomical differences in brain areas implicated in perceptual and other core features of autism revealed by cortical thickness analysis and voxel-based morphometry. *Hum Brain Mapp* 31:556-566.
- Ishai A, Ungerleider LG, Martin A, Haxby JV (2000) The representation of objects in the human occipital and temporal cortex. *J Cogn Neurosci* 12 Suppl 2:35-51.
- Isler JR, Martien KM, Grieve PG, Stark RI, Herbert MR (2010) Reduced functional connectivity in visual evoked potentials in children with autism spectrum disorder. *Clin Neurophysiol* 121:2035-2043.
- Istemic R, Kaplanis PA, Pattichis CS, Zazula D (2010) Multiscale entropy-based approach to automated surface EMG classification of neuromuscular disorders. *Med Biol Eng Comput* 48:773-781.
- Itier RJ, Taylor MJ (2004) Source analysis of the N170 to faces and objects. *Neuroreport* 15:1261-1265.
- Jackson PL, Meltzoff AN, Decety J (2005) How do we perceive the pain of others? A window into the neural processes involved in empathy. *Neuroimage* 24:771-779.
- Jansiewicz EM, Goldberg MC, Newschaffer CJ, Denckla MB, Landa R, Mostofsky SH (2006) Motor signs distinguish children with high functioning autism and Asperger's syndrome from controls. *J Autism Dev Disord* 36:613-621.
- Jeong J (2004) EEG dynamics in patients with Alzheimer's disease. *Clin Neurophysiol* 115:1490-1505.
- Jiao Y, Chen R, Ke X, Chu K, Lu Z, Herskovits EH (2010) Predictive models of autism spectrum disorder based on brain regional cortical thickness. *Neuroimage* 50:589-599.
- Jolliffe T, Baron-Cohen S (1999) A test of central coherence theory: linguistic processing in high-functioning adults with autism or Asperger syndrome: is local coherence impaired? *Cognition* 71:149-185.
- Jolliffe T, Baron-Cohen S (2000) Linguistic processing in high-functioning adults with autism or Asperger's syndrome. Is global coherence impaired? *Psychol Med* 30:1169-1187.
- Jou RJ, Jackowski AP, Papademetris X, Rajeevan N, Staib LH, Volkmar FR (2011) Diffusion tensor imaging in autism spectrum disorders: preliminary evidence of abnormal neural connectivity. *Aust N Z J Psychiatry* 45:153-162.
- Jou RJ, Minshew NJ, Keshavan MS, Hardan AY (2010) Cortical gyrification in autistic and asperger disorders: a preliminary magnetic resonance imaging study. *J Child Neurol* 25:1462-1467.
- Just MA, Cherkassky VL, Keller TA, Kana RK, Minshew NJ (2007) Functional and anatomical cortical underconnectivity in autism: evidence from an FMRI study of an executive function task and corpus callosum morphometry. *Cereb Cortex* 17:951-961.
- Just MA, Cherkassky VL, Keller TA, Minshew NJ (2004) Cortical activation and synchronization during sentence comprehension in high-functioning autism: evidence of underconnectivity. *Brain* 127:1811-1821.
- Kaiser MD, Delmolino L, Tanaka JW, Shiffrar M (2010) Comparison of visual sensitivity to human and object motion in autism spectrum disorder. *Autism Res* 3:191-195.
- Kang X, Jia X, Geocadin RG, Thakor NV, Maybath A (2009) Multiscale entropy analysis of EEG for assessment of post-cardiac arrest neurological recovery under hypothermia in rats. *IEEE Trans Biomed Eng* 56:1023-1031.

- Khateb A, Pegna AJ, Landis T, Mouthon MS, Annoni JM (2010) On the origin of the N400 effects: an ERP waveform and source localization analysis in three matching tasks. *Brain Topogr* 23:311-320.
- Kiehl KA, Laurens KR, Liddle PF (2002) Reading anomalous sentences: an event-related fMRI study of semantic processing. *Neuroimage* 17:842-850.
- Klein A, Sauer T, Jedynak A, Skrandies W (2006) Conventional and wavelet coherence applied to sensory-evoked electrical brain activity. *IEEE Trans Biomed Eng* 53:266-272.
- Kleinhans NM, Richards T, Sterling L, Stegbauer KC, Mahurin R, Johnson LC, Greenson J, Dawson G, Aylward E (2008) Abnormal functional connectivity in autism spectrum disorders during face processing. *Brain* 131:1000-1012.
- Klem GH, Luders HO, Jasper HH, Elger C (1999) The ten-twenty electrode system of the International Federation. *The International Federation of Clinical Neurophysiology, Electroencephalography - Clinical Neurophysiology Supplement* 52:3-6.
- Kliemann D, Dziobek I, Hatri A, Steimke R, Heekeren HR (2010) Atypical reflexive gaze patterns on emotional faces in autism spectrum disorders. *J Neurosci* 30:12281-12287.
- Klinger LG, Dawson G (1995) A fresh look at categorization abilities in persons with autism. In: *Learning and Cognition in Autism* (Schopler, E. and Mesibov, G. B., eds) New York: Plenum.
- Knaus TA, Silver AM, Lindgren KA, Hadjikhani N, Tager-Flusberg H (2008) fMRI activation during a language task in adolescents with ASD. *J Int Neuropsychol Soc* 14:967-979.
- Koch K, Schultz CC, Wagner G, Schachtzabel C, Reichenbach JR, Sauer H, Schlosser RG (2012) Disrupted white matter connectivity is associated with reduced cortical thickness in the cingulate cortex in schizophrenia. *Cortex*.
- Kochunov P, Glahn DC, Lancaster J, Thompson PM, Kochunov V, Rogers B, Fox P, Blangero J, Williamson DE (2011) Fractional anisotropy of cerebral white matter and thickness of cortical gray matter across the lifespan. *Neuroimage* 58:41-49.
- Korkmaz B, Benbir G, Demirebilek V (2006) Migration abnormality in the left cingulate gyrus presenting with autistic disorder. *J Child Neurol* 21:600-604.
- Koshino H, Carpenter PA, Minshew NJ, Cherkassky VL, Keller TA, Just MA (2005) Functional connectivity in an fMRI working memory task in high-functioning autism. *Neuroimage* 24:810-821.
- Koshino H, Kana RK, Keller TA, Cherkassky VL, Minshew NJ, Just MA (2008) fMRI investigation of working memory for faces in autism: visual coding and underconnectivity with frontal areas. *Cereb Cortex* 18:289-300.
- Kucera H, Francis WN (1967) *Computational analysis of present-day American English*. Providence,: Brown University Press.
- Kutas M, Federmeier KD (2011) Thirty years and counting: finding meaning in the N400 component of the event-related brain potential (ERP). *Annu Rev Psychol* 62:621-647.
- Kutas M, Hillyard SA (1980) Reading senseless sentences: brain potentials reflect semantic incongruity. *Science* 207:203-205.
- Kutas M, Hillyard SA (1984) Brain potentials during reading reflect word expectancy and semantic association. *Nature* 307:161-163.
- Kutz M (2003) *Standard handbook of biomedical engineering and design*. New York: McGraw-Hill.

- Lachaux JP, Lutz A, Rudrauf D, Cosmelli D, Le Van Quyen M, Martinerie J, Varela F (2002) Estimating the time-course of coherence between single-trial brain signals: an introduction to wavelet coherence. *Neurophysiol Clin* 32:157-174.
- Lai MC, Lombardo MV, Chakrabarti B, Sadek SA, Pasco G, Wheelwright SJ, Bullmore ET, Baron-Cohen S, Suckling J (2010) A shift to randomness of brain oscillations in people with autism. *Biol Psychiatry* 68:1092-1099.
- Lainhart JE, Piven J, Wzorek M, Landa R, Santangelo SL, Coon H, Folstein SE (1997a) Macrocephaly in children and adults with autism. *Journal of the American Academy of Child and Adolescent Psychiatry* 36:282-290.
- Lainhart JE, Piven J, Wzorek M, Landa R, Santangelo SL, Coon H, Folstein SE (1997b) Macrocephaly in children and adults with autism. *J Am Acad Child Adolesc Psychiatry* 36:282-290.
- Lake DE, Richman JS, Griffin MP, Moorman JR (2002) Sample entropy analysis of neonatal heart rate variability. *Am J Physiol Regul Integr Comp Physiol* 283:R789-797.
- Landrigan PJ (2010) What causes autism? Exploring the environmental contribution. *Curr Opin Pediatr* 22:219-225.
- Lee JE, Bigler ED, Alexander AL, Lazar M, DuBray MB, Chung MK, Johnson M, Morgan J, Miller JN, McMahon WM, Lu J, Jeong E-K, Lainhart JE (2007) Diffusion tensor imaging of white matter in the superior temporal gyrus and temporal stem in autism. *Neurosci Lett* 424:127-132.
- Lemaitre H, Goldman AL, Sambataro F, Verchinski BA, Meyer-Lindenberg A, Weinberger DR, Mattay VS (2010) Normal age-related brain morphometric changes: nonuniformity across cortical thickness, surface area and gray matter volume? *Neurobiol Aging*.
- Leveille C, Barbeau EB, Bolduc C, Limoges E, Berthiaume C, Chevrier E, Motttron L, Godbout R (2010) Enhanced connectivity between visual cortex and other regions of the brain in autism: a REM sleep EEG coherence study. *Autism Res* 3:280-285.
- Leys C, Schumann S (2010) A nonparametric method to analyze interactions: The adjusted rank transform test. *J Exp Soc Psychol* 46:684-688.
- Lieberman MD, Cunningham WA (2009) Type I and Type II error concerns in fMRI research: rebalancing the scale. *Soc Cogn Affect Neurosci* 4:423-428.
- Liu X, Qi H, Wang S, Wan M (2006) Wavelet-based estimation of EEG coherence during Chinese Stroop task. *Comput Biol Med* 36:1303-1315.
- Lo YC, Soong WT, Gau SS, Wu YY, Lai MC, Yeh FC, Chiang WY, Kuo LW, Jaw FS, Tseng WY (2011) The loss of asymmetry and reduced interhemispheric connectivity in adolescents with autism: a study using diffusion spectrum imaging tractography. *Psychiatry Res* 192:60-66.
- Logothetis NK (2002) The neural basis of the blood-oxygen-level-dependent functional magnetic resonance imaging signal. *Philos Trans R Soc Lond B Biol Sci* 357:1003-1037.
- Lombardo MV, Barnes JL, Wheelwright SJ, Baron-Cohen S (2007) Self-referential cognition and empathy in autism. *PLoS One* 2:e883.
- Lord C, Risi S, Lambrecht L, Cook EH, Jr., Leventhal BL, DiLavore PC, Pickles A, Rutter M (2000) The autism diagnostic observation schedule-generic: a standard measure of social and communication deficits associated with the spectrum of autism. *J Autism Dev Disord* 30:205-223.

- Lord C, Rutter M, Le Couteur A (1994) Autism Diagnostic Interview-Revised: a revised version of a diagnostic interview for caregivers of individuals with possible pervasive developmental disorders. *J Autism Dev Disord* 24:659-685.
- Losh M, Capps L (2003) Narrative ability in high-functioning children with autism or Asperger's syndrome. *J Autism Dev Disord* 33:239-251.
- Mak-Fan KM, Taylor MJ, Roberts W, Lerch JP (2011) Measures of Cortical Grey Matter Structure and Development in Children with Autism Spectrum Disorder. *J Autism Dev Disord*.
- Manor B, Costa MD, Hu K, Newton E, Starobinets O, Kang HG, Peng CK, Novak V, Lipsitz LA (2010) Physiological complexity and system adaptability: evidence from postural control dynamics of older adults. *J Appl Physiol* 109:1786-1791.
- Marieb EN, Kollett LS, Zao PZ, Stabler T (2001) Human anatomy & physiology laboratory manual. San Francisco: Benjamin Cummings.
- Mathewson KJ, Jetha MK, Drmic IE, Bryson SE, Goldberg JO, Schmidt LA (2012) Regional EEG alpha power, coherence, and behavioral symptomatology in autism spectrum disorder. *Clin Neurophysiol*.
- McCleery JP, Ceponiene R, Burner KM, Townsend J, Kinnear M, Schreibman L (2010) Neural correlates of verbal and nonverbal semantic integration in children with autism spectrum disorders. *J Child Psychol Psychiatry* 51:277-286.
- McDonald JH (2009) In: *Handbook of Biological Statistics*, pp 160-164 Baltimore, Maryland: Sparky House Publishing.
- McIntosh AR, Kovacevic N, Itier RJ (2008) Increased brain signal variability accompanies lower behavioral variability in development. *PLoS Comput Biol* 4:e1000106.
- McKinley MP, O'Loughlin VD (2006) Human anatomy. Boston: McGraw-Hill Higher Education.
- McPartland J, Dawson G, Webb SJ, Panagiotides H, Carver LJ (2004) Event-related brain potentials reveal anomalies in temporal processing of faces in autism spectrum disorder. *J Child Psychol Psychiatry* 45:1235-1245.
- McRobbie DW (2007) MRI from picture to proton. Cambridge: Cambridge University Press.
- Medvedev AV, Murro AM, Meador KJ (2011) Abnormal interictal gamma activity may manifest a seizure onset zone in temporal lobe epilepsy. *Int J Neural Syst* 21:103-114.
- Michel CM, Murray MM, Lantz G, Gonzalez S, Spinelli L, Grave de Peralta R (2004) EEG source imaging. *Clin Neurophysiol* 115:2195-2222.
- Milne E, Scope A, Pascalis O, Buckley D, Makeig S (2009) Independent component analysis reveals atypical electroencephalographic activity during visual perception in individuals with autism. *Biol Psychiatry* 65:22-30.
- Minshew NJ, Williams DL (2007) The new neurobiology of autism: cortex, connectivity, and neuronal organization. *Arch Neurol* 64:945-950.
- Mizuno T, Takahashi T, Cho RY, Kikuchi M, Murata T, Takahashi K, Wada Y (2010) Assessment of EEG dynamical complexity in Alzheimer's disease using multiscale entropy. *Clin Neurophysiol* 121:1438-1446.
- Monk CS, Peltier SJ, Wiggins JL, Weng SJ, Carrasco M, Risi S, Lord C (2009) Abnormalities of intrinsic functional connectivity in autism spectrum disorders. *Neuroimage* 47:764-772.

- Monk CS, Weng SJ, Wiggins JL, Kurapati N, Louro HM, Carrasco M, Maslowsky J, Risi S, Lord C (2010) Neural circuitry of emotional face processing in autism spectrum disorders. *J Psychiatry Neurosci* 35:105-114.
- Muhle R, Trentacoste SV, Rapin I (2004) The genetics of autism. *Pediatrics* 113:e472-486.
- Murias M, Webb SJ, Greenson J, Dawson G (2007) Resting state cortical connectivity reflected in EEG coherence in individuals with autism. *Biol Psychiatry* 62:270-273.
- Neul JL (2011) Unfolding neurodevelopmental disorders: the mystery of developing connections. *Nat Med* 17:1353-1355.
- Newman AJ, Pancheva R, Ozawa K, Neville HJ, Ullman MT (2001) An event-related fMRI study of syntactic and semantic violations. *J Psycholinguist Res* 30:339-364.
- Newschaffer CJ, Croen LA, Daniels J, Giarelli E, Grether JK, Levy SE, Mandell DS, Miller LA, Pinto-Martin J, Reaven J, Reynolds AM, Rice CE, Schendel D, Windham GC (2007) The epidemiology of autism spectrum disorders. *Annu Rev Public Health* 28:235-258.
- Niedermeyer E (1997) Alpha rhythms as physiological and abnormal phenomena. *Int J Psychophysiol* 26:31-49.
- Norris DG (2006) Principles of magnetic resonance assessment of brain function. *J Magn Reson Imaging* 23:794-807.
- Nunez PL (2000) Toward a quantitative description of large-scale neocortical dynamic function and EEG. *Behav Brain Sci* 23:371-398; discussion 399-437.
- Nunez PL, Silberstein RB, Shi Z, Carpenter MR, Srinivasan R, Tucker DM, Doran SM, Cadusch PJ, Wijesinghe RS (1999) EEG coherency II: experimental comparisons of multiple measures. *Clin Neurophysiol* 110:469-486.
- Nunez PL, Srinivasan R (2006) Electric fields of the brain : the neurophysics of EEG. Oxford ; New York: Oxford University Press.
- Nunez PL, Srinivasan R, Westdorp AF, Wijesinghe RS, Tucker DM, Silberstein RB, Cadusch PJ (1997) EEG coherency I: Statistics, reference electrode, volume conduction, Laplacians, cortical imaging, and interpretation at multiple scales. *Electroencephalogr Clin Neurophysiol* 103:499-515.
- Oberman LM, Hubbard EM, McCleery JP, Altschuler EL, Ramachandran VS, Pineda JA (2005) EEG evidence for mirror neuron dysfunction in autism spectrum disorders. *Brain Res Cogn Brain Res* 24:190-198.
- Oblak AL, Rosene DL, Kemper TL, Bauman ML, Blatt GJ (2011) Altered posterior cingulate cortical cytoarchitecture, but normal density of neurons and interneurons in the posterior cingulate cortex and fusiform gyrus in autism. *Autism Res*.
- Ogawa S, Lee TM, Kay AR, Tank DW (1990a) Brain magnetic resonance imaging with contrast dependent on blood oxygenation. *Proc Natl Acad Sci U S A* 87:9868-9872.
- Ogawa S, Lee TM, Nayak AS, Glynn P (1990b) Oxygenation-sensitive contrast in magnetic resonance image of rodent brain at high magnetic fields. *Magn Reson Med* 14:68-78.
- Oldfield RC (1971) The assessment and analysis of handedness: the Edinburgh inventory. *Neuropsychologia* 9:97-113.
- Ouyang G, Dang C, Richards DA, Li X (2010) Ordinal pattern based similarity analysis for EEG recordings. *Clin Neurophysiol* 121:694-703.
- Owen AM, McMillan KM, Laird AR, Bullmore E (2005) N-back working memory paradigm: a meta-analysis of normative functional neuroimaging studies. *Hum Brain Mapp* 25:46-59.

- Park JH, Kim S, Kim CH, Cichocki A, Kim K (2007) Multiscale entropy analysis of EEG from patients under different pathological conditions. *Fractals-Complex Geometry Patterns and Scaling in Nature and Society* 15:399-404.
- Peng DH, Jiang KD, Fang YR, Xu YF, Shen T, Long XY, Liu J, Zang YF (2011) Decreased regional homogeneity in major depression as revealed by resting-state functional magnetic resonance imaging. *Chin Med J (Engl)* 124:369-373.
- Pennington BF, Ozonoff S (1996) Executive functions and developmental psychopathology. *Journal of Child Psychology and Psychiatry* 37:51-87.
- Percy AK (2011) Rett syndrome: exploring the autism link. *Arch Neurol* 68:985-989.
- Pereda E, Quiroga RQ, Bhattacharya J (2005) Nonlinear multivariate analysis of neurophysiological signals. *Prog Neurobiol* 77:1-37.
- Phillips OR, Clark KA, Woods RP, Subotnik KL, Asarnow RF, Nuechterlein KH, Toga AW, Narr KL (2011) Topographical relationships between arcuate fasciculus connectivity and cortical thickness. *Hum Brain Mapp* 32:1788-1801.
- Picton TW, Bentin S, Berg P, Donchin E, Hillyard SA, Johnson R, Jr., Miller GA, Ritter W, Ruchkin DS, Rugg MD, Taylor MJ (2000) Guidelines for using human event-related potentials to study cognition: recording standards and publication criteria. *Psychophysiology* 37:127-152.
- Pijnacker J, Geurts B, van Lambalgen M, Buitelaar J, Hagoort P (2010) Exceptions and anomalies: an ERP study on context sensitivity in autism. *Neuropsychologia* 48:2940-2951.
- Piven J, Bailey J, Ranson BJ, Arndt S (1997) An MRI study of the corpus callosum in autism. *Am J Psychiatry* 154:1051-1056.
- Poldrack RA, Wagner AD, Prull MW, Desmond JE, Glover GH, Gabrieli JD (1999) Functional specialization for semantic and phonological processing in the left inferior prefrontal cortex. *Neuroimage* 10:15-35.
- Pollonini L, Patidar U, Situ N, Rezaie R, Papanicolaou AC, Zouridakis G (2010) Functional connectivity networks in the autistic and healthy brain assessed using Granger causality. *Conf Proc IEEE Eng Med Biol Soc* 2010:1730-1733.
- Power JD, Fair DA, Schlaggar BL, Petersen SE (2010) The development of human functional brain networks. *Neuron* 67:735-748.
- Quiroga R, Kraskov A, Kreuz T, Grassberger P (2002) Performance of different synchronization measures in real data: a case study on electroencephalographic signals. *Phys Rev E Stat Nonlin Soft Matter Phys* 65:041903.
- Rapin I, Dunn M (2003) Update on the language disorders of individuals on the autistic spectrum. *Brain Dev* 25:166-172.
- Rappelsberger P, Pfurtscheller G, Filz O (1994) Calculation of event-related coherence--a new method to study short-lasting coupling between brain areas. *Brain Topogr* 7:121-127.
- Raymaekers R, Wiersema JR, Roeyers H (2009) EEG study of the mirror neuron system in children with high functioning autism. *Brain Res* 1304:113-121.
- Richman JS, Lake DE, Moorman JR (2004) Sample entropy. *Methods Enzymol* 384:172-184.
- Richman JS, Moorman JR (2000) Physiological time-series analysis using approximate entropy and sample entropy. *Am J Physiol Heart Circ Physiol* 278:H2039-2049.
- Rinehart NJ, Bellgrove MA, Tonge BJ, Brereton AV, Howells-Rankin D, Bradshaw JL (2006) An examination of movement kinematics in young people with high-functioning autism

- and Asperger's disorder: further evidence for a motor planning deficit. *J Autism Dev Disord* 36:757-767.
- Ring H, Sharma S, Wheelwright S, Barrett G (2007) An electrophysiological investigation of semantic incongruity processing by people with Asperger's syndrome. *J Autism Dev Disord* 37:281-290.
- Rippon G, Brock J, Brown C, Boucher J (2007) Disordered connectivity in the autistic brain: challenges for the "new psychophysiology". *Int J Psychophysiol* 63:164-172.
- Rockstroh BS, Wienbruch C, Ray WJ, Elbert T (2007) Abnormal oscillatory brain dynamics in schizophrenia: a sign of deviant communication in neural network? *BMC Psychiatry* 7:44.
- Rossion B, Joyce CA, Cottrell GW, Tarr MJ (2003) Early lateralization and orientation tuning for face, word, and object processing in the visual cortex. *Neuroimage* 20:1609-1624.
- Rousselet GA, Husk JS, Bennett PJ, Sekuler AB (2007) Single-trial EEG dynamics of object and face visual processing. *Neuroimage* 36:843-862.
- Rubenstein JL, Merzenich MM (2003) Model of autism: increased ratio of excitation/inhibition in key neural systems. *Genes Brain Behav* 2:255-267.
- Russo N, Flanagan T, Iarocci G, Berringer D, Zelazo PD, Burack JA (2007) Deconstructing executive deficits among persons with autism: implications for cognitive neuroscience. *Brain Cognition* 65:77-86.
- Russo N, Foxe JJ, Brandwein AB, Altschuler T, Gomes H, Molholm S (2010) Multisensory processing in children with autism: high-density electrical mapping of auditory-somatosensory integration. *Autism Res* 3:253-267.
- Sahyoun CP, Belliveau JW, Soulières I, Schwartz S, Mody M (2010) Neuroimaging of the functional and structural networks underlying visuospatial vs. linguistic reasoning in high-functioning autism. *Neuropsychologia* 48:86-95.
- Sakkalis V, Oikonomou T, Pachou E, Tollis I, Micheloyannis S, Zervakis M (2006) Time-significant wavelet coherence for the evaluation of schizophrenic brain activity using a graph theory approach. *Conf Proc IEEE Eng Med Biol Soc* 1:4265-4268.
- Sakkalis V, Tsiaras V, Michalopoulos K, Zervakis M (2008) Assessment of neural dynamic coupling and causal interactions between independent EEG components from cognitive tasks using linear and nonlinear methods. *Conf Proc IEEE Eng Med Biol Soc* 2008:3767-3770.
- Sankari Z, Adeli H (2011) Probabilistic neural networks for diagnosis of Alzheimer's disease using conventional and wavelet coherence. *J Neurosci Methods* 197:165-170.
- Sato W, Kochiyama T, Yoshikawa S (2011) The inversion effect for neutral and emotional facial expressions on amygdala activity. *Brain Res* 1378:84-90.
- Sawilowsky SS (1990) Nonparametric-Tests of Interaction in Experimental-Design. *Rev Educ Res* 60:91-126.
- Sawyer K (2011) The cognitive neuroscience of creativity: A critical review. *Creativity Research Journal* 23:137-154.
- Scheel C, Rotarska-Jagiela A, Schilbach L, Lehnhardt FG, Krug B, Vogeley K, Tepest R (2011) Imaging derived cortical thickness reduction in high-functioning autism: key regions and temporal slope. *Neuroimage* 58:391-400.
- Schmahmann JD, Weilburg JB, Sherman JC (2007) The neuropsychiatry of the cerebellum - insights from the clinic. *Cerebellum* 6:254-267.

- Schulte-Ruther M, Markowitsch HJ, Fink GR, Piefke M (2007) Mirror neuron and theory of mind mechanisms involved in face-to-face interactions: a functional magnetic resonance imaging approach to empathy. *J Cogn Neurosci* 19:1354-1372.
- Schultz RT, Gauthier I, Klin A, Fulbright RK, Anderson AW, Volkmar F, Skudlarski P, Lacadie C, Cohen DJ, Gore JC (2000) Abnormal ventral temporal cortical activity during face discrimination among individuals with autism and Asperger syndrome. *Arch Gen Psychiatry* 57:331-340.
- Scott JA, Schumann CM, Goodlin-Jones BL, Amaral DG (2009) A comprehensive volumetric analysis of the cerebellum in children and adolescents with autism spectrum disorder. *Autism Res* 2:246-257.
- Seger CA, Peterson EJ, Cincotta CM, Lopez-Paniagua D, Anderson CW (2010) Dissociating the contributions of independent corticostriatal systems to visual categorization learning through the use of reinforcement learning modeling and Granger causality modeling. *Neuroimage* 50:644-656.
- Segonne F, Dale AM, Busa E, Glessner M, Salat D, Hahn HK, Fischl B (2004) A hybrid approach to the skull stripping problem in MRI. *Neuroimage* 22:1060-1075.
- Shamay-Tsoory SG, Lester H, Chisin R, Israel O, Bar-Shalom R, Peretz A, Tomer R, Tsitrinbaum Z, Aharon-Peretz J (2005) The neural correlates of understanding the other's distress: a positron emission tomography investigation of accurate empathy. *Neuroimage* 27:468-472.
- Sharbrough F, Chatrian G-E, Lesser RP, Lüders H, Nuwer M, Picton TW (1991) American Electroencephalographic Society guidelines for standard electrode position nomenclature. *J Clin Neurophysiol* 8:200-202.
- Sheikhani A, Behnam H, Mohammadi MR, Noroozian M, Mohammadi M (2012) Detection of abnormalities for diagnosing of children with autism disorders using of quantitative electroencephalography analysis. *J Med Syst* 36:957-963.
- Sholl DA (1956) The measurable parameters of the cerebral cortex and their significance in its organization. *Prog Neurobiol* 324-333.
- Simmons DR, Robertson AE, McKay LS, Toal E, McAleer P, Pollick FE (2009) Vision in autism spectrum disorders. *Vision Res* 49:2705-2739.
- Singer W, Engel AK, Kreiter AK, Munk MH, Neuenschwander S, Roelfsema PR (1997) Neuronal assemblies: necessity, signature and detectability. *Trends Cogn Sci* 1:252-261.
- Sitges C, Bornas X, Llabres J, Noguera M, Montoya P (2010) Linear and nonlinear analyses of EEG dynamics during non-painful somatosensory processing in chronic pain patients. *Int J Psychophysiol* 77:176-183.
- Soulieres I, Mottron L, Saumier D, Larochelle S (2007) Atypical categorical perception in autism: autonomy of discrimination? *J Autism Dev Disord* 37:481-490.
- Sowell ER, Peterson BS, Kan E, Woods RP, Yoshii J, Bansal R, Xu D, Zhu H, Thompson PM, Toga AW (2007) Sex differences in cortical thickness mapped in 176 healthy individuals between 7 and 87 years of age. *Cereb Cortex* 17:1550-1560.
- Srinivasan R, Winter WR, Ding J, Nunez PL (2007) EEG and MEG coherence: measures of functional connectivity at distinct spatial scales of neocortical dynamics. *J Neurosci Methods* 166:41-52.
- Stam CJ (2005) Nonlinear dynamical analysis of EEG and MEG: review of an emerging field. *Clin Neurophysiol* 116:2266-2301.

- Sundaram SK, Kumar A, Makki MI, Behen ME, Chugani HT, Chugani DC (2008) Diffusion Tensor Imaging of Frontal Lobe in Autism Spectrum Disorder. *Cerebral Cortex* 18:2659-2665.
- Takahashi T, Cho RY, Mizuno T, Kikuchi M, Murata T, Takahashi K, Wada Y (2010) Antipsychotics reverse abnormal EEG complexity in drug-naïve schizophrenia: a multiscale entropy analysis. *Neuroimage* 51:173-182.
- Takahashi T, Cho RY, Murata T, Mizuno T, Kikuchi M, Mizukami K, Kosaka H, Takahashi K, Wada Y (2009) Age-related variation in EEG complexity to photic stimulation: a multiscale entropy analysis. *Clin Neurophysiol* 120:476-483.
- Tamnes CK, Ostby Y, Fjell AM, Westlye LT, Due-Tønnessen P, Walhovd KB (2010) Brain maturation in adolescence and young adulthood: regional age-related changes in cortical thickness and white matter volume and microstructure. *Cereb Cortex* 20:534-548.
- Tang Y, Liu D, Li Y, Qiu Y, Zhu Y (2008) The time-frequency representation of the ERPs of face processing. *Conf Proc IEEE Eng Med Biol Soc* 2008:4114-4117.
- Thakkar KN, Polli FE, Joseph RM, Tuch DS, Hadjikhani N, Barton JJ, Manoach DS (2008) Response monitoring, repetitive behaviour and anterior cingulate abnormalities in autism spectrum disorders. *Brain* 131:2464-2478.
- Thulborn KR, Waterton JC, Matthews PM, Radda GK (1982) Oxygenation dependence of the transverse relaxation time of water protons in whole blood at high field. *Biochim Biophys Acta* 714:265-270.
- Tsiaras V, Simos PG, Rezaie R, Sheth BR, Garyfallidis E, Castillo EM, Papanicolaou AC (2011) Extracting biomarkers of autism from MEG resting-state functional connectivity networks. *Comput Biol Med* 41:1166-1177.
- Tsoneva T, Baldo D, Lema V, Garcia-Molina G (2011) EEG-rhythm dynamics during a 2-back working memory task and performance. *Conf Proc IEEE Eng Med Biol Soc* 2011:3828-3831.
- Ushida T, Ikemoto T, Tanaka S, Shinozaki J, Taniguchi S, Murata Y, McLaughlin M, Arai YC, Tamura Y (2008) Virtual needle pain stimuli activates cortical representation of emotions in normal volunteers. *Neurosci Lett* 439:7-12.
- VanRullen R, Thorpe S (2001) The time course of visual processing: From early perception to decision-making. *Journal of Cognitive Neuroscience* 13:454-461.
- Vidal CN, Nicolson R, DeVito TJ, Hayashi KM, Geaga JA, Drost DJ, Williamson PC, Rajakumar N, Sui Y, Dutton RA, Toga AW, Thompson PM (2006) Mapping corpus callosum deficits in autism: an index of aberrant cortical connectivity. *Biol Psychiatry* 60:218-225.
- Villalobos ME, Mizuno A, Dahl BC, Kemmotsu N, Muller RA (2005) Reduced functional connectivity between V1 and inferior frontal cortex associated with visuomotor performance in autism. *Neuroimage* 25:916-925.
- Visser M, Lambon Ralph MA (2011) Differential Contributions of Bilateral Ventral Anterior Temporal Lobe and Left Anterior Superior Temporal Gyrus to Semantic Processes. *J Cogn Neurosci*.
- Vogel AC, Power JD, Petersen SE, Schlaggar BL (2010) Development of the brain's functional network architecture. *Neuropsychol Rev* 20:362-375.
- Vogt BA, Vogt L, Laureys S (2006) Cytology and functionally correlated circuits of human posterior cingulate areas. *Neuroimage* 29:452-466.

- von Stein A, Sarnthein J (2000) Different frequencies for different scales of cortical integration: from local gamma to long range alpha/theta synchronization. *Int J Psychophysiol* 38:301-313.
- Wallace GL, Dankner N, Kenworthy L, Giedd JN, Martin A (2010) Age-related temporal and parietal cortical thinning in autism spectrum disorders. *Brain* 133:3745-3754.
- Wass S (2011) Distortions and disconnections: disrupted brain connectivity in autism. *Brain Cogn* 75:18-28.
- Wechsler D (1999) Wechsler Adult Intelligence Scale. London: Harcourt Assessment.
- Wegiel J, Kuchna I, Nowicki K, Imaki H, Marchi E, Ma SY, Chauhan A, Chauhan V, Bobrowicz TW, de Leon M, Louis LA, Cohen IL, London E, Brown WT, Wisniewski T (2010) The neuropathology of autism: defects of neurogenesis and neuronal migration, and dysplastic changes. *Acta Neuropathol* 119:755-770.
- Weinstein M, Ben-Sira L, Levy Y, Zachor DA, Ben Itzhak E, Artzi M, Tarrasch R, Eksteine PM, Hendler T, Ben Bashat D (2011) Abnormal white matter integrity in young children with autism. *Hum Brain Mapp* 32:534-543.
- Welchew DE, Ashwin C, Berkouk K, Salvador R, Suckling J, Baron-Cohen S, Bullmore E (2005) Functional disconnectivity of the medial temporal lobe in Asperger's syndrome. *Biol Psychiatry* 57:991-998.
- Welchew DE, Honey GD, Sharma T, Robbins TW, Bullmore ET (2002) Multidimensional scaling of integrated neurocognitive function and schizophrenia as a disconnection disorder. *Neuroimage* 17:1227-1239.
- Willems RM, Ozyurek A, Hagoort P (2008) Seeing and hearing meaning: ERP and fMRI evidence of word versus picture integration into a sentence context. *J Cogn Neurosci* 20:1235-1249.
- Wong TK, Fung PC, Chua SE, McAlonan GM (2008) Abnormal spatiotemporal processing of emotional facial expressions in childhood autism: dipole source analysis of event-related potentials. *Eur J Neurosci* 28:407-416.
- Woodbury-Smith MR, Robinson J, Wheelwright S, Baron-Cohen S (2005) Screening adults for Asperger Syndrome using the AQ: a preliminary study of its diagnostic validity in clinical practice. *J Autism Dev Disord* 35:331-335.
- Zijlmans M, Jacobs J, Kahn YU, Zelman R, Dubeau F, Gotman J (2011) Ictal and interictal high frequency oscillations in patients with focal epilepsy. *Clin Neurophysiol* 122:664-671.